Charles University

Faculty of Science

Study program: Biology

Branch of study: Cellular and Developmental Biology

Specialization: Cell Physiology

Bc. Barbora Burýšková

The effect of 6S-like RNAs on physiological differentiation of *Streptomyces coelicolor*

Vliv 6S-like RNA molekul na fyziologickou diferenciaci *Streptomyces coelicolor*

Diploma thesis / Diplomová práce

Supervisor: RNDr. Jan Bobek, Ph.D.

Prague, 2018

Prohlášení:

Prohlašuji, že jsem závěrečnou práci zpracoval/a samostatně a že jsem uvedl/a všechny použité informační zdroje a literaturu. Tato práce ani její podstatná část nebyla předložena k získání jiného nebo stejného akademického titulu.

V Praze, 04.01.2018

Na tomto místě bych ráda poděkovala svému školiteli Janu Bobkovi za odborné konzultace a pomoc při vyhodnocování výsledků. Dále děkuji Alici Zikové za ochotu a pomoc při získávání koimunoprecipitačních vzorků, Jiřímu Vohradskému z Mikrobiologického ústavu Akademie věd za poskytnutí prostředků a prostoru pro koimunoprecipitační experiment, a Liborovi Krásnému za poskytnutí protilátek a cenných rad. Mé díky patří také Jiřímu Míškovi z Katedry organické chemie Přírodovědecké fakulty za umožnení práce na laserovém skeneru. Děkuji také Ditě Šetinové, Matoušovi Čihákovi, Kláře Šmídové a Jiřímu Pospíšilovi za jejich pomoc, rady a podporu při vypracovávání této práce. V neposlední řadě děkuji za podporu svým rodičům, a Petrovi Taušovi za motivaci a psychickou podporu během studia.

Abstract:

The variety of bacteria and their genomes sometimes causes conservation of homologue molecules to be displayed not in sequence but in secondary and tertiary structures. In the case of the regulatory 6S RNA, sequence homologues have been found in over 100 bacterial species so far. However, none were found in the genus *Streptomyces*. The unique genome of these soil-dwelling bacteria, known for their capacity to produce antibiotics, has a high G/C content and diverges substantially from distantly related bacteria. Yet in the non-coding 6S RNA it is the secondary structure that is crucial for its function. The 6S RNAs trap sigma factors by mimicking target promoter sequences in order to help with switching sets of expressed genes during developmental transitions. 6S-like RNA genes in *Streptomyces coelicolor* have been computationally predicted by comparison of *in silico* modelled secondary structures of known 6S RNAs. The aim of this thesis was the verification of these 6S-like RNA predictions. The experimental approach was based on RNA co-immunoprecipitation (RNA CoIP), as well as RT-PCR from RNA samples. The outcomes of this project are the detection of six novel ncRNA transcripts with possible 6S-like RNA functions, which also served as the wet-lab verification of the *in silico* prediction technique used to identify bacterial ncRNAs on the basis of structure conservation. More research needs to be conducted to resolve the role of the putative 6S-like RNA genes.

Keywords: 6S RNA, sigma factor, *Streptomyces*, antibiotics, physiological differentiation, gene expression

Abstrakt:

Rozmanitost bakterií a jejich genomů může zapříčinit konzervaci funkčních molekulárních motivů na úrovni strukturní místo konzervace na úrovni sekvencí. V případě regulační 6S RNA byly nalezeny sekvenční homology u více než sta bakteriálních druhů. U bakterií rodu *Strepomyces* však nebyl nalezen žádný. Jedinečný genom těchto bakterií, důležitých pro svou schopnost produkce antibiotik, má vysoký obsah G-C párů bází a je představitelem unikátních genomů fylogeneticky staré větve Aktinobakterií. Funkce nekódující 6S RNA je dána její sekundární strukturou. 6S RNA svou strukturou napodobují cílové promotorové sekvence a vychytávají tak sigma faktory, které jsou součástí transkripčního aparátu. Tímto napomáhají přepínání souborů exprimovaných genů během vývojových přechodů. Pomocí porovnání *in silico* predikovaných sekundárních struktur známých 6S RNA byl vytvořen počítačový model, který predikoval 6S-like RNA u Streptomycet. Cílem této práce bylo ověřit expresi těchto 6S-like RNA predikovaných u *Streptomyces coelicolor* pomocí RT-PCR a RNA koimunoprecipitace (RNA CoIP). Výsledkem této práce je detekce šesti nových ncRNA transkriptů, které by mohly být homology 6S RNA u Streptomycet. Tato zjištění rovněž potvrdila *in silico* predikční metodu, kterou byly nalezeny nekóducíjí bakteriální RNA na základě strukturní homologie. Aby mohla být určena funkce těchto nalezených RNA, je třeba pokračovat ve výzkumu.

Klíčová slova: 6S RNA, sigma faktor, *Streptomyces*, antibiotika, fyziologická diferenciace, genová exprese

Table of Contents

Abbreviations

BSA	Bovine serum albumin
CCR	Carbon catabolite repression
c-di-GMP	Cyclic diguanosine monophosphate
CoIP	Co-Immunoprecipitation
CTD	C-terminal binding domain
DBD	DNA binding domain
dTTP	Deoxythymidine triphosphate
ECF	Extracytoplasmic function
EtOH	Ethanol
GlcNAc	N-acetylglucosamin
HGT	Horizontal gene transfer
HRP	Horse radish peroxidase
IPTG	Isopropyl β-D-1-thiogalactopyranoside
MetOH	Methanol
NaAc	Sodium acetate
ncRNA	Non-(protein)-coding RNA
O/N	Over night
PBS	Phosphate buffered saline
PCD	Programmed cell death
RIPA buffer	Radioimmunoprecipitation assay buffer
RNAP	RNA polymerase
RT buffer	Reverse transcriptase buffer

RT	Room temperature
RT-PCR	Reverse transcription PCR
TBE buffer	Tris-borate-EDTA buffer
TE buffer	Tris-EDTA buffer
TF	Transcription factor
WB	Western blot
WT	Wild type

1 Introduction

Streptomycetes are gram-positive soil bacteria, resembling fungi with their filamentous growth and the production of haploid spores by an aerial mycelium emerging from the vegetative mycelium in soil. Since the majority of clinically used antibiotic compounds comes from *Streptomyces* species, these bacteria are extremely important in medicine. With multidrug resistant bacteria on the rise, research is focused on the discovery of novel compounds with antimicrobial activity. Cryptic gene clusters of streptomycetes, that are not expressed under standard conditions, could represent an untapped source of such compounds. Therefore, elucidating the molecular mechanisms of gene expression regulation in streptomycetes is an important task.

As in other bacterial phyla, a major group of the 800 genes encoding transcriptional regulators in streptomycetes are sigma factors. These dissociable subunits of RNA polymerase alter the affinity of the transcriptional machinery to distinct promoter motifs and thus regulate sets of expressed genes in response to external or internal stimuli. In *E. coli* and many other bacteria, a non-coding regulatory RNA – 6S RNA regulates the RNA polymerase (RNAP) holoenzyme by mimicking the open promoter complex and enabling the complex to transcribe DNA. Due to the GC – rich genome of streptomycetes and their phylogenetic distance from other bacterial phyla, no 6S homologs were identified in this genus yet. Considering the 65 sigma factors that *Streptomyces coelicolor* harbors, we hypothesized that a proportional amount of 6S RNAs could be present.

Our laboratory focuses on research of antisense RNAs in *S. coelicolor* gene expression regulation (Šetinová, manuscript in press) as well as *Streptomyces* physiological differentiation and associated changes in secondary metabolism during the life cycle (Bobek et al., 2017). This thesis focuses on primary research of the molecular mechanisms of gene expression regulation by searching for 6S-like RNAs in *S. coelicolor*. In addition to our hypothesis, this search was prompted by the *in silico* prediction of 6S RNA candidates in *S. coelicolor* by Josef Pánek. There are still many blank spaces in the model of *Streptomyces* gene expression regulation and this thesis should contribute to the knowledge.

2 Literature Review

2.1 Streptomycetes classification

Streptomycetes are soil-dwelling bacteria and the largest genus of Actinobacteria. Actinobacteria are a phylum of Gram positive bacteria with terrestrial as well as aquatic specimen, unique in a high GC genomic DNA content. Actinobacteria are decomposers and contribute significantly to soil buffering and hummus formation. Their origin is dated back to 2 – 1.5 billion years ago when the atmosphere began to get oxygenated, and streptomycetes emerged 450 million years ago, soon after terrestrial plants colonized earth's land (Heckman et al., 2001). Nevertheless, besides the saprophytic soil dwelling filamentous specimen, the phylum of actinobacteria also includes symbiotic nitrogen fixing bacteria (genus *Frankia*), intracellular pathogens (*Mycobacterium tuberculosis*, *Mycobacterium leprae*; reviewed in Cosma et al., 2003) or extracellular pathogens (*Corynebacterium diphteriae*, *Nocardia* spp., *Propionibacterium* spp.; reviewed in Ventura et al., 2007) as well as commensal species inhabiting the human gut (*Bifidobacterium* spp.; Eckburg et al., 2005) and skin microbiota (*Corynebacterium* spp.; Chiller et al., 2001).

2.2 Habitat and Ecology

The characteristic habitat of streptomycetes is soil, and an easy way to determine the presence of these bacteria is the familiar earthy smell of the volatile alcohol geosmin, which the bacteria produce as one from the plethora of compounds created by their secondary metabolism (Gerber & Lechevalier, 1965). Their growth rates in soil communities are slower than those of most bacteria and fungi, but the production of powerful extracellular enzymes and a variety of inhibitors of cellular processes (antibiotics, fungicides, cytostatics, immune response modulators, plant growth modulators; Hopwood, 2007) enables them to exploit a large variety of carbon and nitrogen resources (cellulose, chitin, xylan, lignin) and repel other species from taking over their area of growth (Wohl & McArthur, 2001). Regarding their ability to compost a variety of insoluble materials and the evolutionary conservation level of the genes involved, streptomycetes are

thought to have played a role in the formation of primeval soil. On top of that, the diversity of genes encoding extracellular enzymes between different *Streptomyces* species suggests the importance of cooperation in mixed *Streptomyces* communities (Chater et al., 2010). Streptomycetes also play a role in rhizosphere symbiosis. With the exception of the pathogenic *Streptomyces scabies*, causing potato scab (Lerat et al., 2009), they grow endophytically thus protecting the roots of plants from fungal pathogens by acting as growth competitors, by the release of secondary metabolites (Sardi et al., 1992), and they are also able to produce plant growth hormones, e.g. auxin, which leads to increased nutrient assimilation and growth of the symbiotic plants (Manulis et al., 1994). *Streptomyces griseoviridis* isolated from sphagnum peat in Finland is even used as a protective biological fungicide commercially sold to this day in agriculture, significantly increasing the yield of grown crops (Mycostop; Lahdenpera, 2000; Tahvonen, 1988).

In 1995, Moran et al. ruled out the possibility that *Streptomyces* spores found in marine environments are solely stray spores of terrestrial specimen. Further investigation has shown evidence of streptomycetes being indigenous to the marine environment, inhabiting various habitats and forming symbioses with marine invertebrates (Pathom-Aree et al., 2006; Seipke et al., 2012). Not long after, the focus of scientists turned towards bioprospecting for the unexplored marine microbial communities and the hunt for secondary metabolites of marine streptomycetes had begun (Lozada & Dionisi, 2015). The emerging diversity of *Streptomyces* bioactive secondary metabolites has been first reviewed in Dharmaraj, 2010, and subsequent research focuses on biotechnological as well as biopharmaceutical application of newly found compounds (Hassan et al., 2017).

2.3 Life cycle and morphological differentiation

Streptomycetes exhibit characteristic similarities with the fungal growth cycle and ecological role. They have a sophisticated life cycle which involves phases of complex physiological differentiation. Their colonies produce a filamentous multicellular vegetative mycelium to create a larger surface area for nutrient absorption from soil, which is aided by the production and secretion of extracellular enzymes. In response to nutrient depletion, an aerial mycelium starts to form. This structure depends energetically on the supportive vegetative

mycelium, which undergoes programmed cell death (PCD) to release the nutrients needed by the proliferative hyphae. In concert with the aerial mycelium formation, antibiotics are produced to defend the vegetative mycelium from processing by other microorganisms. The upper parts of the aerial hyphae septate and further give rise to metabolically silenced spores, which are dispersed and can slumber over the decades until favorable conditions trigger their germination (Haselwandter & Ebner, 1994; reviewed in McCormick & Flärdh, 2011; **Fig.1**).

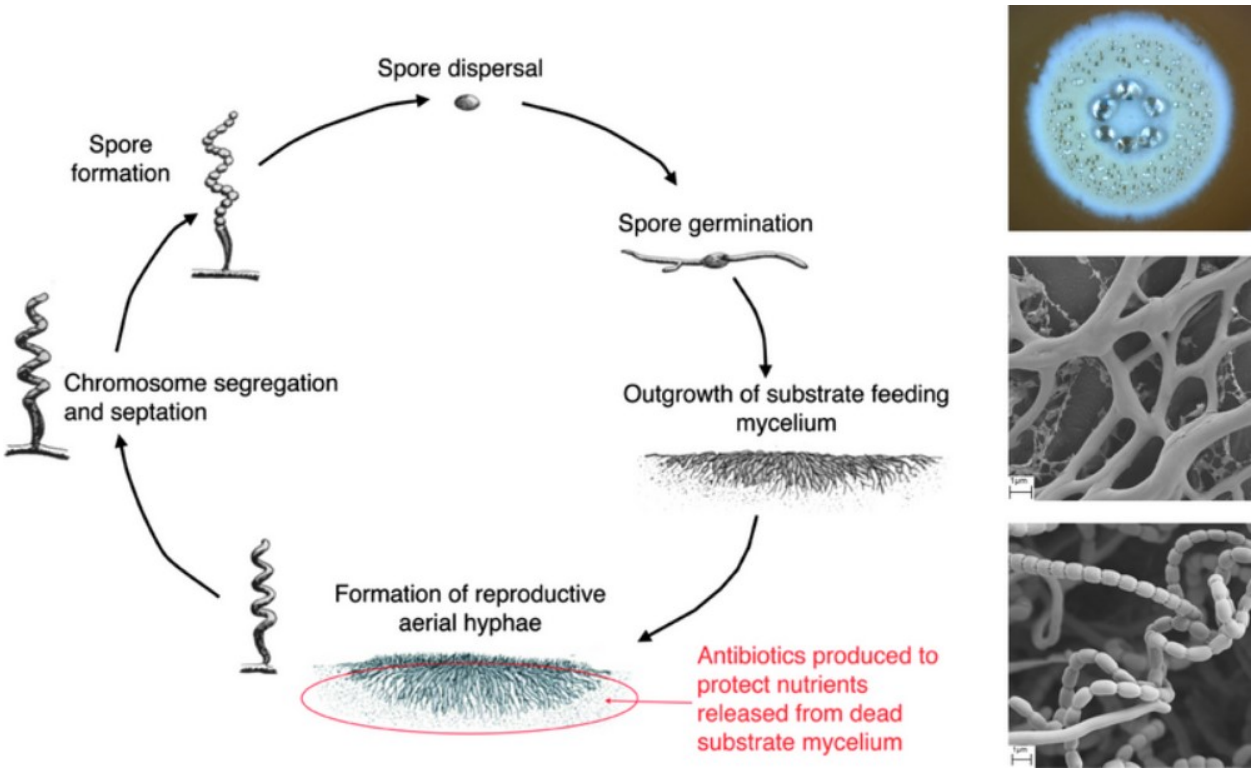

Figure 1. General outline of the *Streptomyces* life cycle which is described in the text above. The pictures on the right show a colony of *Streptomyces* spp. isolated from *Allomerus* ants (40×; top), and scanning electron micrographs of the vegetative mycelium (400×; middle) and aerial mycelium with spore chains (400×; bottom) of *Streptomyces coelicolor*. The scale bar represents 1µm. Adapted from (Seipke et al., 2012).

2.3.1 Vegetative growth

The root system-like *Streptomyces* substrate mycelium is formed by two important features. Firstly, unlike the isotropic growth of the lateral cell walls in *Escherichia coli*, dependent

on the bacterial actin homologue MreB (Carballido-López, 2006), *Streptomyces* vegetative hyphae grow at their tips. This apical growth is coordinated by the essential protein DivIVA. The protein localizes to the tips of the growing hyphae and is responsible for recruiting the peptidoglycan biosynthesis machinery (Flärdh, 2003). DivIVA also localizes to foci in the lateral walls and marks the points of new branch growth (Hempel et al., 2008). New insights have shown additional proteins cooperating with DivIVA and the complex has been termed a "polarisome" (Fuchino et al., 2013). Secondly, *Streptomyces* cell wall extension and branching are independent of cell division. Also, chromosome replication is not linked to cytokinesis and therefore an extensive multicellular mycelium is formed (Elliot et al., 2008).

2.3.2 Stimuli leading to developmental transition

In response to unfavorable conditions (nutrient depletion, environmental stress) the *Streptomyces* developmental program is affected, and an aerial mycelium starts to form, in order to produce spores that will dispatch the colony to a safer environment. Presence of high-energy nutrients in soil promotes mycelium growth and represses developmental processes including aerial mycelium development. The preferred substrate of streptomycetes is N-acetylglucosamin (GlcNAc) and its abundance in soil is closely monitored (Romero-Rodríguez et al., 2016). Uptake of GlcNAc has a pleiotropic effect on *Streptomyces* development and the blue pigmented actinorhodin antibiotic production. Under rich conditions, it inhibits development, whereas under famine conditions it promotes development and actinorhodin production (Rigali et al., 2008). This mechanism senses the release of nutrients from the vegetative mycelium undergoing PCD and through a series of molecular signals, aerial (reproductive) hyphae start to form (Miguélez et al., 1999). Utilization of preferred substrates can disrupt processing and absorption of less favored substrates. This phenomenon is called carbon catabolite repression (CCR) or glucose repression (Görke & Stülke, 2008). Due to the fluctuations of carbon sources during the developmental transition from vegetative to aerial mycelium many antibiotics are subject to CCR, and this is therefore extensively studied (Hošťálek, 1980; Sanchez et al., 2010; Urem et al., 2016).

2.3.3 Erection of aerial hyphae

To grow outside of the moist and supporting substrate, *Streptomyces* hyphae must create a hydrophobic coat. This is achieved by chaplin and rodlin protein families. These proteins are secreted and polymerize into a filamentous hydrophobic sheath that reduces the surface tension of water above the mycelium and enables growth upwards (Claessen et al., 2003; Tillotson et al., 1998). Additionally, SapB - an amphipathic lantibiotic-like protein - is secreted to act as a biosurfactant of top of the transitioning mycelium (Kodani et al., 2004). In wild type *S. coelicolor*, SapB is not produced during growth on minimal medium and its absence in the hydrophobic sheath does not impair aerial mycelium growth (Willey et al., 1991).

On a cellular signaling level, the complete morphological transition is subject to the master regulator BldD (Bld stands for bald, as the mutants in *bld* genes lack the fuzzy aerial mycelium), which represses most genes encoding developmental regulators (Den Hengst et al., 2010). Though the specific upstream factors regulating BldD are not known (an exception is BldD repression by PhoP under phosphate limitation conditions; Allenby et al., 2012), new research has shown that it acts in a complex with the bacterial second messenger cyclic diguanosine monophosphate (c-di-GMP; **Fig.2**; Tschowri et al., 2014). One of the genes derepressed by the BldD-(c-di-GMP) complex decay is *bldN* (**Fig3**). This gene encodes σ^{BldN} (one of the 64 or more sigma factors in streptomycetes, see chapter **2.6**), which in turn directs the transcription of all genes encoding chaplin and rodlin proteins (Bibb et al., 2012). AdpA (formerly recognized as BldH; Champness, 1988) is another developmental regulator expressed when BldD-(c-di-GMP) repression is alleviated. AdpA controls the expression of a gene encoding a regulatory tRNA – *bldA* (Bush et al., 2015). BldA is the only tRNA that can recognize a rare UUA codon (see chapter **2.4**), thus streptomycetes have assigned BldA a very unique function by designing a new mechanism of post-transcriptional regulation (Chater & Chandra, 2008). When expressed, BldA helps express several genes involved in the developmental program (and much more genes that are not involved in development), which leads to the expression of SapB and a positive feedback loop to *adpA* (Higo et al., 2011).

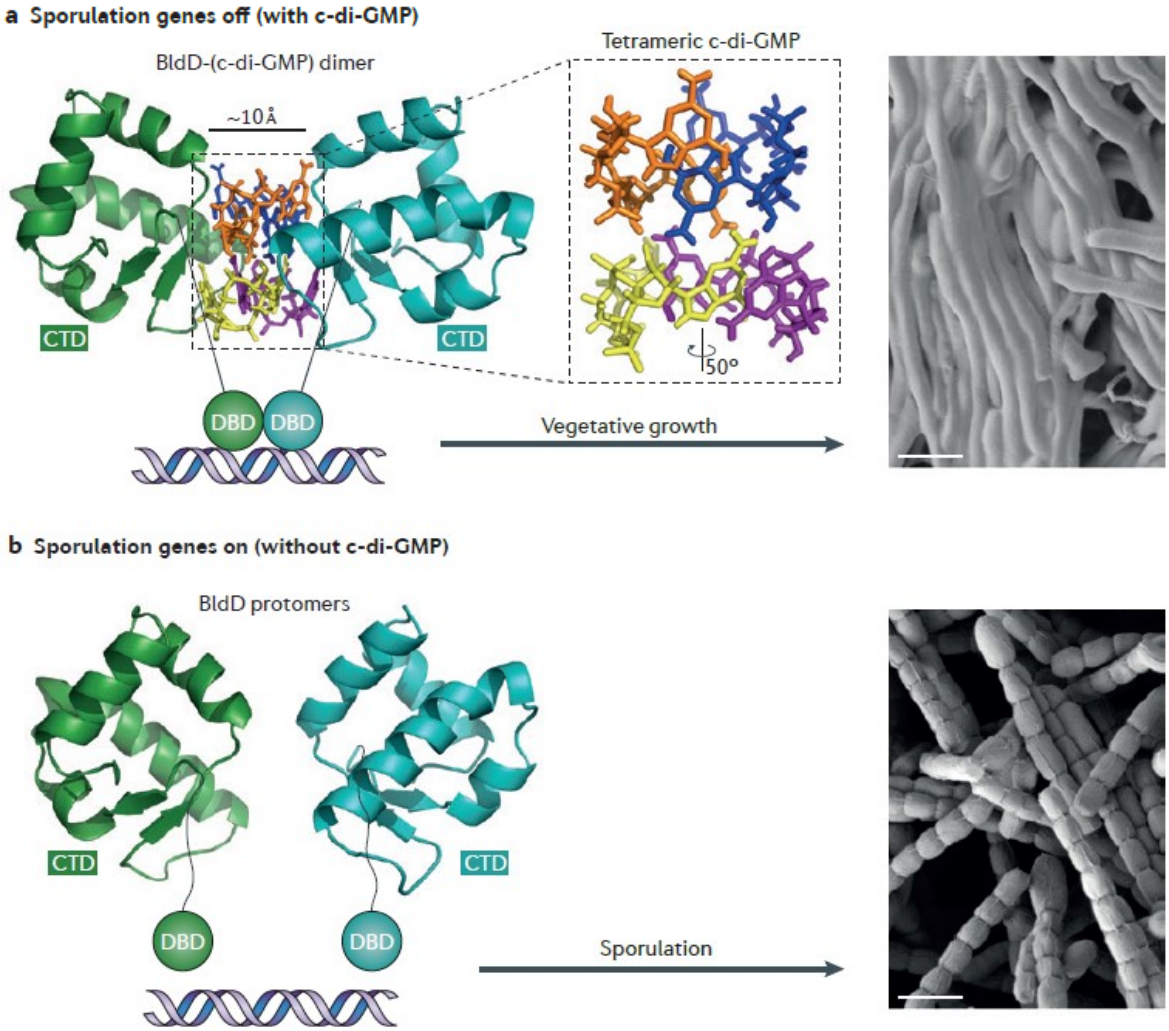

Figure 2. BldD-(c-di-GMP) as a master regulator of developmental transition in Streptomycetes. **a)** The bacterial second messenger c-di-GMP tetramer controls the DNA binding capacity of BldD by mediating its dimerization. **b)** After a drop in c-di-GMP concentration levels, the complex dissociates and the repression of BldD-(c-di-GMP) regulated genes ceases. This activates the extensive transcriptional cascade leading to sporulation. DBD – DNA binding domain; CTD – C-terminal domain; The scale bar represents 2μm. Adapted from (Bush et al., 2015).

2.3.4 Sporulation septation and chromosome segregation

In comparison to the vegetative hyphae, chromosome replication in the elongating aerial hyphae is highly upregulated. The cells contain up to 100 copies of the chromosome and are called the "sporogenic cells" (Ruban-Ośmiałowska et al., 2006). The transition from aerial growth to

sporulation septation is strongly coordinated by two putative transcription factors that most likely work together – WhiA and WhiB (Whi stands for white, as the mutants in *whi* genes cease to transform their white aerial hyphae into pigment containing spores; Bush et al., 2015; Flärdh et al., 1999). Firstly, the transcription of a polarisome associated cytoskeletal protein FilP is repressed and thereby apical growth is stopped. At the same time the *ftsZ* gene, derepressed by the BldD-(c-di-GMP) complex disintegration, is activated, and FtsZ (the tubulin homologue in bacteria) forms a ladder like structure, marking future septa between spores (Bush et al., 2013; Den Hengst et al., 2010; Flärdh et al., 2000). Another gene activated by WhiA(-WhiB?) is *ftsK*. The FtsK DNA translocase helps with segregation of the DNA away from the closing septa (Bush et al., 2013).

2.3.5 Spore maturation

The later stages of sporulation are launched by the expression of the sigma factor σ^{WhiG}. Like *ftsZ*, *whiG* is subject to repression alleviation by BldD-(c-di-GMP) complex disintegration and WhiA(-WhiB?) activation (**Fig.3**). The sigma factor σ^{WhiG} activates transcription of *whiH* and *whiI*. The cell division process is regulated by *whiH*, yet the mechanisms are still unknown (Flärdh et al., 1999). *WhiI* regulates the transition of aerial hyphae into mature spores and its product is

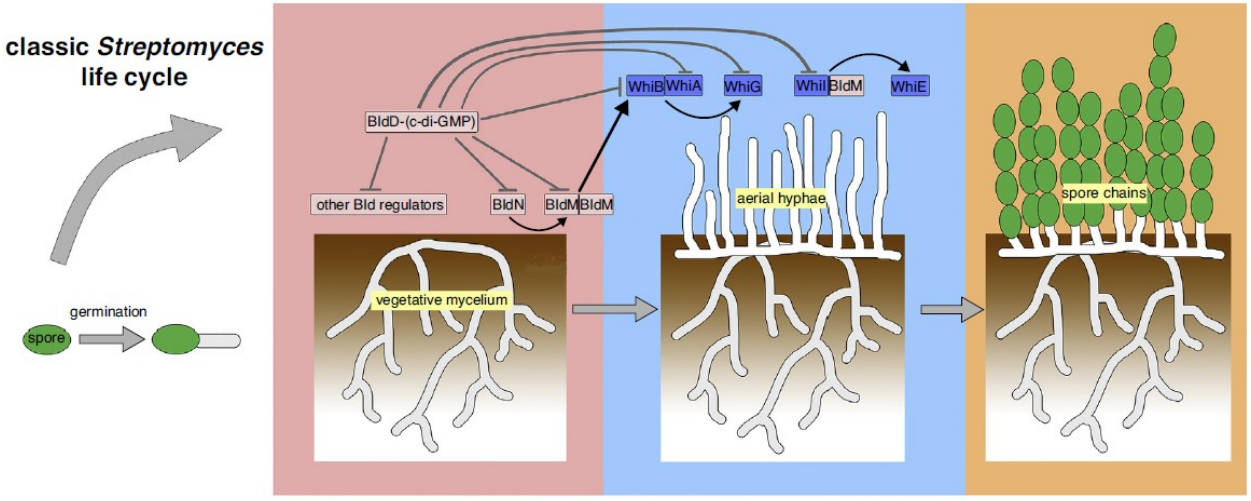

Figure 3. Basic overview of the regulatory cascade involved in *Streptomyces* developmental transitions. From the left: a single germ tube emerges from the germinating spore. The streptomycete enters the vegetative growth phase and a mycelium is formed. In response to external stimuli, the BlD-(c-di-GMP) repression ceases and *bld* genes and subsequently *whi* genes get activated and guide the aerial mycelium formation and sporulation. Adapted from (Jones & Elliot, 2018).

thought to operate in concert with the σ^{BldN} transcribed BldM, creating a two-component checkpoint mechanism for the finale of the complex developmental transition into a haploid reproductive state of being (Al-Bassam et al., 2014). This involves the rounding of spores and production of a 30-50 nm thick cell wall that is resistant to lysozyme. The bacterial actin MreB is involved in the spore wall formation (Mazza et al., 2006). Interestingly, this protein is no longer present in non-sporulating actinomycetes. The chaplin and rodlin layer on the surface of spores reorganizes and creates a hydrophobic coat, making the spore watertight (Flärdh & Buttner, 2009). The last spore maturation step is WhiI-BldM mediated WhiE activation and subsequent expression of enzymes involved in synthesis of the grey polyketide spore pigment (Kelemen et al., 1998).

2.3.6 Spore dispersal and germination

Metabolically silenced spores are dispersed by wind currents, water, or animals. The disaccharide trehalose is thought to protect dormant cells from desiccation and other environmental stresses, and later act as an energy source during germination (Sola-Penna & Meyer-Fernandes, 1998; Fillinger et al., 2001). Water is the minimal requirement for the awakening of dispersed spores. Heat shock, mechanical disruption of the outer spore coating or addition of L-amino acids or bivalent ions to the medium induce germination (Bobek et al., 2017; Eaton & Ensign, 1980), but the precise mechanism of germination induction is still unknown. During germination, streptomycetes produce an autoregulatory germination inhibitor called Germicidin A. A prospective role of this autoinhibition could be the preservation of a fraction of dormant spores from unfavorable surrounding conditions (Aoki et al., 2011; M. Čihák, 2017).

2.4 Genome

As a representative of the Actinomycetales specimen with a sophisticated life cycle, streptomycetes have a linear chromosome capped by terminal proteins at the 5'ends. Next to the capping terminal proteins, large – up to hundreds of kilobases - terminal inverted repeats protect telomeres of *Streptomyces* chromosomes (reviewed in Chaconas & Chen, 2005). In 2002, when the genome of *Streptomyces coelicolor* A3(2) was sequenced, it was found to have the largest number of genes discovered in a bacterium at that time. The chromosome is 8,6 Mb long with a

72% GC content, almost 8000 genes and a centrally located *OriC* (Bentley et al., 2002). The large chromosome has a specific organizational structure common to most Actinobacteria. The core region holds essential core genes syntenous in most Actinomycetales. Regions flanking the core contain genes specific for streptomycetes and the terminal regions contain diverse sets of genes in separate *Streptomyces* species (Ventura et al., 2007). *Streptomyces coelicolor* A3(2) has two plasmids, the linear 365 kb long SCP1 and the smaller, 31 kb, circular SCP2. The strain used in this thesis, *Streptomyces coelicolor* M145, is a prototrophic derivative of the wild-type strain A3(2) lacking the two plasmids and a 1Mb long terminal inverted repeat sequence which probably arose by unequal recombination within the terminal inverted repeats between copies of transposable elements (Bentley et al., 2002; Weaver et al., 2004). *S coelicolor* was chosen as the model species by David Hopwood, the pioneer in *Streptomyces* genetics (Hopwood, 1999), due to the easily detectable production of the red prodiginines and blue actinorhodin antibiotics. Since the production of these antibiotics coincides with developmental transitions (in a manner that enables pinpointing the onset of transition; Jeong et al., 2016), development altering mutation can be detected by the naked eye, making *S. coelicolor* a research-friendly species. Horizontal gene transfer (HGT) has been thought to play a big role in *Streptomyces* divergence by acquisition of secondary metabolism clusters and resistance or pathogenicity genes. While this is true, by calibrating the HGT rate to the ancient age of *Streptomyces* existence, HGT turns out to be quite rare (10 genes acquired and maintained per one million years) and less impactful than previously thought, with vertically inherited point mutations and homologous recombination being the main driving force of *Streptomyces* evolution (McDonald & Curie, 2017). Due to the GC-rich *Streptomyces* genome, their codons are often skewed to a G or C in the last position. This makes the rare UUA leucine codon even more interesting. In *S. coelicolor*, 145 genes contain TTA codons, and these are mainly genes of secondary metabolism cassettes and genes involved in developmental differentiation. Since secondary metabolism and morphological transitions are linked, the TTA codon was thought to have a regulatory role. This has been confirmed by description of a developmentally regulated tRNA (BldA), recognizing the UUA codon (see chapter **2.3.3**; Chater & Chandra, 2008; Ventura et al., 2007).

2.5 Transcriptional regulators – overview

In bacteria, the most common manner of gene expression control is the regulation of transcription initiation. Considering the elaborate *Streptomyces* life cycle with all its morphological forms, and the rich habitats overflowing with stimuli, it is no surprise that streptomycetes encode nearly 800 transcription regulator genes (Barakat et al., 2010). These molecules mediate external and internal signal transduction to the cellular operating center, the chromosome, and can be divided into one- or two-component transcription factors (Romero-Rodríguez et al., 2015). The executive molecules (response regulators) in transcription regulating cascades are proteins capable of binding DNA – transcription factors (TFs). These act in different ways to activate or repress transcription: repression by competition for binding sites with activators; binding at promoter sequences to create physical hindrance to the transcription machinery; binding downstream of promoters to enable transcription elongation; activation by stabilizing the initiation complex (RNAP holoenzyme – promoter sequence) and stimulating the "open" complex formation (reviewed in Lee et al., 2012).

The two-component regulation systems typically consist of membrane bound sensor kinases (usually histidine or serine/threonine kinases) and DNA binding response regulators. When sensor kinase specific stimuli are detected by the extracellular part of the sensor kinase, autophosphorylation of the intracellular kinase domains occurs and these can in turn phosphorylate their cognate response regulators, which act as transcription factors and repress or activate the stimuli specific response genes (**Fig.4**; Podgornaia & Laub, 2013). Next to the two-component systems, bacteria have a range of molecules with both sensory and executive domains capable of transducing similar signals as the two-component systems. Moreover, it has been found that these one-component systems could in fact be the dominant nutrient sensing mechanism, due to the fast route between input and output domains that are present on the same molecule (Ulrich et al., 2005). Another type of transcriptional regulators widely used to direct transcription in bacteria are sigma (σ) factors. σ factors are dissociable subunits of the RNA polymerase (RNAP) core, which is assembled from five subunits (β, β', α, α, ω). By binding of σ to the RNAP core enzyme, the RNAP holoenzyme with assigned promoter specificity is formed. Bacteria usually possess more types of σ factors that are activated under different conditions and by directing transcription help equip the

cells with molecules needed in different situations (Losick & Pero, 1981; Helmann & Chamberlin, 1988).

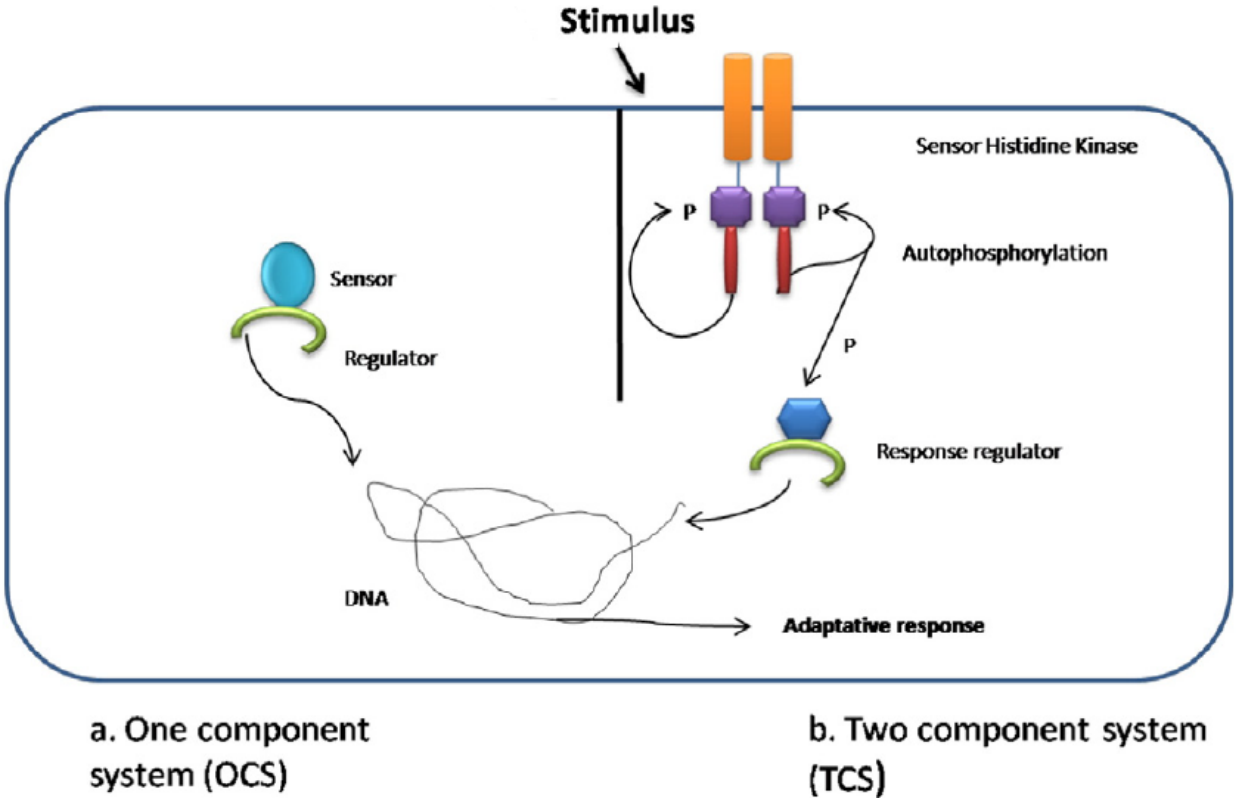

Figure 4. Scheme of one-component and two-component signal transduction systems in bacteria. **a)** Example of a one component system consisting of one molecule with a sensory domain and a regulatory domain. **b)** Example of a two component system consisting of a sensory histidine kinase and an independent regulator. Adapted from (Romero-Rodríguez et al., 2015).

2.6 Sigma (σ) factors

Bacterial sigma factors can be classified in two distinct families based on their homology to *E. coli* sigma factors - the housekeeping σ^{70} (RpoD) and the enhancer dependent σ^{54} (σ^{N}; unrelated by sequence to σ^{70}; Buck et al., 2000). The σ factors can also be grouped by promoter specificity. Housekeeping σ factors are responsible for essential gene transcription during growth. Alternative σ factors transcribe special regulons in response to changing conditions, stress or developmental transitions. The σ^{70} family can be divided into 4 phylogenetically and structurally distinct groups, with group 1 comprising housekeeping σ factors and groups 2-4 comprising alternative σ factors (reviewed by Paget, 2015). The structural differences, and a structural model of σ^{70} in the RNAP transcription initiation complex are shown below (**Fig.5**).

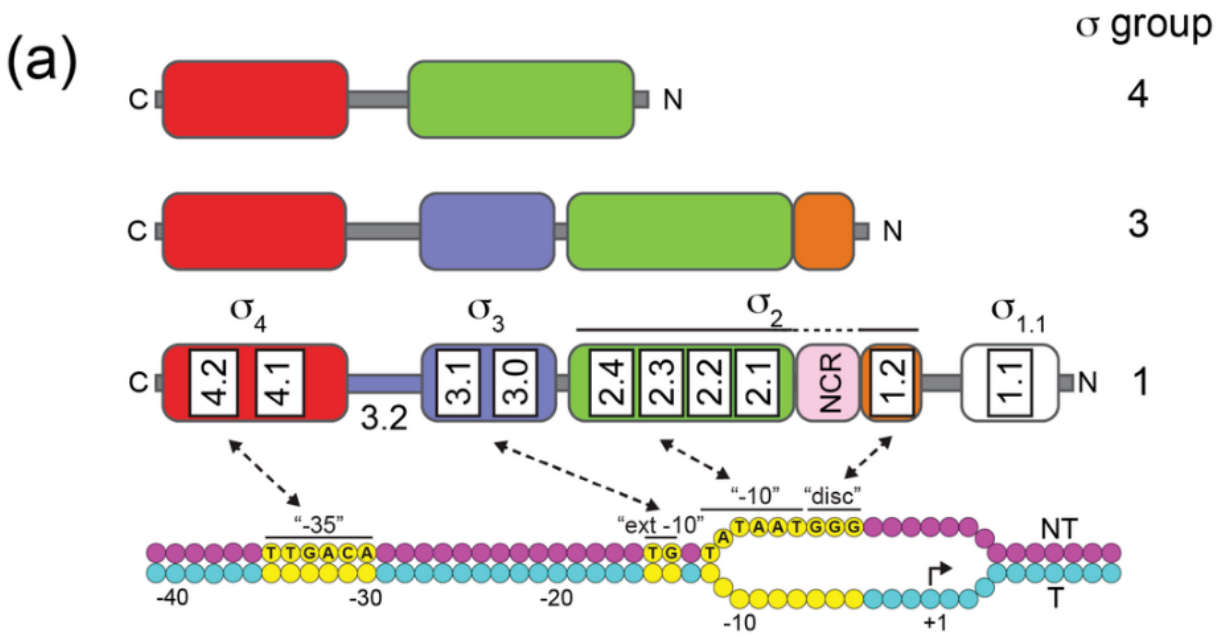

Figure 5. The σ^{70} family domain organization, recognized promoter motifs and a structural model representation. **a)** Domain organization of σ factor groups (1, 3, 4) and σ^{70} (group 1) consensus with the *E. coli* promoter DNA. Non-template (NT) strand, magenta; template (T) strand, cyan; key consensus promoter elements contacted by σ, yellow ("−35", −35 element; "ext −10", extended −10 element; "−10", −10 element; "disc", discriminator); nonconserved region (NCR; variable in size and structure among Group 1 σ factors), pink; **b)** (see next page) Structural model of *E. coli* σ^{70} in a transcription initiation complex with RNA polymerase. The surface representations of σ^{70} domains and promoter DNA are colored as in (a). The β, α and ω RNAP subunits are not depicted. The location of the σ finger close to template strand DNA and nascent RNA (yellow) is depicted. Adapted from (Paget, 2015).

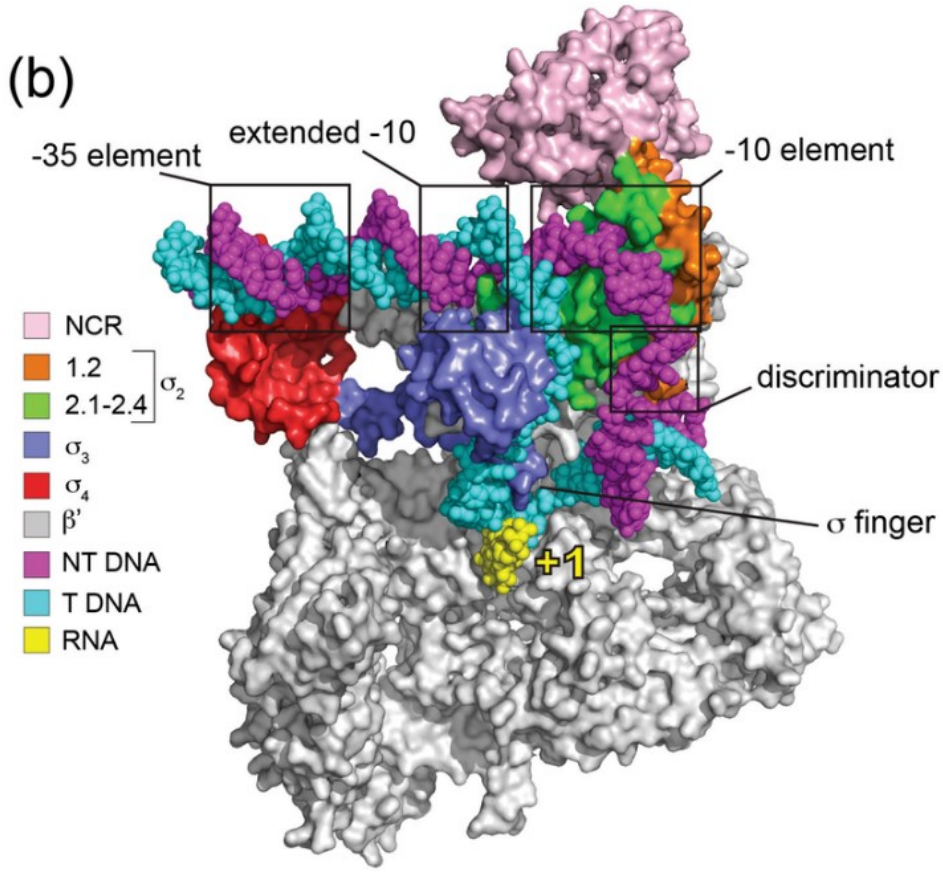

Streptomyces coelicolor has an astonishing number of 64 σ factors, which can be divided in four groups, correlating with the σ^{70} family division (Bentley et al., 2002; Gruber & Gross, 2003). *S. coelicolor* has one principal σ factor belonging to the first group (housekeeping σ factors), called HrdB (HrdB for homologue of RpoD). Group 2, structurally closely related to group 1 (they lack $\sigma_{1.1}$), comprises three non-essential σ factors (HrdA, C, D) with yet unknown functions (Buttner & Lewis, 1992). The promoters recognized by group 2 σ factors only differ in one nucleotide in the extended -10 element (Becker & Hengge-Aronis, 2001). Group 3 is structurally and functionally diverse and so are the recognized promoters. Analogous bacterial σ factors governing flagellum biosynthesis, heat shock response, general stress, and sporulation belong to this group (Paget & Helmann, 2003). In streptomycetes, both σ^{WhiG} and σ^{BldN} (see chapter development) are members of this group, as well as 9 paralogues of the stress responsive σ^{B} of *Bacillus subtilis* (Chater et al., 1989; Viollier et al., 2003; Dalton et al., 2007). Expression profiles of these σ factors have validated the link between *Streptomyces* stress responses and regulatory pathways governing developmental transitions (Vohradsky et al., 2000; Bobek et al., 2014). Group

4 is the largest, most diverse and phylogenetically distant from σ^{70}. σ factors of this group can sense and respond to stimuli generated outside of the cell or in the cell membrane, and are thus called extracytoplasmic function (ECF) σ factors. A representative of *S. coelicolor* group 4 σ factor is σ^{R}, which triggers the response to oxidative stress by activating more than 100 genes (Paget et al., 1998; Kallifidas et al., 2010). Promoters recognized by ECF σ factors contain a -35 "AAC" motif and diversity in the -10 element, which is recognized by a variable loop located on the σ_2 2.3 domain (see **Fig.5a**). By replacing the loop with another from a different ECF σ factor, a switch in specificity was observed and the variable loop is thus thought to be a modular element which expands ECF factor diversity (Staroń et al., 2009; Campagne et al., 2014).

2.6.1 Sigma (σ) factor regulation

Being one of the main regulatory pathways of gene expression, the activity of sigma factors also must be controlled. The most basic way of such control is the competition between σ factors for the RNAP core enzyme. It has been found that *E. coli* σ^{70} has a higher affinity for the polymerase complex than alternative σ factors (Maeda et al., 2000). One theory suggests that with the lower general rate of transcription during starvation, the rise in free RNAP would heighten the proportion of RNAP: σ^{70} and thus facilitate alternative σ binding (Mauri & Klumpp, 2014). The cellular concentration of σ factors can be controlled by means of transcription, translation and protein turnover. An example of transcriptional level control is the auto-induced signal amplification loop of σ^{SigN} expression, where a basal level of σ^{SigN} is present from pre-developmental expression and continues to promote its own expression from a second promoter in the *sigN* gene (Dalton et al., 2007). Some σ factors have an inhibitory N-terminal extension, which makes them "pro - σ" factors that are activated by proteolysis of the extension (Paget, 2015). On the other hand, some ECF σ factor groups have large C-terminal extensions with possible regulatory or localization functions, which also could affect the availability or activity of the σ factors (Jogler et al., 2012).

A more direct way of sigma factor regulation is sequestering by anti-σ factors. These are often co-transcribed with σ factor genes, but unlike σ factors do not have conserved sequences. Anti-σ factors are modular, where the sensory domain can respond to signals designating the release of the σ-anti-σ complex (Campbell et al., 2008). Although inhibition by anti-σ factors is

more prevalent in alternative σ factors, even housekeeping σ factors can be sequestered by this mechanism as in *E. coli* σ^{70}. The anti-σ factor Rsd binds to the σ_2 and σ_4 domains of σ^{70} thereby disabling the interaction with the β subunit of RNAP and the promoter "-35 element" (Jishage & Ishihama, 1998; Patikoglou et al., 2007). Anti-σ factors exert one of two mechanisms of σ sequestration – the helical proteins either insert between the σ_2 and σ_4 domains, or stabilize the σ factor by wrapping around it and pushing the σ_2 and σ_4 domains together, disabling bonds with DNA and RNAP in both cases (**Fig.6**; Paget, 2015).

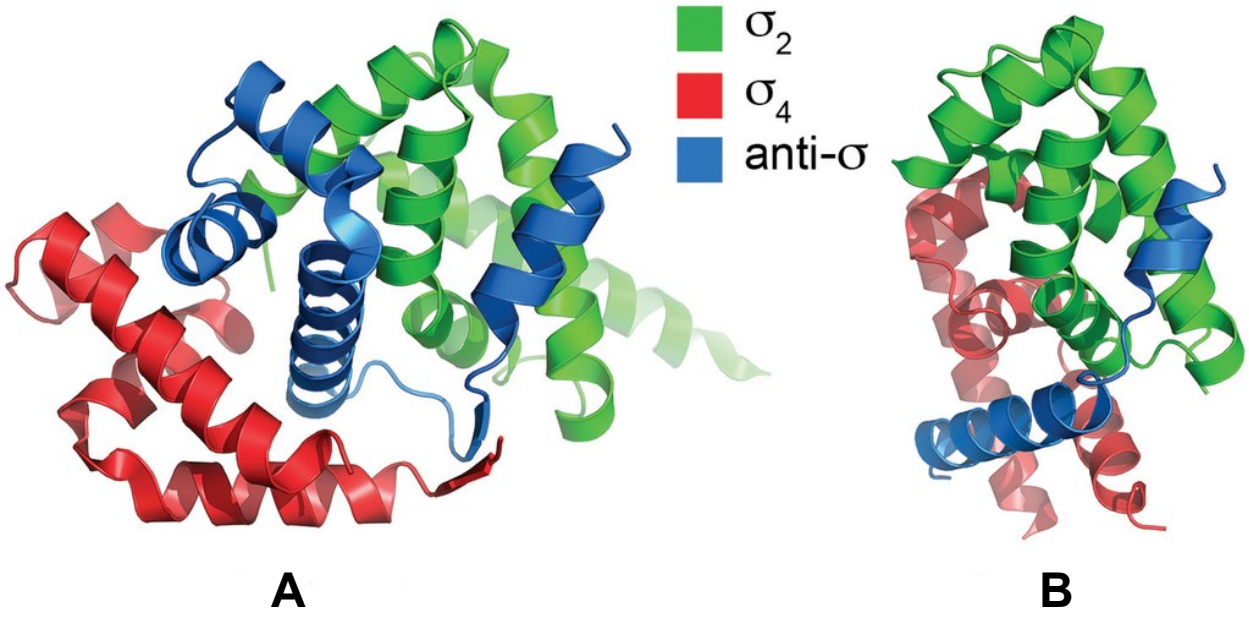

Figure 6. Structural model representation of σ factor inhibition by anti-σ factors. **a)** Inhibition by anti-σ factor (blue) intercalation between the σ_2 (green) and σ_4 (red) domains. **b)** Inhibition by anti-σ factor wrapping around the σ_2 and σ_4 domains. Only the σ-binding domains of the anti-σ factors are shown. Adapted from (Paget, 2015).

2.7 6S RNA

Another way of affecting sigma factor activity is its competitive inhibition with 6S RNA. 6S RNA is a small non-coding RNA (ncRNA) first described in *Escherichia coli* (Brownlee, 1971). Because of its highly conserved secondary structure mimicking the epitope of a melted promoter sequence, it is bound by the σ factor and disables RNAP holoenzyme docking on DNA and transcription initiation. Unlike the anti-σ factors, 6S RNA binds to the whole RNAP holoenzyme and does not interact with the core or σ^{70} alone. The secondary structure of the 6S RNA (of *E. coli*, 184bp) can be described as a central bulge flanked by irregularly paired stem regions forming an A-form RNA helix (**Fig.7**; Kondo et al., 2013). Through mutational analysis of the central bulge it has been found, that the secondary structure, not the sequence, determines the function of 6S RNA (Trotochaud &Wassarman, 2005). The 6S RNA – RNAP holoenzyme association depends largely on the σ^{70} region 4.2 where a stretch of positively charged amino acid residues binds the 6S RNA A-helix (see red square in **Fig.8a**). The association of protein and RNA widens the 6S RNA major groove so that it mimics the B-helix of DNA (σ^{70} 4.2 is the same region involved in binding of the -35 promoter element on DNA; **Fig.5** and **Fig.8b**; Klocko & Wassarman, 2009; Chen et al., 2017). Interestingly, the *E. coli* 6S RNA has no or only nonspecific affinity to other, even closely related, σ factors in complex with RNAP. At the same time, results of Steuten et al., (2013), have shown a possible sequence dependency in addition to the secondary structure requirements

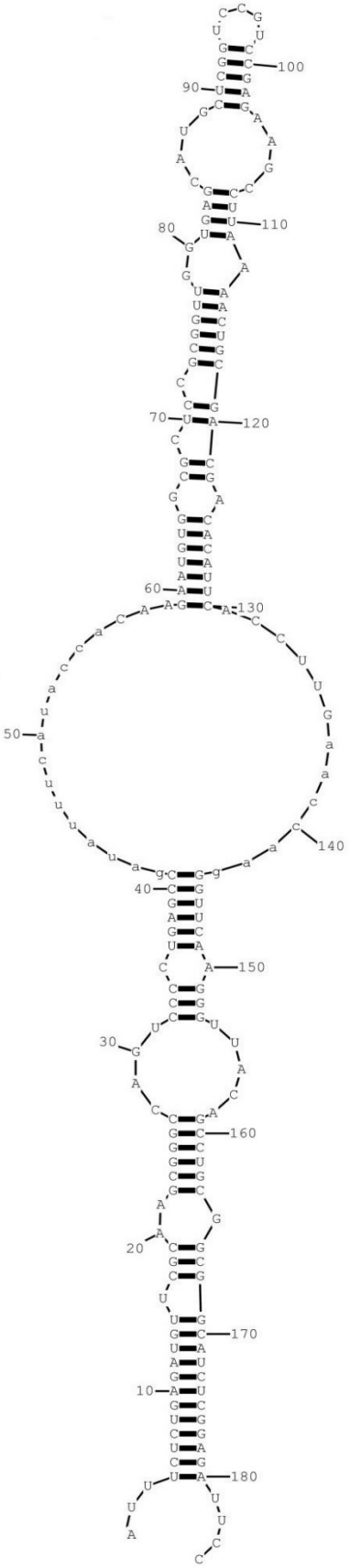

Figure 7. To the right: Secondary structure representation of the *E. coli* 6S RNA (184 bp). Adapted from (Pánek et al., 2008).

for σ^{70}-RNAP recognition. Chen et al., (2017) have confirmed the sequence dependency of certain amino acid residues on the σ^{70} region 4.2. This could indicate a more complex interaction linked to differences of various RNAP holoenzyme preference for 6S RNA.

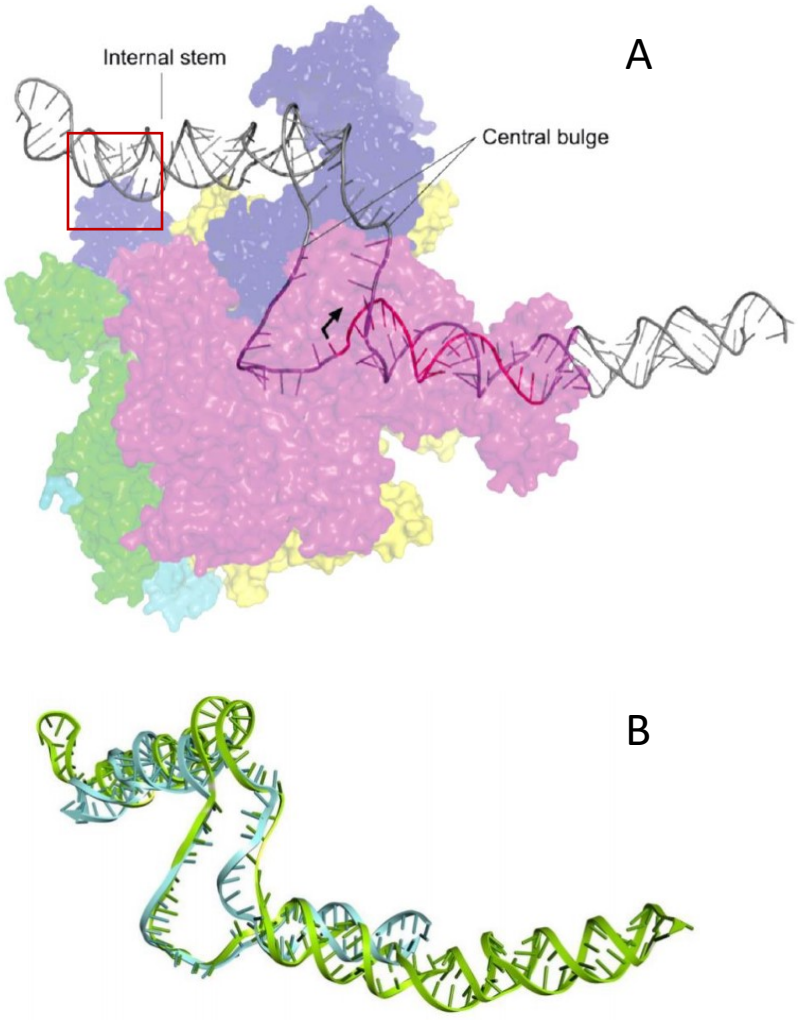

Figure 8. a) A structural model of the *E. coli* 6S RNA-RNAP complex. 6S RNA grey; pRNA template region of 6S RNA, red; The central bulge and internal stem are depicted as well as the pRNA transcription start site (arrow). The *E .coli* σ^{70} (pdb ID: 4igc) is displayed as a transparent surface. σ^{70}, dark blue; β', yellow; β, magenta; αI, green; αII, teal. The red square indicates the σ^{70} 4.2 region and its proximity to the 6S RNA A-helix (internal stem). Adapted from (Steuten et al. 2014). **b)** Overlap of the spatial structures of promoter DNA and 6S RNA derived from complexes. DNA promoter, teal; 6S RNA, green. Adapted from (Steuten et al., 2013).

6S RNA of *E. coli* is transcribed form the only copy of the *ssrS* gene, containing two promoter sequences (Hsu et al., 1985). The transcription is terminated by Rho factor, a protein that binds to C-rich regions of 3' downstream sequences (Graham, 2004; Chae et al., 2011). The proximal promoter (P1) is recognized by σ^{70} and generates a 288bp long 6S RNA precursor. The distal promoter (P2) is recognized by both σ^{70} and the *E. coli* stationary phase sigma factor (σ^{S}), and produces a long, 503bp precursor. Both molecules are processed at the 5'and 3' ends by ribonucleases, and the matured 184bp 6S RNA becomes functional (Kim & Lee, 2004, Chae et al., 2011). Expression of the *ssrS* gene results in stationary growth phase accumulation (10-fold) and the main regulatory implication of 6S RNA in *E. coli* is the inactivation of housekeeping σ70 in order to tip the scales in favour of the alternative σ^{S} (Wassarman & Storz, 2000). Next to RNAP-σ^{70} inhibition, the bound 6S RNA also serves as a template for synthesis of a short (14-20 nt) RNA product – pRNA (Wassarman & Saecker, 2006; Gildehaus et al., 2007). The position of the start site for pRNA synthesis, U44, has been mapped in the proximity of the RNAP active centre (Steuten et al., 2013). pRNA is transcribed as a result of outgrowth from stationary phase and nutrient availability and destabilizes the 6S RNA-RNAP holoenzyme complex to free the inhibition of housekeeping gene transcription (Wassarman & Saecker, 2006). The destabilization is based on perfect complementarity of pRNA to 6S RNA and thus the formation of a pRNA:6S RNA hybrid that triggers refolding of the 6S RNA secondary structure. Consequently, the central bulge loses its single stranded structure by hairpin formation on each side of the bulge, dispatching both the 6S RNA and the σ^{70} from RNAP (Steuten & Wagner, 2012). The same expression profile of 6S RNA, with its highest concentration during stationary phase as in *E. coli*, can be observed in numerous bacteria. However, many bacteria exhibit different expression characteristics demonstrating the functional diversity of 6S RNA. In some phototrophic cyanobacteria, 6S RNA accumulates in the exponential growth phase (*Synechococcus*; Watanabe et al., 1997), or helps with adaptation to the dark-light cycle (Axmann et al., 2007; Rediger et al., 2012). In *Bacillus subtilis*, two different 6S RNAs with divergent function are expressed: 6S-1 RNA, with a similar expression profile as in *E. coli*, and 6S-2 RNA, exhibiting constant expression throughout the cell cycle (Cavanagh & Wassarman, 2013). The expression profile of 6S RNA in human pathogen *Helicobacter pylori* is the same as for 6S-2 RNA of *B. subtilis* (Sharma et al., 2010). Interestingly, in the case of *Burkholderia*, expression levels of 6S RNA change upon stress induced by reactive oxygen species (Peeters et al., 2010).

2.8 The search for 6S-like RNAs

Based on sequence conservation, 6S RNA candidates have been predicted in many different bacterial species. The 6S RNA was found to be as widespread as ncRNAs with important cellular roles, such as tRNA, 5S RNA, SRP RNA and others, pointing out its relevant role (although *ssrS* deletion mutants are viable). Some bacteria had more than one 6S RNA copy (Barrick et al., 2005). Although an analysis of 6S RNA homologues in this study followed the 16S phylogenetic tree, only one predicted homologue was found in Actinobacteria, which could be caused by the uniqueness of Actinobacteria in terms of their GC rich genome and general phylogenetic distance from other bacterial phyla. Later it was found that the genetic neighbourhood and localization (synteny) context can be helpful when searching for poorly conserved homologues (Heueis et al., 2014). This approach, together with other methods was used in further studies searching for ncRNAs. Pánek et al., (2008), performed a blast search of conserved intergenic regions between the two sequenced *Streptomyces* genomes at the time – *S. coelicolor* and *S. avermitilis*. By this approach, the first 6S RNA candidate in streptomycetes was found and its expression confirmed by both northern blot and reverse transcription PCR (RT-PCR). Although many groups have tried identifying ncRNAs in *Streptomyces* so far, there has been a very small overlap in their findings (Pánek et al., 2008; Swiercz et al., 2008; Vockenhuber et al., 2011; Heueis et al., 2014). This emphasizes the importance of wet-lab verification of biocomputational research. In 2010, Pánek et al. came up with a novel approach of finding 6S RNA homologues using *in silico* designed suboptimal secondary structures (i.e. higher than minimal free energy) of common 6S RNAs to create a functional template for the search (**Fig.9**). The group identified two 6S-like RNAs in *S. coelicolor* and one in *Mycobacterium smegmatis* and verified their expression. The candidate from *M. smegmatis* was later found to be Ms1 - a novel ncRNA interacting with RNAP (but not a 6S RNA; Hnilicová et al., 2014). Another study detected one of the predicted *S. coelicolor* 6S RNA candidates as well as its binding to the RNAP core and production of small transcripts, similar to pRNA (Mikulík et al., 2014).

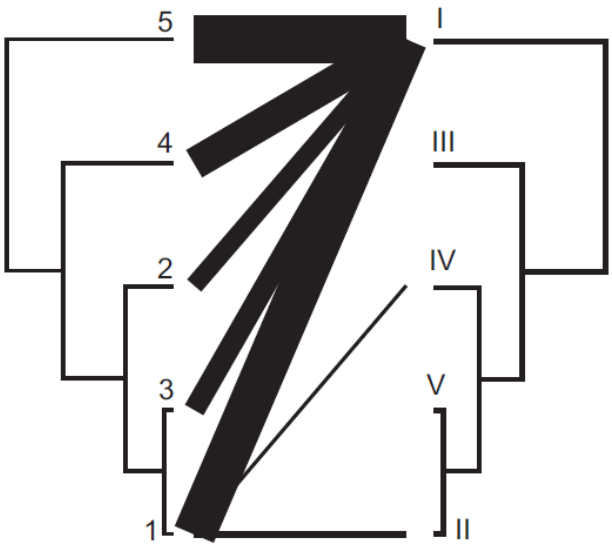

Figure 9. Comparison of sequence homology and structural analogy of suboptimal 6S RNAs structures. 147 6S RNAs were clustered using similarity trees of sequences (left tree) and suboptimal structures (right tree). The sequence similarity scores ware pair-wise BLAST E-values, and RNAdistance scores for the best-scoring suboptimal structures are used in the suboptimal structure similarity tree. The connecting lines indicate positions of sequences and best-scoring structures of single 6S RNAs in both trees. The line width is proportional to the number of 6S RNAs included in the line. Adapted from (Pánek et al., 2010).

3 Aims of the thesis

The main aim of the thesis is the verification of 6S-like RNAs in *Streptomyces coelicolor*. A 6S-like RNA is a small non-coding RNA that inhibits the RNAP holoenzyme by binding to any σ subunit.

Two distinct approaches were set up to achieve this goal:

- RNA coimmunoprecipitation (RNA CoIP) using antibodies against HA-tagged HrdB sigma factor, produced in a mutant *S. coelicolor* strain, and subsequent isolation and sequencing of the co-precipitated RNAs
- Validation of *in silico* predicted *Streptomyce*s 6S-like RNAs

The secondary aim of the thesis was characterizing the found 6S-like RNAs with focus on transcript size and expression profiles (under various growth conditions). The outputs would contribute to the elucidation of the possible regulatory functions of the 6S-like RNA candidates.

4 Materials and Methods

4.1 Bacterial strains

***Streptomyces coelicolor* M145 wild type (WT)**

***Streptomyces coelicolor* M145: *HrdB-HA (epitope tagged)* mutant**: Courtesy of Jiří Vohradský, Laboratory of Bioinformatics at the Institute of Microbiology of the Czech Academy of Sciences

***Escherichia coli* SURE Competent Cells (Stratagene)**: *e14-(McrA-) Δ(mcrCB-hsdSMR-mrr)171 endA1 gyrA96 thi-1 supE44 relA1 lac recB recJ sbcC umuC::Tn5 (Kanr) uvrC [F′ proAB lacIqZΔM15 Tn10 (Tetr)]*. (Genes listed signify mutant alleles. Genes on the F′ episome, however, are wild-type unless indicated otherwise).

***Escherichia coli* TOP 10 (Thermo Fisher)**: *F- mcrA Δ(mrr-hsdRMS-mcrBC) φ80lacZΔM15 ΔlacX74 nupG recA1 araD139 Δ(ara-leu)7697 galE15 galK16 rpsL(StrR) endA1 λ-*

4.2 Plasmids

pTrcHis A (Thermo Fisher): Isopropyl β-D-1-thiogalactopyranoside (IPTG) inducible, multiple cloning site vector with an N-terminal polyhistidine tag, N-terminal Xpress™ epitope for detection of expressed products and an enterokinase cleavage site for fusion tag removal. The vector map is visualized in **Fig.10**.

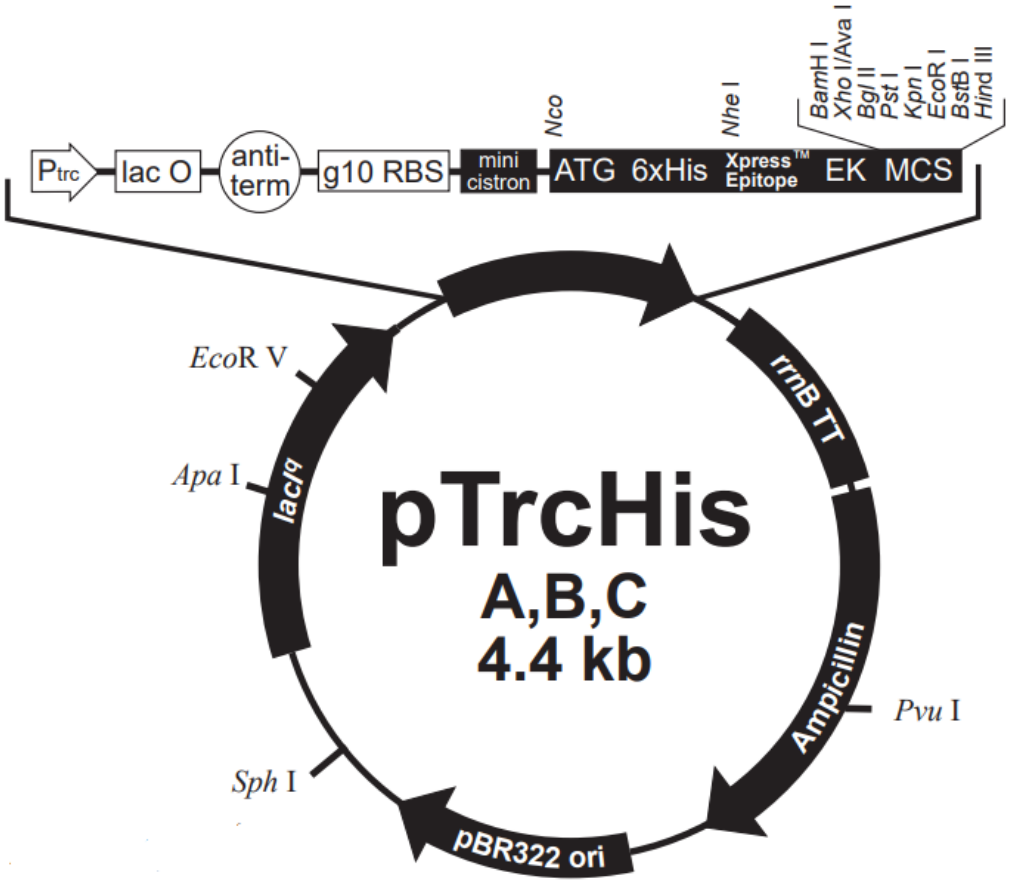

Figure 10. Vector map of pTrcHis A, B, C. (Adapted from Thermo Fisher online catalog; pTrcHis A, B, & C Bacterial Expression Vectors under Documents)

pCR™4-TOPO® TA Vector (Thermo Fisher): IPTG inducible expression vector optimized for direct ligation of Taq-amplified sequences (by means of facilitated ligation with topoisomerase I attached to the cleaved ends of the vector) and subsequent sequencing, with ampicillin and kanamycin resistance cassettes. The vector map is visualized in **Fig.11**.

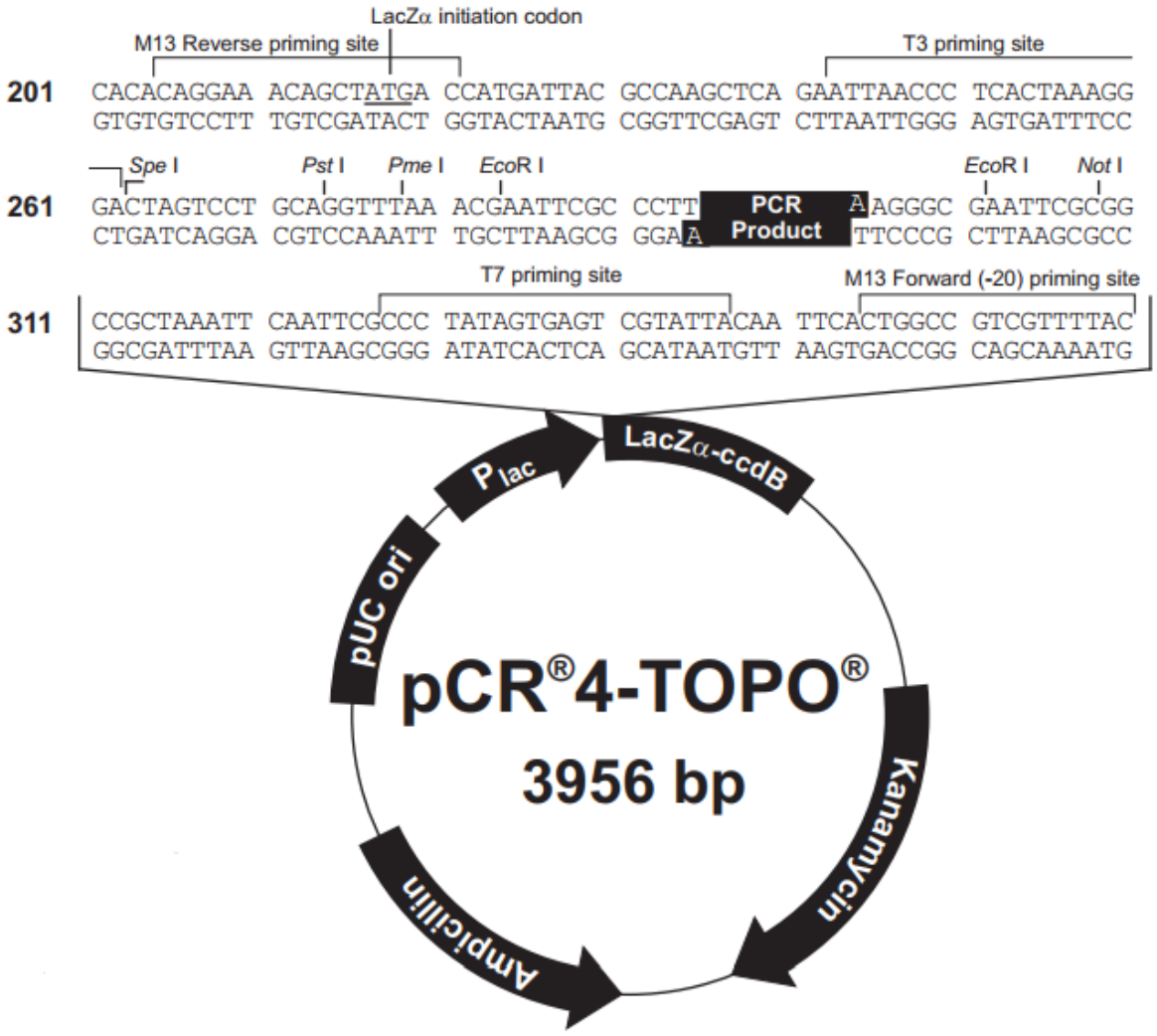

Figure 11. Vector map of pCR™4-TOPO® TA Vector. (Taken from Thermo Fisher online catalog; TOPO® TA for sequencing supplementary information)

4.3 Growth media

R2YE (Kieser et al., 2000) rich medium

103 g Sucrose (Lach-Ner)
0,25 g K_2SO_4 (Lach-Ner)
10,12 g $MgCl_2 \cdot 6H_2O$ (Lach-Ner)
10 g Glucose (Lach-Ner)
0,1 g Difco Casaminoacids (Oxoid)
Fill up to a final volume of 800 ml with Distilled water.
Autoclave and add the following sterile solutions:
10 ml KH_2PO_4 (0,5%; Lach-Ner)
80 ml $CaCl_2 \cdot 2H_2O$ (3,68%; Lach-Ner)
15 ml L-proline (20%; Roth)
100 ml TES buffer (5,73%, pH 7.2; Sigma)
2 ml Trace element solution *
5 ml NaOH (1M; Lach-Ner)
50 ml Difco yeast extract (10%; Oxoid)

* $ZnCl_2$ 40 mg; $FeCl_3 \cdot 6H_2O$ 200 mg; $CuCl_2 \cdot 2H_2O$ 10 mg; $MnCl_2 \cdot 4H_2O$ 10 mg; $Na_2B_4O_7 \cdot 10H_2O$ 10 mg; $(NH_4)_6Mo_7O_{24} \cdot 4H_2O$ 10 mg; 1000 ml Distilled water

Lysogeny Broth (LB; Lennox) medium:

10 g Tryptone (Oxoid)
5 g Yeast extract (Oxoid)
5 g NaCl (Lach-Ner)
1 g Glucose (Lach-Ner)
Fill up to a final volume of 1000 ml with Distilled water.

4.4 Antibiotics

Ampicillin (Applichem) used at a concentration of 50 μg/ml in growth media

Tetracycline (Applichem) used at a concentration of 10 μg/ml in growth media

4.5 Antibodies

Anti-HA High Affinity, Rat monoclonal IgG antibody (Roche)

RNA pol β Antibody, Mouse monoclonal IgG antibody (diluted 500x for WB; Santa Cruz)

IgG from rat serum (Sigma-Aldrich)

IgG from mouse serum (Sigma-Aldrich)

Anti-HA-Peroxidase, High Affinity, Rat monoclonal IgG antibody (diluted 10000x for WB; Roche)

Anti-Mouse IgG (Fc specific)–Peroxidase antibody produced in goat, polyclonal (diluted 10000x for WB; Sigma-Aldrich)

4.6 Sterilization

All autoclavable solutions, glassware, pipettes and microtubes were sterilized at high pressure and temperature higher than 105°C in a pressure cooker. Solutions that could not be autoclaved were filtered through sterile acrodisc syringe filters with pore size 0,2μm. Glassware and tweezers used for aseptic manipulation of any kind or plating bacteria were sterilized by wetting in denatured ethanol (EtOH) and burning over a Bunsen burner.

4.7 Cultivation of bacteria

4.7.1 Cultivation on plates

Spores of the wild type (WT) *Streptomyces coelicolor* strain M145 were plated on solid R2YE medium (Kieser et al., 2000) covered with sterilized cellophane sheets. The plates were incubated at 28,5 °C for 33, 46, and 60 hours respectively. The cultivation time correlates with the growth phase desired – exponential growth, transition phase and stationary phase. The mycelium was harvested with a spatula from the top of the cellophane.

4.7.2 Cultivation in liquid medium

Spores of the WT *Streptomyces coelicolor* strain M145 as well as the mutant strain HrdB-HA - created at the Bioinformatics lab of Jiří Vohradský, Institute of Microbiology, ASCR – were inoculated into 500ml spiked flasks containing 100 ml R2YE liquid growth medium and incubated at 30°C while shaking at 200 rpm. The culture was harvested at 22h incubation time, when 50 ml of culture was used to create the first sample (exponential growth phase, WT T22 and HrdB-HA T22). Another 2,5 ml of the culture were used to inoculate spiked flasks containing 100 ml of fresh R2YE liquid medium to avoid overgrowth of the bacteria. More samples were obtained at 34 and 48 hours respectively.

4.7.3 Cultivation of *Escherichia coli*

Escherichia coli glycerol stocks were thawed on ice and spread on LB media plates containing necessary antibiotics (ampicillin (50 µg/ml), tetracycline (10 µg/ml)). The plates were incubated at 37°C O/N for colonies to form.

4.8 Preparing calcium competent *E. coli* cells

A frozen glycerol stock of *E. coli* SURE Competent Cells (Stratagene; 100 µl) was plated onto a LB plate with tetracycline (10 µl/ml). The plate was incubated at 37°C over-night (O/N). The next day a starter culture of cells was prepared by inoculating 10 ml of LB medium containing tetracycline (10 µl/ml) with a single *E. coli* colony from the LB plate. The culture was grown at 37°C O/N in a shaker at 200 rpm. Next, 200 ml of LB media with tetracycline (10 µl/ml) were inoculated by 2 ml of the starter culture and grown at 37°C in a shaker at 200 rpm until the OD_{600} reached 0,37 (after 1,45 hours; the OD was checked often). After reaching the desired density the culture was immediately put on ice and chilled for 30 minutes with occasional swirling. The cells were kept at 4°C for the rest of the procedure. The 200ml culture was split in four 50ml Falcon tubes (50 ml in each) and centrifuged for 15 minutes at 3000 g force and 4°C. The supernatant was decanted, and the harvested cells were gently resuspended in 20 ml of ice cold $MgCl_2$ solution (100mM). After another centrifugation for 15 minutes at 2000 g force and 4°C the supernatant was removed, 20 ml of ice cold $CaCl_2$ solution (100mM) was added and the tubes were incubated on ice for 30 minutes. The cells were collected by centrifugation for 15 minutes at 2000 g force and 4°C, the supernatant was removed, and the pellets were resuspended in 10 ml of ice cold $CaCl_2$ solution (85mM) with 15% (v/v) glycerol. The four fractions were combined in one fresh and chilled Falcon tube. The cells were collected by centrifugation for 15 minutes at 1000 g force and 4°C and the supernatant was decanted so that the cells could be resuspended in a smaller volume of 2 ml of ice cold $CaCl_2$ solution (85mM) with 15% (v/v) glycerol. The OD_{600} was measured - OD_{600} = 50 – and aliquots of 100 µl were pipetted into sterile 1,5ml microcentrifuge tubes to be stored in -80°C until use.

4.9 Obtaining the RNA samples

4.9.1 RNA Coimmunoprecipitation (RNA CoIP)

Note: the CoIP experiment (including subsequent Western blot, chapter 4.9.1.1, and RNA isolation after CoIP, chapter 4.9.1.2) was conducted at the Bioinformatics laboratory at IMB, CAS and thus established protocols were used, some of which differ from protocols used in experiments conducted at the primary laboratory at IIM, 1.MF. RNA isolation and gel electrophoresis are thus described two times

Streptomycete mycelium in culture harvested from solid and liquid growth media was crosslinked by addition of 38% formaldehyde to a final concentration of 1% (v/v) and cultivated for 30 minutes at 30°C and 200 rpm. The crosslink reaction was stopped by slowly adding chilled glycine to a final concentration of 125mM while mixing the culture. After a 5min incubation at room temperature (RT) the culture samples were transferred into 50ml tubes and centrifuged for 5 minutes at 4000 g force and 4°C. The pellet was washed four times with cold phosphate buffered saline (PBS) until loosened properly and centrifuged for 5 minutes at 4000 g force and 4°C. The crosslinked and washed pellets were deep-frozen with liquid nitrogen and stored at -80°C.

The frozen mycelium pellets were thawed on ice and 5 ml of RIPA buffer supplemented with RNase inhibitor (RNasin® Plus RNase Inhibitor; Promega; 800 U/50 ml of buffer) and protease inhibitor (cOmplete™ Mini EDTA-free Protease Inhibitor Cocktail 7x; 150 µl/50 ml of buffer) was added to each pellet. For each *Streptomyces* strain (WT and HrdB-HA) and cultivation means (liquid or solid) the different growth cycle samples (T22, T34, and T48 for liquid media and T34, T46, and T60 for solid media) were joined into one sample that was further used for the CoIP procedure. The samples were sonicated as follows: samples from liquid cultivation for 4 cycles of 10s sonication with 0,5 amplitudes and following a 1-minute chill on ice, samples from solid cultivation (on plates) 4 cycles of 15s sonication with 0,5 amplitudes and following a 1-minute chill on ice. The lysates were then centrifuged in a Beckman centrifuge with rotor JA.25-50 for 20 minutes at 20 000 g force and 4°C. The supernatant was transferred info fresh and chilled 50ml tubes.

To dispose of non-specific debris reacting with agarose beads the protein lysates were precleared. Protein-G Plus Agarose (Santa Cruz) beads were preequilibrated by a 3x wash with 1

ml RIPA buffer, resuspension and centrifugation for 30 seconds at 11000 g force. After adding 25 µl of agarose beads to each lysate sample (20 ml) these were incubated for one hour at 4°C. The precleared lysates were centrifuged for 2 minutes at 9000 g force and 4°C to separate then from the agarose beads. Next, the amount of protein in the lysates was measured using the Pierce BCA Protein Assay Kit (Thermo Fisher) and the lysates were divided into samples and controls for immunoprecipitation.

Each immunoprecipitation sample contained an amount of lysate with 4 mg of protein. For this amount, 2 µg of primary antibody was added to the samples and these were incubated at 4°C over-night (O/N). Control samples, later used for western blot (WB), contained half the amount of input protein and were immunoprecipitated with only 1 µg of primary antibody. The next day, Protein-G Plus Agarose (Santa Cruz) beads were preequilibrated with a 3x wash with 1 ml RIPA buffer, resuspension and centrifugation for 30 seconds at 11000 g force. Incubation of samples with 50 µl of beads added in each continued for 5 hours at 4°C. Centrifugation for 30 seconds at 11000 g force and 4°C followed for the beads to settle. Then they were washed as follows:

3x 1 ml RIPA buffer
4x 1 ml LiCl Wash buffer
2x 1 ml RIPA buffer
2x 1 ml TE buffer

After the last wash 200 µl of elution buffer was added to each sample and these were frozen to ease the elution of the RNA-protein coimmunoprecipitate from the beads. The samples then were thawed on ice and 1 µl (40 U) of RNase inhibitor was added during the process. The elution was finished by a 15-minute incubation at 50°C (samples for WB analysis were eluted in 40 µl of elution buffer and 10 µl of formamide loading dye by heat - 90°C, 15 min). The samples were then centrifuged for 5 minutes at 14 000 g force, the supernatant was transferred to new RNase free microcentrifuge tubes. The RNA-protein coimmunoprecipitates were de-crosslinked by addition of NaCl (final concentration 200mM), 2 µl Proteinase K (1,5 U; Thermo Fisher) and incubation at 50°C for one hour while adding 1 µl (40 U) of RNase inhibitor every 15 minutes. The de-crosslinked samples were further used for RNA isolation.

PBS: 137mM NaCl, 2,7mM KCl, 10mM $Na_2HPO_4 \cdot 2H_2O$, 1,8mM KH_2PO_4 (pH 7,4 for 1x dilution)

RIPA buffer: 50mM Tris (pH 8 – adjusted with HCl), 150mM NaCl, 0,5% (v/v) Triton, 0,5% (w/v) Sodium deoxycholate, 0,075% (w/v) SDS, 1mM EDTA

LiCl Wash buffer: 100mM Tris (pH 8,5 – adjusted with HCl), 0,5M LiCl, 0,5% (v/v) Triton, 0,5% (w/v) Sodium deoxycholate, 1mM EDTA

TE buffer: 10mM Tris (pH 8 – adjusted with HCl), 10mM EDTA

Elution buffer: 50mM Tris (pH 8 – adjusted with HCl), 10mM EDTA

Note: Protease Inhibitor Cocktail (7x) 150 µl/50 ml was added to RIPA buffer, 100 µl/50 ml added to LiCl Wash buffer, 50 µl/50 ml added to TE buffer. RNase inhibitor (800U/50 ml) was added to all buffers. Elution buffer contained a higher concentration of RNase inhibitor (200U/ml).

4.9.1.1 Western blot (as a control for IP)

4.9.3.1.1 Protein SDS-PAGE with precast gels

Polyacrylamide gradient gels NuPAGE Bis-Tris Mini Gels (Novex) were installed into the vertical electrophoresis tray and the 2x NuPAGE SDS running buffer (Novex) diluted to 1x concentration was poured inside. Protein samples were mixed with 5x formamide loading buffer and denatured at 99°C for 15 minutes before loading 25 µl of sample on the gel. Six µl of the prestained protein marker (7-175 kDa; NEB) was also loaded. The apparatus was plugged into a voltage source and electrophoresis was run for 30 minutes at 200 V. The gel was released from the apparatus, washed in the running buffer and further used for Western blot analysis.

4.9.3.1.2 Blotting proteins from PAGE gel on solid surface

Electroblotting was used to transfer proteins from the gel on a microporous polyvinylidene difluoride membrane. Pieces of chromatography paper (Whatman), plastic sponges and the gels were all soaked in blotting buffer (48mM Tris, 39mM glycine, 0,0375% (w/v) SDS, 20% (v/v) MetOH) while the polyvinylidene difluoride membranes were activated in pure methanol

(MetOH). One sponge was covered with three pieces of Whatman paper and the gel which was covered with the polyvinylidene difluoride membrane. On top came three more pieces of Whatman paper and a second sponge. The “sandwich” structure was secured with two plastic clamp pieces and installed into a wet electroblotting machine filled with blotting buffer. The apparatus was run for 30 minutes at 260 mA. The success of the electroblot was checked by observing the transferred protein size marker on the membrane. The membrane was used right away for immunodetection of CoIP targets.

4.9.3.1.3 Immunodetection of protein targets

Membranes with blotted proteins were submerged in a solution of 5% milk in PBS-T and incubated for 1hour on a shaker to block the membrane. Two washes with phosphate buffered saline + 0,05% (v/v) Tween20 (PBS-T) followed and the primary antibody diluted in a solution of PBS-T with 1,5% milk was added, and the membranes were incubated for 1,5 or 3 hours. Next the membranes were washed with PBS-T two times and the secondary antibody was added (also diluted in a solution of PBS-T with 1,5% milk). The incubation with the secondary antibodies conjugated with horse radish peroxidase (HRP) were carried out in the dark. The treated membranes were washed again two times in PBS-T, incubated with Super signal® West Pico chemiluminescent substrate (Thermo Fisher) and exposed to photographic film in a dark casette for 15 s, 1 min, 2 min and 10 min. The films were developed in an automatic film developer and a digital image of the films was taken with a scanning machine.

4.9.1.2 RNA isolation following CoIP

Samples ready for RNA isolation were mixed with Phenol-Chloroform-Isoamylalcohol (1:1:24, pH6,6) in a volume ratio 1:1, vortexed for 2 minutes and centrifuged for 15 minutes at 14500 g force and 4°C. The upper aqueous phase was carefully transferred into fresh microcentrifuge tubes and the Phenol-Chloroform-Isoamylalcohol isolation process was repeated one more time. The aqueous phase containing the RNA was precipitated by adding ethanol (EtOH) 96% in a volume ratio 2,2:1, sodium acetate (NaAc; 3M) in a volume ratio 0,1:1 and 1 µl (40 U) of RNase inhibitor. The mixture was precipitated at -80°C for 5 minutes and another 25 minutes at -20°C. Centrifugation for 15 minutes at 14500 g force and 4°C created an RNA pellet. The supernatant was removed, and the pellet was washed once with 0,5 ml chilled isopropanol (-20°C) and once with 0,5 ml 70% EtOH (-20°C). Centrifugation for 10 minutes at 14500 g force and 4°C and subsequent removal of the supernatant followed each wash. The remaining EtOH was removed with a small pipette tip, the microcentrifuge tubes were left open shortly for the EtOH to fully dissipate and the pellets were dissolved in 30 µl nuclease free water (Gibco) containing 3 µl (120 U) of RNase inhibitor.

The last step in purifying the RNA was treatment with DNase I. For this we used the DNA-free Kit (Ambion). The RNA samples were incubated with DNase I buffer and enzyme for 30 minutes at 37°C. To stop the reaction the DNase inactivation reagent was added, and the microcentrifuge tubes were lightly mixed for 2 minutes at RT. The reagent was separated from the sample by centrifugation for 1,5 minutes at 10000 g force and the samples (supernatant) were transferred into fresh microcentrifuge tubes for storage at -80°C. The RNA concentration was measured by Qubit 3 Fluorimeter using a high sensitivity detection kit and alternatively by nanodrop.

4.9.2 RNA isolation (total RNA from plates)

The cultivated *Streptomyces coelicolor* WT strain M145 mycelium, grown on Petri dishes with R2YE solid medium covered with cellophane, was harvested with a sterilized spatula and transferred into chilled 50ml Falcon tubes containing 3 grams of 0,5mm glass beads. Immediately, ice cold TRIzol™ Reagent (Ambion) was added to the Falcon tubes (1 ml for 100 mg of mycelium). The samples were homogenized by vortexing with the glass beads for 30 seconds with a subsequent 30 second chill on ice. The vortex – chill cycle was repeated eight times for each tube. The homogenized solution was transferred to a new Falcon tube and 3 ml of fresh TRIzol™ Reagent were used to rinse the beads and added to the new tube which was frozen to -20°C until all samples were ready for further processing.

After thawing all samples on ice, the microcentrifuge tubes were centrifuged for 2 minutes at 14000 g force and 4°C. The mycelium debris settled on the bottom and the supernatant was transferred to a new Falcon tube and chilled on ice for 5 minutes. Next, 0,2 ml of chloroform per 1 ml of TRIzol™ Reagent was added to the tubes. The solution was mixed, chilled on ice for 3 minutes and centrifuged for 15 minutes at 12000 g force and 4°C. The upper aqueous phase was transferred to microcentrifuge tubes and 0,5 ml of chilled isopropanol per 1 ml of TRIzol™ Reagent was added. The solution was mixed and incubated at RT for 10 minutes to precipitate the RNA. After centrifugation for 10 minutes at 12000 g force and 4°C the supernatant was removed, and the gel-like pellet was washed in 1 ml of ice cold ethanol. At this step, a part of the material was stored at -80°C.

The microcentrifuge tubes with the pellet in ethanol were vortexed and centrifuged for 5 minutes at 7500 g force and 4°C. The supernatant was discarded, and the rest of the ethanol was removed with a 10ml pipette tip. The RNA pellet was resuspended in 40 µl of nuclease free water (Gibco) and 5 µl (200 U) of RNase inhibitor (RiboLock RNase Inhibitor; Fermentas) was added. After measuring the RNA concentration and purity on Nanodrop the RNA could be further treated by DNase I (200U/µl; Invitrogen). The reaction design:

50 µl RNA
25 µl DNase I buffer (10x)

10 µl DNase I enzyme (2000 U)

<u>165 µl nuclease free H_2O</u>

250 µl final volume **30min, 37°C**

The DNase treated RNA was chilled on ice and extracted with 1:1 Phenol-Chloroform-Isoamylalcohol (25:24:1; pH 4; AppliChem). The mixture was vortexed for 30 seconds and centrifuged for 10 minutes at 14000 g force and 4°C. The upper phase containing the RNA was transferred to a fresh tube and a volume of 1/10 of 3M sodium acetate (pH 5,5) was added in addition to 2,5 volumes of 96% ethanol. In this mixture, the RNA was precipitated in the freezer (-20°C) over night (O/N).

After centrifugation of the precipitate for 10 minutes at 14000 g force and 4°C the RNA pellet was washed with 1 ml of ethanol (75%) by flinching. Finally, the sample was centrifuged for 5 minutes at 14000 g force and 4°C, the pellet was dried by removing residual ethanol and dissolved in 40 µl of nuclease free water (Gibco) and 5 µl (200 U) of RNase inhibitor was added. The RNA concentration and purity were checked on the nanodrop Biospectrometer (Eppendorf) and the samples were stored at -80°C.

4.10 Exploring the RNA samples

4.10.1 Poly-adenyl(A) Tailing of RNA

The purified isolated RNA of unknown sequence was poly(A) tailed so that adaptors permitting further RNA manipulation could be attached. The *E. coli* Poly(A) Polymerase enzyme (NEB) was used to tail our RNA samples. The reaction was designed as follows:

15 µl RNA sample (in nuclease free H_2O)
2 µl *E. coli* Poly(A) Polymerase Reaction Buffer 10x
2 µl ATP (10mM)
1 µl Poly(A) Polymerase Enzyme (5 U)
20 µl final volume **30 min, 37°C**

The reaction was stopped by directly proceeding to the cleanup step carried out by the QIAquick Nucleotide Removal Kit (Quiagen) according to the manufacturers protocol. The purified poly(A) tailed RNA was eluted in nuclease free H_2O (Gibco) preheated to 60°C and was stored in -80°C until further use.

4.10.2 Primer Extension

RNA samples were polyadenylated by the *E. coli* Poly(A) Polymerase. Primers used for hybridization with the end labeled RNA were a poly(T) primer (NV18xT) and a poly(T) primer with an additional adaptor sequence (NV18xT+32N). In the case of *in silico* predicted sequences, reverse complementary primers were labeled. Firstly, the primers had to be labeled on their 5'-ends by a phosphorus isotope [$\gamma - {}^{32}P$]. For that the T4 polynucleotide kinase (PNK) was used to add [$\gamma - {}^{32}P$]-ATP to the primers. The reaction was as follows:

2 µl primer (100µM)
2 µl reaction buffer A [forward reaction] 10x (Thermo Fisher)
0,5 µl [$\gamma - {}^{32}P$]-ATP (10 µCi/µl)
1 µl T4 PNK enzyme (10 U/µl; Thermo Fisher)
14,5 µl nuclease free H_2O (Gibco)
20 µl final volume **1h, 37°C**

Next, the labeled primers were purified by the QIAquick Nucleotide Removal Kit (Quiagen) according to the manufacturers protocol. The isotope labeled primers (primers*) then were used to reverse transcribe the RNA. The reverse transcription (RT) reaction:

2 µl RNA
4 µl dNTP mix (each at 2,5mM)
2 µl primer* (10µM)
4 µl Prime Script RT Buffer (5x)
1 µl RNase inhibitor (40 U)
1 µl Prime Script Reverse Transcriptase (200 U; Takara)
6 µl nuclease free H_2O (Gibco)
20 µl final volume **1h, 42°C**

The synthesized cDNA was frozen to -20°C and later run on a denaturing polyacrylamide gel. The gel was dried between cellophane sheets O/N (or alternatively dehydrated in (95% v/v) ethanol; Fadouloglou et al., 2000), sealed in sheet protector and was exposed to a storage phosphor screen placed in an autoradiography cassette. The resulting image was taken by the Typhoon FLA 7000 (GE Life Sciences) laser scanner at the Laboratory of Chemical Biology and Catalysis lead by Jiří Míšek, Department of Organic Chemistry at the Faculty of Science.

4.10.3 SMARTer PCR cDNA synthesis (Clontech)

Polyadenylated RNA samples were used as an input for reverse transcription using the CDS primer (3' SMART CDS Primer II A) together with the SMART II oligonucleotide adaptor (SMARTer II A Oligonucleotide). The method takes advantage of the terminal transferase activity of the SMARTScribe reverse transcriptase, where the enzyme adds a few nucleotides to the end of the transcribed sequence. The SMARTer oligonucleotide adaptor base-pairs with the overhang stretch and extends the template which is subsequently replicated by the reverse transcriptase. The flanked ssDNA is then amplified by long distance PCR using the CDS PCR primer (5' PCR Primer II A) which binds to the ssDNA sequence on both 3' and 5' end flanking regions added in the first reaction (**Fig. 12**).

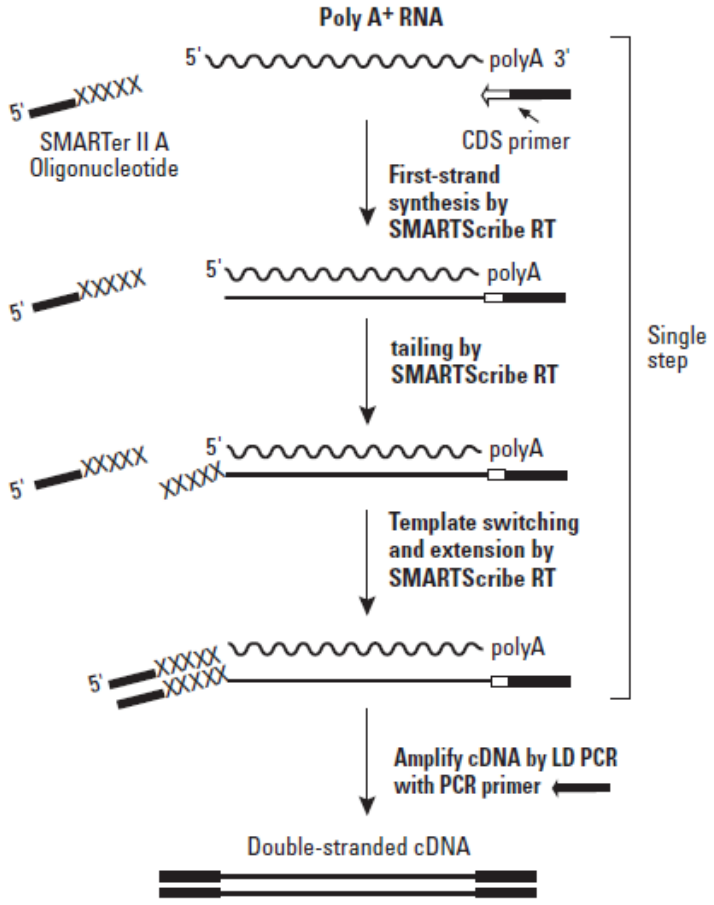

Figure 12. Flowchart of SMARTer cDNA synthesis. The SMARTer II A Oligonucleotide, 3' SMART CDS Primer II A, and 5' PCR Primer II A all contain a stretch of identical sequence. (Adapted from SMARTer™ PCR cDNA Synthesis Kit User Manual, PT4097-1, Clontech)

The reverse transcription reaction was designed with respect to the SMARTer™ manual:

1 or 2 µl polyA$^+$ RNA
1 µl SMARTer II A Oligonucleotide
1 µl 3' SMART CDS Primer II A
1 or 2 µl nuclease free H_2O (Gibco)
5 µl final volume **10 min, 72°C**

After incubation, the reaction was placed on ice for 2 minutes and the following mix was added:

2 µl First-Strand Buffer (5x)
1 µl dNTP mix (each at 2,5mM)
1 µl SMARTScribe™ Reverse Transcriptase (100 U)
10 µl final volume **1 h, 42°C**

The reverse transcribed sequences with added flanking regions containing the 5' PCR Primer II A complementary reads were amplified by PCR in Thermal Cycler TC-24/H (Bioer Technology Co., Ltd.; the amplification program can be found in the box at the right side of the reaction design):

2 µl RT reaction containing ssDNA
2,5 µl Complete PCR Buffer (10x)
2 µl dNTP mix (each at 2,5mM)
2 µl 5' PCR Primer II A
0,5 µl Taq Polymerase (5 U)
16 µl nuclease free H_2O (Gibco)
25 µl final volume

	95°C 3 min
40x	**95°C 15 sec**
	65°C 30 sec
	68°C 1 min
	68°C 5 min
	4°C ∞

At the end of the PCR reaction, the samples were cooled to 4°C and the amplified DNA was visualized by agarose electrophoresis. The cDNA was further stored at -20°C.

4.10.4 One-step RT-PCR

The primers were designed 18-20mers with no or low chance of creating cross dimers. The melting temperature difference of primer pairs was lower than 2°C. The primers were designed manually and analyzed online with the Multiple Primer Analyzer from Thermo Fisher Scientific (available at https://www.thermofisher.com/, 9th November 2016). The full predicted sequences can be found in the supplementary data.

The one-step reverse transcription PCR (RT-PCR) reaction was composed of two established protocols. In the first step, the RNA with reverse transcriptase buffer (RT Buffer) and the primers was denatured, only after that the enzyme mix (reverse transcriptase and polymerase) are added so that RT-PCR can begin. The reaction was prepared on ice. Scheme of the reaction:

2 µl RNA (1µg +)
5 µl Prime Script RT Buffer (5x)
1 µl primer mix (each at 10µM)
9 µl nuclease free H_2O (Gibco)

5 min, 65°C

+

2,5 µl dNTPs (each at 2,5mM)
2,5 µl High GC Enhancer (5x, from OneTaq® Polymerase, NEB)
2,5 µl bovine serum albumin (BSA, 1 mg/ml)
0,2 µl Super Taq™ Polymerase (5 U/µl)
0,3 µl Prime Script Reverse Transcriptase (200 U; Takara)
25 µl final volume **40 min, 49°C**

Right after the reverse transcription step (40 min, 49°C) the reaction was heated up to loosen the bonds between RNA and its complementary reverse transcribed DNA and amplification was carried out in Thermal Cycler TC-24/H (Bioer Technology Co., Ltd.) according to the outlined chart:

	94°C 5 min
	94°C 30 sec
30x	**X°C 30 sec**
	68°C 45 sec
	68°C 5 min
	4°C ∞

Products of the one-step RT-PCR reaction are visualized by agarose electrophoresis.

4.10.5 Northern blot

To determine the true size of the predicted 6S-RNA sequences, total *S. coelicolor* RNA was run on a 6% denaturing polyacrylamide gel (Electrophoresis), and analyzed by Northern blot. Electroblotting was used to transfer the RNA from the gel on a microporous, positively charged Nylon membrane (SensiBlot Plus Nylon Membrane; Fermentas). Pieces of chromatography paper (Whatman), the Nylon membrane and the gel were all soaked in Transfer Buffer (NorthernMax®, Ambion). The transfer stack was assembled on the bottom electrode of a Semi-dry transfer unit (TE77XP, Hoefer) in the following order: 3 pieces Whatman paper, membrane, gel, 3 pieces Whatman paper. A small amount of Transfer Buffer was poured additionally on top of the "sandwich structure" to keep it wet and the apparatus was closed and run for 45 minutes at 240 mA. By exposure to UV light twice for 3 seconds at 120 mJ/cm^2 in the HL-2000 HybriLinker^{TM} Hybridization Oven/UV Crosslinker (UVP) the blotted RNA was crosslinked to the still-wet membrane and stored at -20°C until used for hybridization.

As hybridization probes we used isotope labeled oligonucleotides (PCR rev. primers used for the RT-PCR experiment and probe complementary to *S. coelicolor* 5S rRNA). The T4 polynucleotide kinase (T4 PNK) was used to add [γ – ^{32}P]-ATP to the 5' ends of the probes. The reaction was as follows:

2 µl primer (100µM)
2 µl Reaction Buffer A [forward reaction] 10x (Thermo Fisher)
0,5 µl [$\gamma - {}^{32}P$]-ATP (10 µCi/µl)
1 µl T4 PNK enzyme (10 U/µl; Thermo Fisher)
14,5 µl nuclease free H_2O (Gibco)
20 µl final volume **1h, 37°C**

The labeled probes were purified by the QIAquick Nucleotide Removal Kit (Quiagen) according to the manufacturers protocol and eluted into 80 µl nuclease free H_2O (Gibco). These were stored in -20°C. The membranes were prehybridized in hybridization tubes with 15 ml ULTRAhyb Buffer (preheated to 68°C; NorthernMax®, Ambion) for 50 minutes at 42°C. Next, the isotope labeled probes were denatured by heat treatment at 90°C for 2 minutes and 20 µl of probe was added to the ULTRAhyb Buffer in the hybridization tubes. The membranes were hybridized O/N at 42°C and washed in 15 ml Low Stringency Wash Solution #1 (NorthernMax®, Ambion) two times for 5 minutes. The membranes were further sealed in sheet protector and exposed to a storage phosphor screen placed in an autoradiography cassette. The resulting image was obtained by Typhoon FLA 7000 (GE Life Sciences).

4.10.6 Quantitative PCR (qPCR)

To determine the expression profiles of the expressed 6S-RNA predictions, RT reaction was used to convert RNA from three different growth phases to cDNA. The cDNA was subsequently amplified in a light cycler (Applied Biosystems 7300 Real-Time PCR System) using Maxima SYBR Green/ROX qPCR Master Mix (2X; Thermo Fisher) and the same primers as in the one-step RT-PCR experiment. After optimization, 5 ng of input RNA was used for each RT reaction. Aliquots were further used for duplicates of the quantitative amplification reaction. The RT reaction was carried out on ice and as indicated below:

1 µl RNA (5ng)
2,5 µl Prime Script RT Buffer (5x)
0,3 µl reverse complementary primer (10µM)
1,5 µl dNTPs (each at 2,5mM)
7 µl nuclease free H_2O (Gibco)
5 min, 65°C

+

0,3 µl Prime Script Reverse Transcriptase (200 U; Takara)

12,5 µl final volume **40 min, 49°C**

10 min, 95°C

From the RT reaction, 2 µl were diluted by 8 µl of nuclease free H_2O (Gibco). 5 µl were then used as input cDNA for each sample duplicate. The qPCR reaction was prepared at RT and is outlined below:

5 µl cDNA
12,5 µl Maxima SYBR Green/ROX qPCR Master Mix (2X)
0,3 µl primer mix (each at 10µM)
7,2 µl nuclease free H_2O (Gibco)
25 µl final volume

	95°C 10 min
40x	**95°C 15 sec**
	X°C 30 sec
	72°C 30 sec
	72°C 5 min
	4°C ∞

The amplification curves were analyzed, C_t values were exported, and the relative expression of samples was calculated using the $\Delta\Delta C_t$ method (Haimes & Kelley, 2010). The amplified DNA was stored at -20°C.

4.11 Looking at the products

4.11.1 Electrophoresis

4.11.1.1 Agarose Gel Electrophoresis

1-2% agarose gels were prepared by mixing the appropriate amount of agarose (Sigma) with the desired volume of Tris-borate-EDTA (TBE) buffer (depending on the gel size; e.g., 0,6 g of agarose with 60 ml TBE for a 1% gel) and boiling the solution in a microwave until the agarose is dissolved. After cooling the agarose solution to ~50°C, GelRed™ nucleic acid stain was added (8 µl/100 ml of solution; 10000x; Biotium), mixed, and the solution was poured into prepared casting trays with combs. After the gel had solidified the comb was removed and the samples were mixed with Loading Dye (6x) to a final concentration of 1x Loading Dye and loaded together with a DNA molecular weight Marker (O'Gene Ruler; Thermo Fisher). The apparatus was plugged into a voltage source and electrophoresis was run for 40-60 minutes at 12 V/cm of gel. After the electrophoresis was completed, the gel was placed on an UV transilluminator and photographed.

TBE buffer: 89mM Tris (pH 7,6 – adjusted with HCl), 89mM boric acid, 2mM EDTA

4.11.1.2 Polyacrylamide gel electrophoresis (PAGE)

6% polyacrylamide denaturing gels were made by mixing 8 ml of 6% acrylamide solution containing Urea (6M) and MOPS Buffer (0,2M; NorthernMax®, Ambion) with 40 µl ammonium persulfate (10%) and 8 µl Tetramethylethylenediamine. RNA or DNA samples were mixed with formamide loading dye (5x) to a final concentration of 1x formamide loading dye and denatured at 65°C for 15 min before they were loaded on the gel together with 4 µl of DNA molecular weight Marker. The gel was run in MOPS Buffer at 120V (12V per centimeter of gel) for 1 hour. After the gel was taken out of the apparatus, the marker lane was cut off and put in 15 ml MOPS Buffer containing 3 µl of GelRed™ nucleic acid stain where it was incubated for 10 minutes, washed in fresh MOPS Buffer for 5 minutes and photographed on an UV transilluminator. The gel was washed in MOPS Buffer for 5 minutes before carrying on to subsequent procedures.

4.11.2 Cloning of cDNA products

4.11.2.1 Preparation of inserts

The cDNA products (10 µl of the PCR reaction) were run on a 1,5% agarose gel. The desired product gel bands were excised using a scalpel and placed in nuclease free microcentrifuge tubes. The products were extracted from the gel using the GeneJET Gel Extraction Kit (Thermo Fisher) and eluted into 40 µl of nuclease free H_2O (Gibco). The purified products were stored at -20°C. Since all the products were amplified by Taq polymerase, they had single 3'-adenine overhangs.

4.11.2.2 Manual TA cloning

We obtained the pTrcHis A plasmid (Thermo Fisher) from Protean, s. r. o. The vector was already cut at the XhoI restriction site, treated with Klenow fragment to blunt the ends and dephosphorylated to disable circularization. In our laboratory, the plasmid was T-tailed by the following reaction using deoxythymidine triphosphate (dTTP; adapted from Marchuk et al., 1991):

3 µl pTrcHis A plasmid (~500ng)
10 µl Taq Polymerase PCR Complete Buffer (10x)
20 µl dTTP (10mM)
1 µl Taq Polymerase enzyme (5U/µl)
16 µl nuclease free H_2O (Gibco)
50 µl final volume **1 hour, 70°C**

Right away the ligation reaction was mixed. The vector/insert ratio was 1:3.

4 µl T4 DNA Ligase Buffer (5x)
7 µl insert (PCR product; 150 ng)
5 µl vector (straight from T-tailing reaction; 50 ng)
1 µl T4 DNA Ligase (1U/µl)
8 µl nuclease free H_2O (Gibco)
25 µl final volume **O/N, 14°C**

The ligation reaction was immediately used for transforming *E. coli* SURE Competent Cells. 100 µl aliquots were thawed on ice. Just when the cells started to turn into an icy mash 1,5 µl of the ligation reaction was mixed into the mash with a pipette. The cells were put on ice for 30

minutes and then heat-shocked at 42°C for 45 seconds. Following a two-minute rest on ice, 0,9 ml of fresh LB medium with no antibiotics was added to the cells and these were incubated at 37°C for one hour while swiftly rotating in the hybridization oven. Finally, the cells were plated on LB plates containing ampicillin (50 µg/ml) and tetracycline (10 µg/ml) and incubated O/N at 37°C.

The success of TA cloning was inspected by restriction analysis. 10 ml of LB medium containing ampicillin (50 µg/ml) and tetracycline (10 µg/ml) were inoculated by single colonies of the transformed cells and incubated at 37°C and 190 rpm O/N. The cultures were centrifuged 5 minutes at 6000 g force, the supernatant was discarded, and the cells were used for minipreparation of plasmid DNA with the GeneJET Plasmid Miniprep Kit (Thermo Fisher). The plasmid DNA was used in the endonucleolytic cleavage reaction:

7 µl nuclease free H_2O (Gibco)
2 µl NEBuffer™ 3.1 (10x)
10 µl plasmid DNA (~ 0,5 µg)
0,5 µl BamHI (5 U; Thermo Fisher)
0,5 µl EcoRI (5 U; Thermo Fisher)
20 µl final volume **1,5 hours, 37°C**

The restriction analysis products were visualized by agarose electrophoresis.

4.11.2.3 TOPO TA Cloning Kit (Thermo Fisher)

Since our PCR products had identical forward and reverse primer sequences attached it was necessary to clone them in a plasmid (pCR™4-TOPO TA Vector) that contained its own pair of suitable primer sequences. The ligation reaction:

1,5 µl insert (PCR product; 30 ng)
1 µl Salt Solution (1,2M NaCl; 0,06M $MgCl_2$)
0,5 µl pCR™4-TOPO TA Vector
3 µl nuclease free H_2O (Gibco)
6 µl final volume **5 min, RT**

Right after the incubation time has passed, 1,5 µl of the ligation reaction were used to transform 25 µl of TOP 10 *E. coli* competent cells. The cells were thawed, and the ligation reaction swirled into the still icy cells. After a 20-minute incubation on ice the cells were heat-shocked at

42°C for 30 seconds. Following a two-minute rest on ice, 250 µl of fresh LB medium with no antibiotics was added to the cells and these were incubated at 37°C for one hour while rotating in the hybridization oven. Finally, the cells were plated on LB plates containing ampicillin (50 µg/ml), X-gal (40 mg/ml) and IPTG (0,1M) and incubated O/N at 37°C.

Blue-white selection was a good indication of which colonies obtained a vector with the ligated insert. Nevertheless, colony PCR was performed with M13 primers (encoded in the vector) to confirm the transformants containing our insert. Sterile toothpicks were used to dab single colonies and transfer the adhered cells into PCR tubes where the reaction was mixed:

x µg Transformant DNA
2 µl GC Buffer (5x; NEB)
2 µl dNTP mix (each at 2,5mM)
0,5 µl M13 forward primer
0,5 µl M13 reverse primer
0,3 µl One Taq Polymerase (NEB)
14,5 µl nuclease free H_2O (Gibco)
20 µl final volume

	94°C 5 min
40x	**94°C 15 sec**
	59°C 30 sec
	68°C 30 sec
	68°C 5 min
	4°C ∞

The results of colony PCR were visualized by agarose electrophoresis. The desired inserts were excised and extracted from the gel using the GeneJET Gel Extraction Kit (Thermo Fisher).

4.11.3 Sequencing

DNA product identity was checked by Sanger sequencing at the DNA Sequencing Laboratory located at Viničná 7, Biology Departments, Faculty of Science. The sequences were analyzed using the software Geneious 10.2.2 available at http://www.geneious.com/ , 20th April 2016.

5 Results

5.1 RNA CoIP

To find potential 6S-like RNAs in *Streptomyces coelicolor* we coimmunoprecipitated RNA bound to the Streptomyces housekeeping sigma factor HrdB using the *Streptomyces coelicolor* A3(2) M145: *HrdB-HA* (epitope tagged) mutant. To expand the scope of our search (explore other regulatory RNAs) we also coimmunoprecipitated RNA interacting directly with the RNA polymerase core (β subunit) from *Streptomyces coelicolor* A3(2) M145 WT, even though such an RNA would not be a 6S RNA, characterized by binding to sigma factors. We prepared samples from liquid and solid cultivation to investigate possible differences in the expression profiles of genes of interest.

5.1.1 Immunoprecipitation

The amounts of protein in lysates obtained from homogenizing mycelia from liquid as well as solid cultivation of the *S. coelicolor* WT and HrdB-HA mutant were measured using the Pierce BCA Protein Assay Kit (Thermo Fisher). This information was used to optimize the immunoprecipitation experiment.

Lysate samples		µg of protein/ul	x µl containing 4 mg of protein
Liquid growth medium	HrdB-HA	1,513	2642
	WT	1,941	2060
Solid growth medium	HrdB-HA	3,117	1284
	WT	1,765	2265

Table R1. Table of lysate protein concentrations. The column on the right shows the amount of lysate used for immunoprecipitation with 4 mg of total protein as input.

Western blot analysis with the same respective antibodies used in the IP experiment served as a control of the procedure. Each IP sample had a non-specificity control treated with IgG corresponding to the used antibody. The anti-HA IP sample had a second, negative control where

the WT lysate was immunoprecipitated with the anti-HA antibody. The WB results are shown in the pictures below. For HrdB-HA IP (**Fig.R1**), the samples had a large band between 46 and 58 kDa where HrdB sigma factor (56 kDa) is located (Shinkawa et al., 1995). The IgG non-specificities control as well as the WT negative control did not show any significant banding (very light bands appeared at 10 min exposition). Non-specificities were present in both HrdB-HA lysates in contrast to WT lysates. The samples from solid medium cultivation show some additional banding in comparison with the liquid cultivation samples.

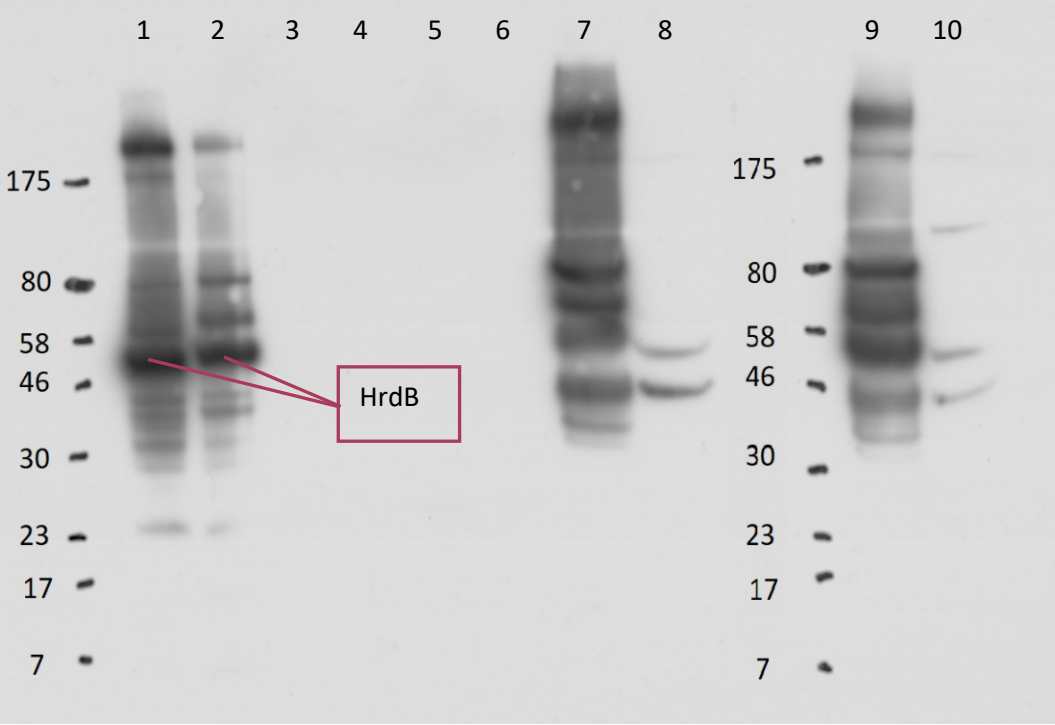

Figure R1. WB analysis with Anti-HA-Peroxidase rat monoclonal IgG antibody (diluted 10000x for WB). Image obtained from photographic film exposed for 1 min. Size standards of a broad range protein marker are indicated (in kDa). sm - solid medium; lm - liquid medium; Ab - antibody. Sample description in numbered lanes: **1**: sm HrdB-HA, anti-HA Ab; **2**: lm HrdB-HA, anti-HA Ab; **3**: sm HrdB-HA, rat IgG Ab; **4**: lm HrdB-HA, rat IgG Ab; **5**: sm WT, anti-HA Ab; **6**: lm WT, anti-HA Ab; **7**: sm HrdB-HA, lysate; **8**: sm WT, lysate; **9**: lm HrdB-HA, lysate; **10**: lm WT, lysate; The position of the HrdB (CoIP target) band is indicated by red lines.

Surprisingly the RNAP β IP samples (**Fig.R2**) did not show any band at 128/144 kDa where the *S. coelicolor* RNA pol β should be. The two large bands in the IgG non-specificities control were the IgG light and heavy chains. Only one band at about 175 kDa appeared in the lysate samples. A band of this size could signify a slowly migrating RNAP β' (Babcock et al., 1997). Altogether, the RNAP β subunit was not immunoprecipitated.

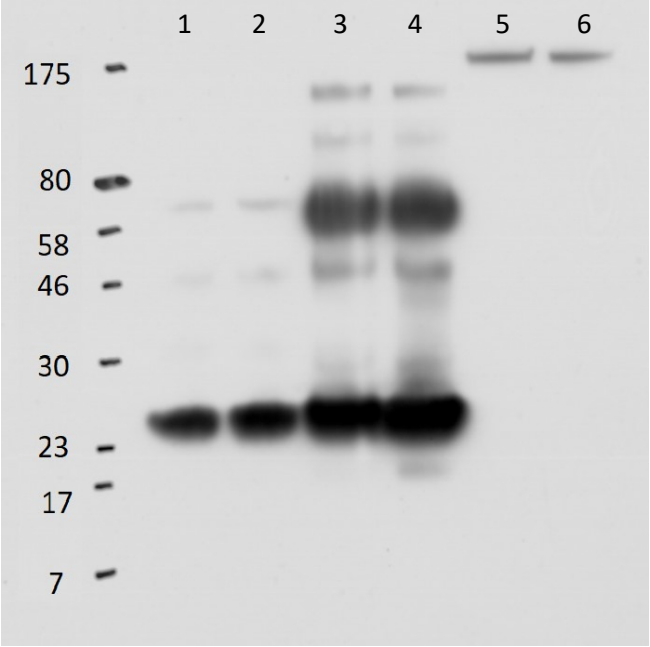

Figure R2. WB analysis with anti - RNA pol β mouse monoclonal IgG antibody (diluted 500x for WB). Image obtained from photographic film exposed for 1 min. Size standards of a broad range protein marker are indicated (in kDa). Sm - solid medium; lm - liquid medium; Ab - antibody. Sample description in numbered lanes: **1**: sm WT, anti-RNAP β Ab; **2**: lm WT, anti-RNAP β Ab; **3**: sm WT, mouse IgG Ab; **4**: lm WT, mouse IgG Ab; **5**: sm WT, lysate; **6**: lm WT, lysate;

5.1.2 RNA isolation – following CoIP

The amounts of acquired RNA from CoIP samples were lower than 0,2 ng/µl and not measurable with Qubit 3 Fluorimeter using a high sensitivity detection kit. Total RNA acquired from lysates (no IP) was measured - 2,4 µg/µl for the sample cultivated on solid medium and 1,13 µg/µl liquid medium sample - with nanodrop. This was a control of our CoIP RNA isolation method.

5.2 Analyzing old (2015) RNA CoIP samples

5.2.1 Primer extension

The primer extension method conducted with the old CoIP RNA input sample (HrdB-HA cultivated in liquid medium with a WT control sample; HrdB2015; WT2015) did not lead to detection of any RNA in the sample.

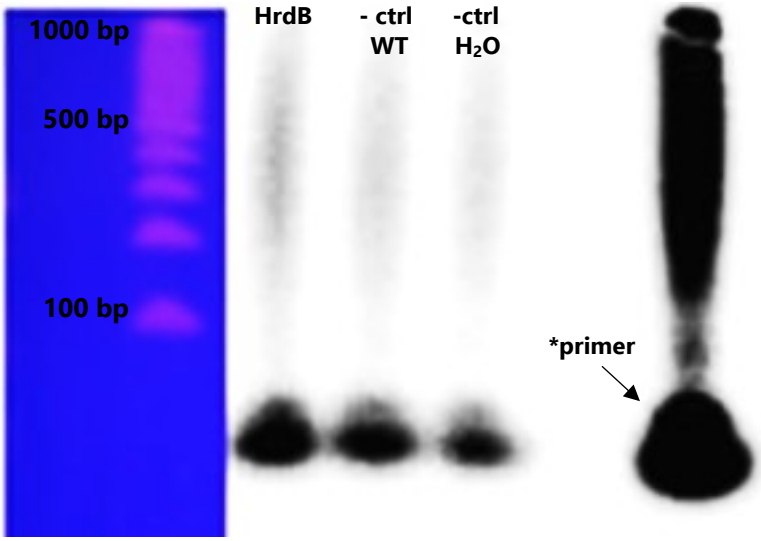

Figure R3. Primer extension results. Samples run on an 6% acrylamide gel. DNA size standards of a low range (100 bp +) nucleic acid marker are indicated. Samples from left to right: HrdB-HA RNA coIP; WT RNA CoIP control; H_2O negative control; blank lane; 5 µl isotope-labeled primer;

5.2.2 SMARTer PCR cDNA synthesis

Reverse transcription and amplification using the commercial kit lead to the detection of a 150 - 300 bp band in the HrdB2015 sample (**Fig.R4a**). This broad band was excised, purified and 0,5 µl of the DNA was amplified using the same primers (from the SMARTer PCR cDNA synthesis kit) one more time to separate the product. After the second amplification, a main band at 170 bp appeared with two lighter bands surrounding the main product (**Fig.R4b**). The main product was excised, purified and sequenced. The sequencing was not successful and after realizing that the cause was the same primer sequence on both ends of our product (present in SMARTer PCR adaptors) the purified product was cloned.

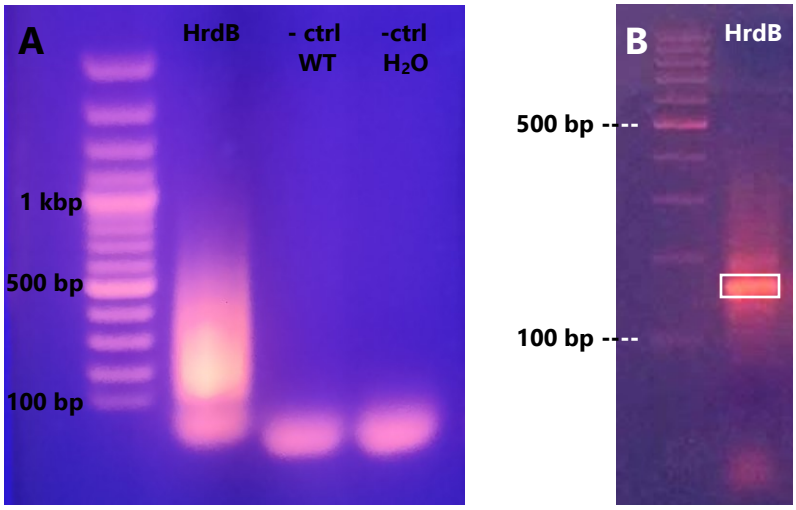

Figure R4. SMARTer PCR cDNA synthesis results. a) Samples run on a 2% agarose gel. DNA size standards of a low range (100 bp +) nucleic acid marker are indicated. Samples from left to right: HrdB-HA RNA coIP; WT RNA CoIP control; H_2O negative control; **b)** Sample run on a 1,5% agarose gel. The excised DNA band is indicated by the white rectangle.

5.2.3 Cloning and Sequencing the found RNA

The efficiency of competent cell preparation was evaluated from O/N cultivated plates. Transformed *E. coli* SURE Competent Cells (tetracycline resistant) obtained the ampicillin resistance cassette from the pTrcHis A vector and colonies grew on the Tet + Amp supplemented LB plates. Mock transformed *E. coli* SURE Competent Cells were also plated. No colonies appeared on the control plate as expected. Next, a restriction analysis was performed using BamHI and EcoRI restriction enzymes. The digestion product was expected to be ~210 bp long. No expected product was observed after running the samples on a 1,5% agarose gel. After ordering the TOPO TA Cloning Kit the insert was ligated in the commercial vector and the TOP 10 competent cells were transformed and plated. Twenty-three colonies were picked by blue/white selection and analyzed by qPCR. The desired outcome was a ~370 bp product (the insert-less sequence was 201 bp long). The results are shown in **Figure R5**.

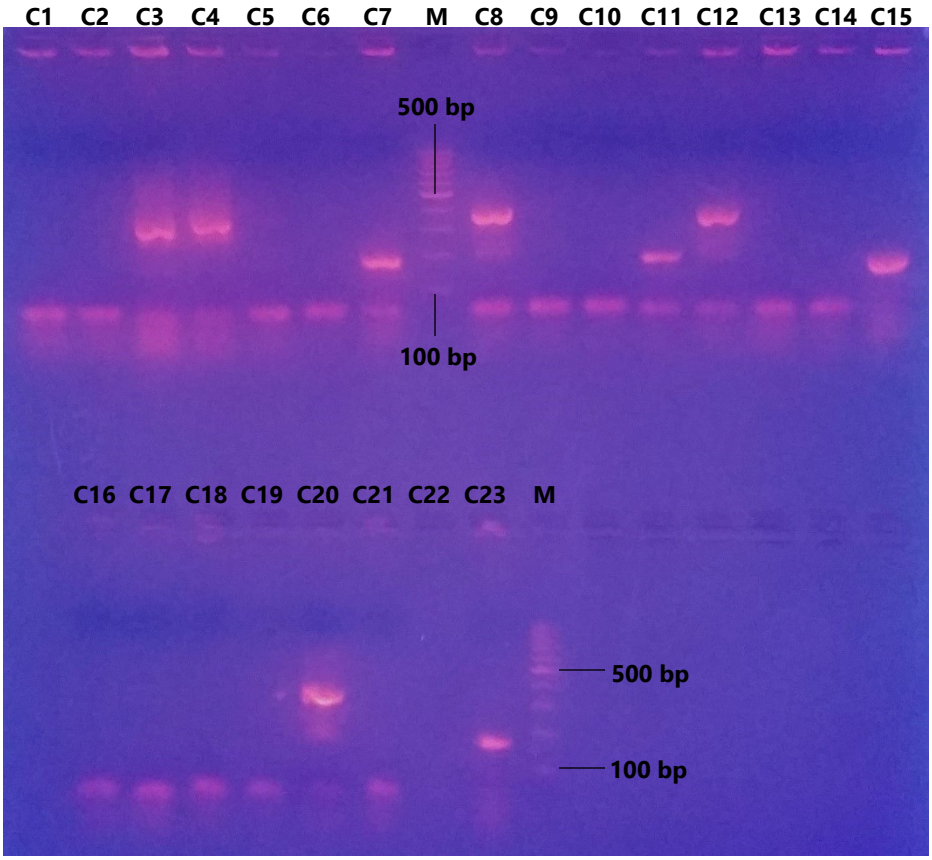

Figure R5. Colony PCR results. Twenty-three blue colonies were analyzed to assess the ligation efficiency. C – clone; The PCR product with the cloned insert can be seen in clones 3,4,8,12 , and 20.

The investigated insert was present in five clones. It was purified from the agarose gel and sequenced. The insert sequence was mapped on the *Streptomyces coelicolor* A3(2) M145 genome using the NCBI online Nucleotide Blast available at https://blast.ncbi.nlm.nih.gov/Blast.cgi, 12th May 2016. The alignment revealed, that our explored insert sequence was a stretch of RNA belonging to the Streptomyces 16S ribosomal RNA and thus was only a contamination of the RNA CoIP sample (**Fig.R6**).

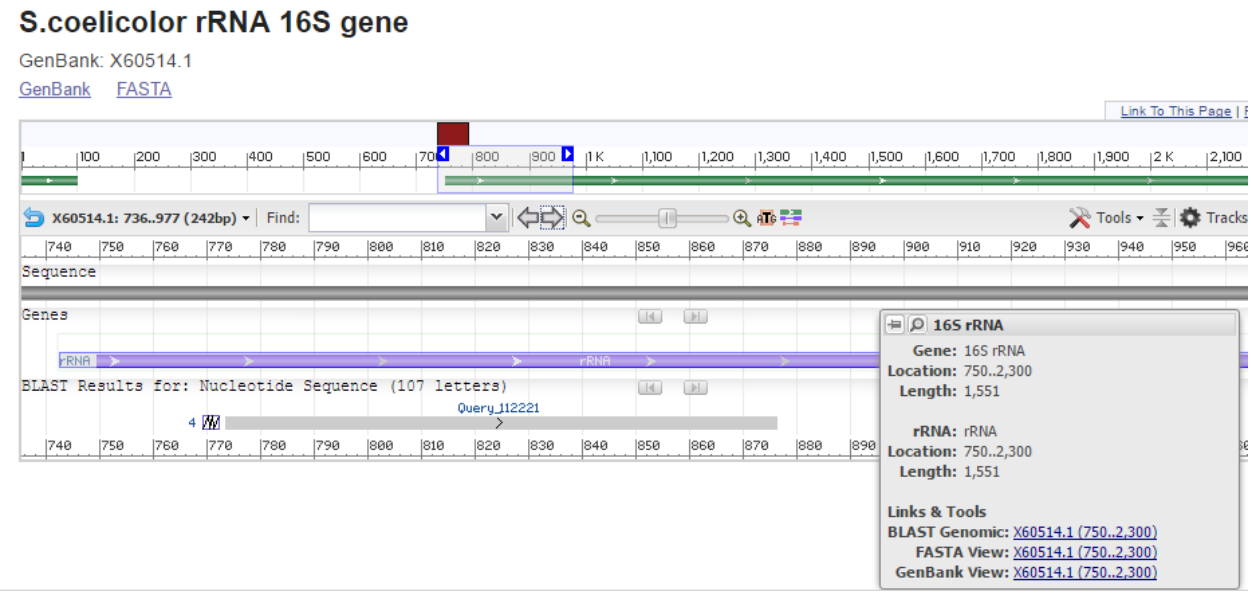

Figure R6. Sequenced insert mapped on *S. coelicolor* genome. Alignment carried out with BLASTN 2.6.1+ (Altschul etal., 1997). Aligmnet score for the blast was >200.

5.3 Verifying expression of *in silico* predicted 6S RNAs

5.3.1 RNA isolation (total RNA from plates)

S. coelicolor total RNA isolations from the exponential growth phase (T33), transition phase (T46) and stationary phase (T60) were finalized by measuring the amounts of isolated RNA. Due to DNA contamination, some of the samples had to be treated with DNase a second time which significantly lowered the yields. DNase treated RNA concentration and purity are shown in the table below.

RNA isolation	T 33		T46		T60	
	[µg/µl]	$A_{260/280}$	[µg/µl]	$A_{260/280}$	[µg/µl]	$A_{260/280}$
1st isolation	0,399	2,01	0,316	2,07	0,202	2,04
2nd isolation	7,34	2,06	10,3	2,09	2,5	2,10

Table R2. Concentration and purity of isolated total RNA. The lower amounts of RNA from the first isolation were caused by additional DNase treatments and subsequent purification.

5.3.2 One-step RT-PCR

The RT-PCR reaction using primers designed for the *in silico* 6S RNA predictions confirmed the expression of all but one predicted RNA sequences. The 6Sc8 product was only visible in the first round of RT-PCR. In each reaction, a positive control (of the method) was included. I used mouse thymus RNA (1 µg/µl) from FirstChoice RLM RACE Kit (Ambion) with the respective primers included in the kit (final PCR product is 217 bp long). A negative control for the positive control (without reverse transcriptase (RT) enzyme) was initially also included to rule out the possible reverse transcriptase activity of the Taq polymerase (Myers & Gelfand, 1991). As a negative control, I mixed reactions without reverse transcriptase for every RNA sample. In the first round of RT-PCR some of the negative controls contained products, and these RNA samples were treated with DNase a second time. After the second purification, in the second round of RT-PCR only one negative control contained a light band. All products were subsequently verified by sequencing. The results for each 6S RNA prediction (6Sc1, 6Sc2, 6Sc3, 6Sc5, 6Sc6, 6Sc7, 6Sc8 (6Sc4 has already been described in literature, see chapter **6.2**)) are shown in the table below together with primers and annealing temperatures used, and expected product sizes (**Table R3**). A representative gel photograph of the 6Sc3 and 6Sc5 RT-PCR results is shown below (**Fig.R7**). All of the 6Sc sequences were predicted in intergenic regions. 6Sc2 is located at an interesting position, close to the gene encoding the HrdB sigma factor. At the time, I received the *in silico* predictions, the position of the 6Sc7 sequence was shown to overlap with a putative transposase gene (see supplementary data). Two technical replicates of RT-PCR were conducted.

6S-like RNA	primers		T_m	$T_{annealing}$ used	product size	6S-like RNA expression overview		
						T33	T46	T60
6Sc1 intergenic	6Sc1for	5'-TGGACGGCTGTTGGTACGCA-3'	67°C	59°C	**186 bp**	✓	✓	✓
	6Sc1rev	5'-GCTTGTGCAGATGCGCCAACG-3'	67°C					
6Sc2 intergenic	6Sc2for	5'-ACGTTCCCGCTCGTGGCTT-3'	67°C	59°C	**171 bp**	✓	✓	✓
	6Sc2rev	5'-CTCCGGGCACGTCCTCATGA-3'	67°C					
6Sc3 intergenic	6Sc3for	5'-CATCTGAGGCACCCTAGCGT-3'	64°C	55°C	**166 bp**	✓	✓	✓
	6Sc3rev	5'-ACAAACAGGGCGCTCCAC-3'	63°C					
6Sc5 intergenic	6Sc5for	5'-CGAACGCCGCATGTCGGT-3'	66°C	55°C	**185 bp**	✓	✓	✓
	6Sc5rev	5'-ATCACGACCGAACCTTTGCGG-3'	65°C					
6Sc6 intergenic	6Sc6for	5'-CAAAGTGGCTGCCTAAAGC-3'	59°C	52°C	**174 bp**	X	X	✓
	6Sc6rev	5'-ACTTTCCCTACTTCATCAAGGC-3'	59°C					
6Sc7 gene overlap	6Sc7for	5'-CTCGGCAGCACCACGAACC-3'	67°C	59°C	**190 bp**	✓	✓	✓
	6Sc7rev	5'-GAACATCGGGGACCGCGAG-3'	66°C					
6Sc8 intergenic	6Sc8for	5'-CAGTCTCCCCTCATGCCTGGT-3'	66°C	59°C	**136 bp**	X	X	X
	6Sc8rev	5'-GAAACGGGCGCGGGAGAC-5'	67°C					
Endogenous control								
5S RNA	5Sfor	5'-TTCGGTGGTCATAGCGTAGG-3'	65°C	55°C	**110 bp**	✓	✓	✓
	5Srev	5'-GGCGTCCTACTCTCCCACAG-5'	66°C					

Table R3. Primers used for RT-PCR and expected product sizes. Melting temperatures taken from the Multiple Primer Analyzer from Thermo Fisher Scientific (available at https://www.thermofisher.com/, 9th November 2016). Primers for the endogenous control used in both RT-PCR (CoIP samples) and qPCR are included. A quick overview of the results is included. ✓ - expressed, X - not expressed.

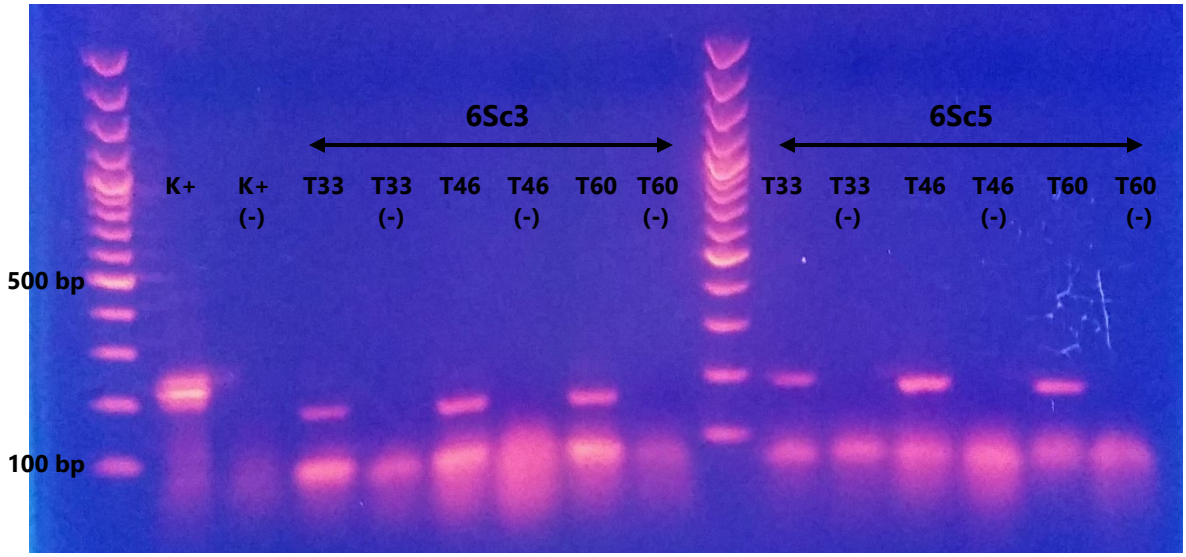

Figure R7. Expression of 6Sc3 and 6Sc5 from *S. coelicolor* RNA. Samples run on a 1,5% agarose gel. DNA size standards of a low range (100 bp +) nucleic acid marker are indicated. Expression of both 6Sc3 (166 bp) and 6Sc5 (185 bp) in all three growth phases can be seen. All the negative control samples are clear.

5.4 Determining the size and the expression profiles of the 6S RNA predictions

5.4.1 Northern blot

Determining the true size of the 6S RNA prediction transcripts by northern blot was not achieved. No signal was obtained from the membranes hybridized with probes complementary to the 6S RNA predictions. Troubleshooting was conducted, and by dot-blotting probes straight on the nylon membrane I confirmed that the probes were successfully labeled (**Fig.R8**). A dot-blot of total RNA was hybridized with the 6Sc3 complementary probe and no signal was obtained.

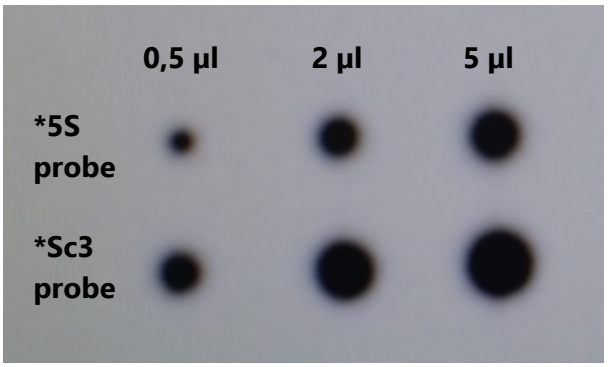

Figure R8. Isotope labeled probe dot-blot - troubleshooting. The control probe (*5S probe) and one of the experimental probes (*6Sc3) dot-blotted on a positively charged nylon membrane in three different concentrations (0,5 µl, 2 µl and 5 µl respectively blotted onto one dot).

5.4.2 Primer extension

A method for visualizing the 5' end size of the predicted transcripts was using primer extension. The method was successful, but primer extension products appeared only in the 6Sc7 (gene overlap) samples and the positive control (5S RNA). Negative controls (a mix of T33, T46 and T60 RNA samples without RT enzyme) were included and all the negative control lanes were clear (**Fig.R9**, **Fig.R10**). The smeared edges of the gels are caused by gel shrinking during dehydration in EtOH, which also enhances the obtained signal (see chapter **4.10.2**).

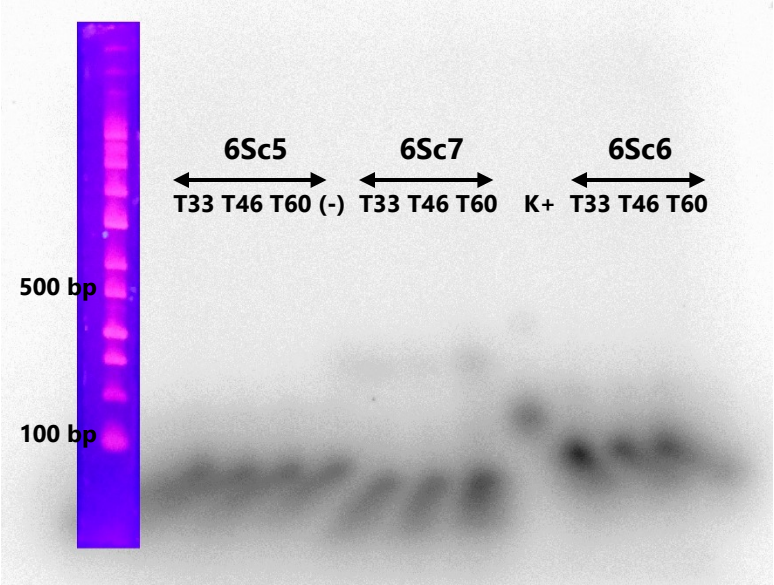

Figure R9. Primer extension results – 6Sc5, 6Sc6, 6Sc7. A light band was found in the positive control lane at ~450 bp. In all the 6Sc7 samples a light band was located at ~300 bp. No products were found in 6Sc5 and 6Sc6 samples.

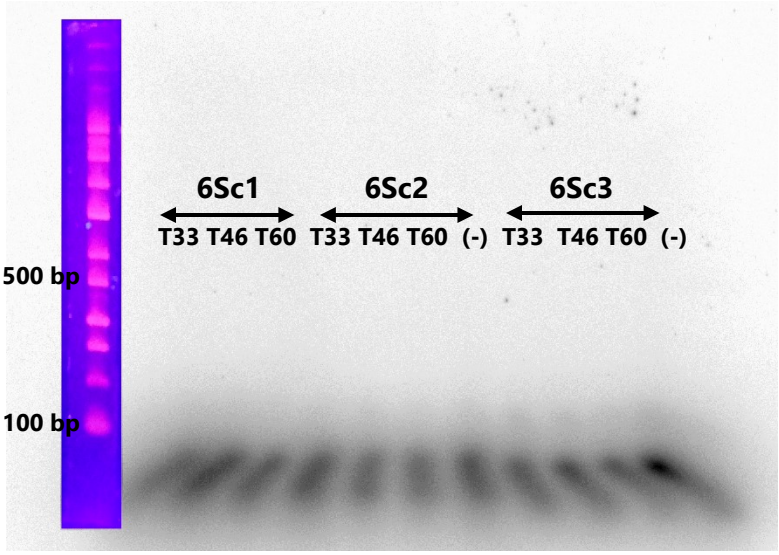

Figure R10. Primer extension results – 6Sc1, 6Sc2, 6Sc3. No products were found in 6Sc1, 6Sc2 and S6c3 samples, nor in the negative control samples.

5.4.3 Quantitative PCR (qPCR)

Total RNA (T33, T46, T60) was used for relative quantification of expression of the 6S RNA prediction transcripts during the *Streptomyces* growth phases on solid R2YE medium (T33 - exponential growth phase, T46 – transition phase, T60 – stationary phase). The ribosomal 5S RNA was used as an endogenous control. The primers used can be found in Table R.3. After optimization, 5 ng of input RNA were used in each RT reaction. As a negative control, I mixed reactions without reverse transcriptase for every RNA sample. All samples were carried out in duplicate. The qPCR experiment showed a nice amplification curve for 5S RNA and a 20-cycle difference between the 5S RNA sample and negative control (no RT enzyme added; **Fig.R11**). The C_t values (threshold cycle – the number of the cycle after which a real signal was obtained) of the 6S RNA predictions however had inconsiderable differences from their negative controls. This means that the method worked well, but the results are not conclusive.

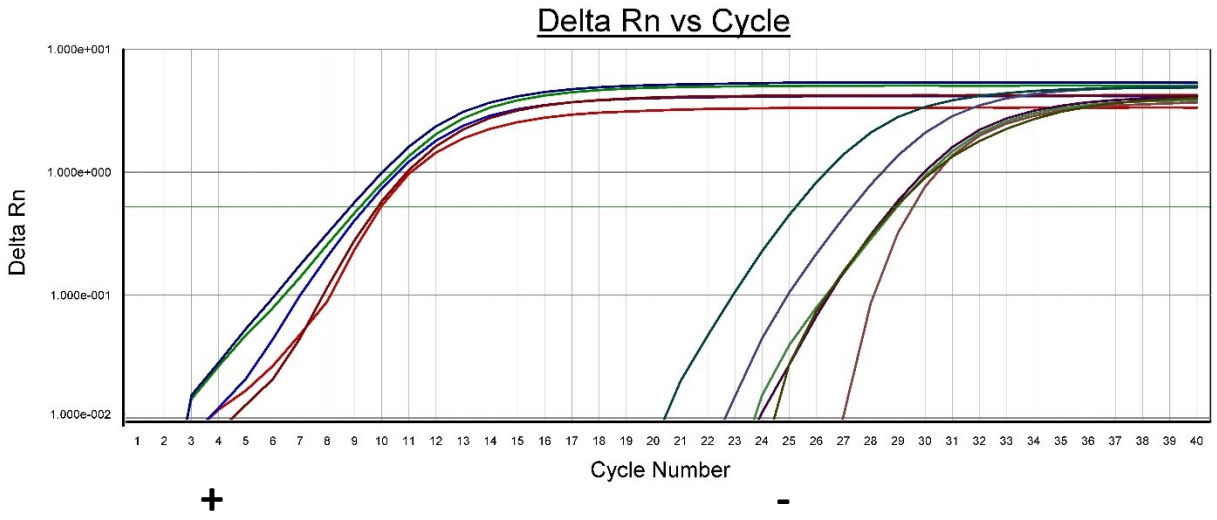

Figure R11. qPCR results – 5S RNA endogenous control amplification plot. The amplification curves of 5S RNA endogenous control (**+**) and a corresponding negative control (no RT enzyme; **-**) The curves of the positive samples show a constant expression level. Delta Rn – Reporter value normalized to reference signal (ROX).

5.5 Verifying the presence of *in silico* predicted 6S RNAs in new (2017) CoIP samples

The RNA samples obtained by CoIP with HrdB have been used as an input for one-step RT-PCR. Primers for the ribosomal 5S RNA were used to create a positive control (by amplification with total RNA – no CoIP) and an endogenous control of the Co-IP samples. None of the *in silico* predicted 6S RNAs has been amplified from the HrdB CoIP samples, and as expected due to the unsuccessful immunoprecipitation of RNAP β, none were detected in RNAP β CoIP samples. The 5S RNA positive control showed a clear band. The 5S RNA endogenous control showed amplification in both HrdB and RNAP β CoIP samples. All negative control samples (no RT enzyme) were clear. Below, a summary of the results is shown (**Table R4**).

CoIP sample ↓	**6Sc1**	**6Sc2**	**6Sc3**	**6Sc5**	**6Sc6**	**6Sc7**	**6Sc8**	**5S RNA**
sm HrdB	X	X	X	X	X	X	X	✓
sm RNAP β	X	X	X	X	X	X	X	✓

Table R4. Results overview of RT-PCR using CoIP samples. Expression of in silico predictions and the 5S RNA endogenous control from the solid medium (sm) RNA CoIP samples. ✓ -expressed, X - not expressed.

6 Discussion

Due to the important antibiotic producing properties of streptomycetes, research has been mainly focused on their secondary metabolism and accompanied by genome mining for cryptic secondary metabolism clusters for exploitation in medicine (reviewed in Baltz, 2017). Meanwhile, the morphological and physiological differentiation that streptomycetes undergo during their intricate life cycle is less vigorously studied, and the underlying molecular mechanisms are still not fully understood (Buttner & Lewis, 1992; Flärdh et al., 1999; Tschowri et al., 2014). As in all other bacteria, σ factors are major contributors to the gene expression shifts underlying the responses to extracellular conditions and ensuing cellular transitions (Vohradský et al., 2000). Various means of σ factor regulation in streptomycetes have been studied already (Dalton et al., 2007; Otani et al., 2013; Kormanec et al., 2016), but due to the complicated search for ncRNAs in the phylogenetically distant Actinobacteria (Menzel et al., 2009), the 6S RNA inhibition pathway was omitted. The discovery of a ncRNA capable of binding the RNAP core, with a behaviour comparable to 6S RNA (Mikulík et al., 2014) prompted us to suspect the presence of yet unidentified 6S-like RNAs. Considering the impressive amount of σ factors present in streptomycetes, we hypothesize that a proportional number of regulatory ncRNAs may be present (Bentley et al., 2002). This would follow the trend observed in other bacterial species (Watanabe et al., 1997; Axmann et al., 2007; Cavanagh & Wassarman, 2013). To inspect our hypothesis, we combined bottom up and bottom down techniques. Since we had a clear target (6S-like RNAs) we were able to narrow down our search by applying RNA CoIP (also referred to as co-purification of sRNAs; Sharma & Vogel, 2009). We took advantage of the *S. coelicolor* M145: *HrdB*-HA epitope tagged mutant strain, created by insertional mutagenesis at the laboratory of Jiří Vohradský. Using this mutant strain, we were able to coimmunoprecipitate RNA together with the housekeeping σ^{HrdB}. Our bottom up technique was based on validation of 6S-like RNA *in silico* predictions by one-step RT-PCR. Although novel, high throughput methods were not implemented in this thesis, the sensitive RT-PCR method delivered data that verify the expression of 6 of the 7 predicted 6S-like RNA sequences. Nevertheless, the expressed transcripts were not detected in CoIP samples, ruling out their interaction with σ^{HrdB}. This result does however not rule out their 6S-like RNA function, since *S. coelicolor* has many more σ factors with possible affinities to the predicted transcripts.

For the detection of 6S-like RNAs in *S. coelicolor*, two complementing approaches were employed. The first was based on our definition of what a 6S-like RNA is: A 6S-like RNA is a small non-protein-coding RNA that inhibits the RNAP holoenzyme by binding to any σ subunit. Therefore, in the first approach I was searching for the 6S RNA where it should be bound. RNA CoIP with antibodies against HA-tagged HrdB (the Streptomyces housekeeping σ factor) and alternatively RNAP β subunit was carried out and the output RNA was searched either non-specifically, with the aim to detect any RNA present (see chapter **5.1** and **5.2**), and specifically by using primers for *in silico* predicted 6S-like RNAs (see chapter **5.5**). The second approach was based on the bioinformatic work of Josef Pánek, who predicted 6S-like RNAs *in silico* based on structure conservation. Total RNA isolated from *S. coelicolor* samples in three different growth phases was used for identifying the expression of these predicted 6S-like RNAs. After verifying the expression of the *in silico* predicted sequences, the size and expression profiles of the RNAs were further studied (see chapter **5.3** and **5.4**). A flowchart of my work is depicted below.

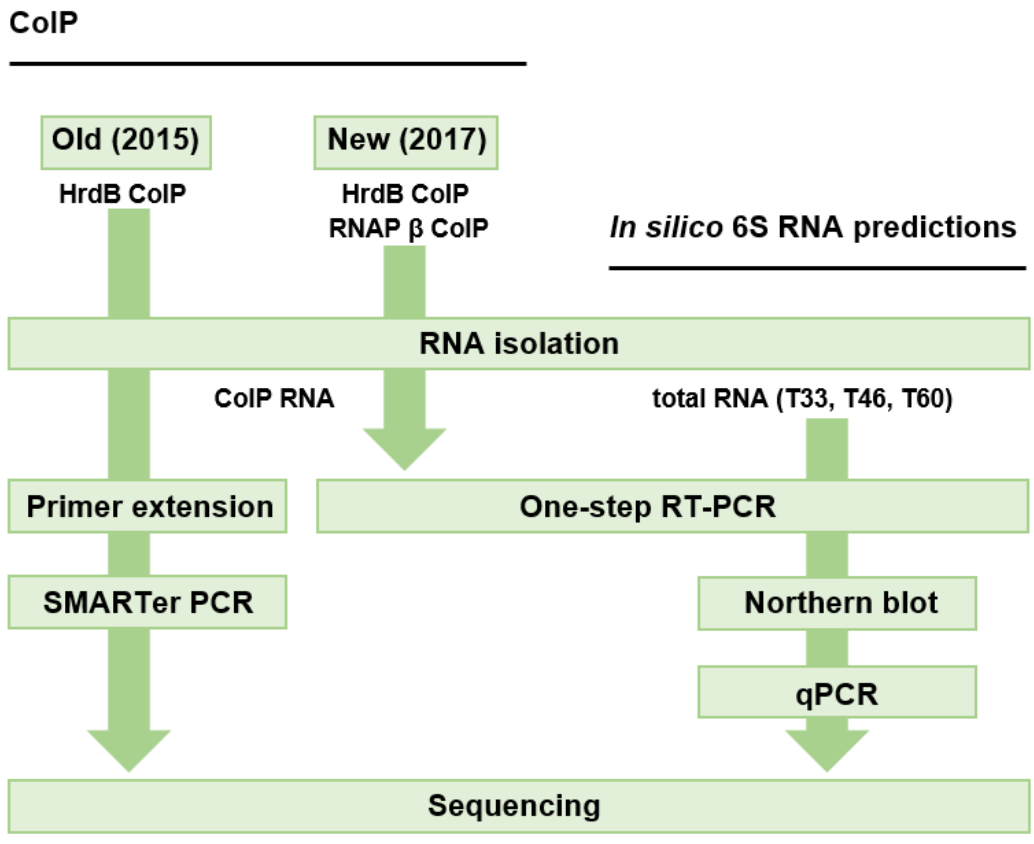

Figure 13. Flowchart of the experimental structure. The two different approaches are depicted on top.

6.1 Bottom-down search for 6S-like RNAs (In old CoIP samples)

The first experiments were carried out on complete CoIP RNA samples (referred to as Old, 2015). I obtained these samples from the laboratory of Bioinformatics at CAS. These only included RNA co-immunoprecipitated with the housekeeping σ factor HrdB. The first conducted experiment was primer extension, which did not detect any RNA in the RNA-CoIP sample. Another method, SMARTer PCR cDNA synthesis, lead to the detection of a broad cDNA band in the 150 - 300bp range. After purification and reamplification of this DNA, a main product of 170 bp was detected. The difference in results using the two methods can be accounted to the missing amplification step in primer extension, making SMARTer PCR a significantly more sensitive method (Dean et al., 2002). Since the SMARTer PCR method adds the same sequences to the ends of reverse transcribed products, the DNA had to be cloned prior to sequencing (see **Fig.12**). The first attempt by manual TA cloning of the fragment did not work out. Colonies of SURE *E. coli* cells after transformation indicated that the transformation and competent cells are faultless, but the restriction reaction did not show any insert. A possible explanation is the confusion in thymidine triphosphate labeling (TTP; automatically considered a 2' - deoxynucleotide), since it can also be labeled as 2' – deoxythymidine triphosphate (dTTP) and thus the 2', 3' – dideoxythymidine triphosphate used could be labeled as ddTTP. In the case of adding TTP (labeled as dTTP) the reaction would create a poly-T 3' – overhang and the ligation reaction would not be successful (Sanger et al., 1977). Using the TOPO-TA cloning kit, the DNA fragment has been cloned successfully. Sequencing results revealed, that the found RNA was a fragment of the ribosomal 16S RNA, sheared by sonication of the lysate samples during preparation for RNA CoIP.

6.2 Validation of 6S RNA *in silico* predictions

Hence, we decided to take a different approach. The bioinformatic work of Josef Pánek already led to identification of new small RNAs in streptomycetes and Mycobacteria in the past (Pánek et al., 2008; 2011). Interestingly, although the former study was based on sequence conservation and functional features, and the latter on conservation of suboptimal secondary

structures, both approaches led to the identification of an identical *S. coelicolor* 6S RNA candidate. The expression of this regulatory RNA candidate was verified, and a publication described its non-constitutive expression, pRNA synthesis and binding capacity for the RNAP core (named 6Sc4 in our data and omitted in this thesis; Mikulík et al., 2014). Pánek et al. studied a native template (the *E. coli* 6S RNA) to observe that it does not fit a structural model with optimal (minimal) free energy, but a structure with a higher than minimal free energy instead. This observation critically shifts the mindset of a biologist taught to believe how molecules acquire their structure. The prediction of ncRNAs exploiting common suboptimal structures, coupled with candidate selection based on sequence functional features (intergenic location, promoter and terminator positioning, etc.) has managed to overcome the lack of sequence specificity that disabled the homology based discovery of ncRNA sequences in Actinomycetes so far (Barrick et al., 2005; Pánek et al., 2010). Pánek et al. included a criterion that distinguished the predicted ncRNAs from 3' UTRs of upstream genes by searching for the 5' flanking termination sites. Our laboratory acquired seven 6S RNA candidate sequences from Josef Pánek through personal communication (one already described in Pánek et al., 2011, as Sc1) and the wet-lab verification of their presence in *S. coelicolor* became part of my thesis.

Using an optimized one-step RT-PCR protocol (Kreader, 1996), I verified the expression of all but one 6S RNA prediction – the 6Sc8 was only expressed in one of two technical replicates and thus I did not regard it as a positive. Sequencing analyses confirmed that all products corresponded to the expected products. Sequencing results of both 6Sc6 and 6Sc8 were poor due to a low DNA yield, yet consensus of the usable data with the predicted sequences still enabled their verification. These results, where novel putative transcripts have been validated, confirmed the rational approach of the prediction technique employed (Pánek et al., 2010) and the subsequent goal was studying the expression levels of the transcripts and determining their possible regulatory roles. Since the ncRNA predictions have been chosen based on similarity in *S. coelicolor* and *S. avermitilis*, the chance that only transcriptional "noise" has been detected is low (Lybecker et al., 2014). The next step was determining the true size of the transcript and a possible regulatory function, based on differential expression during the S. coelicolor growth cycle. We decided to conduct a Northern blot analysis to determine the transcript size. During the work we encountered many problems caused either by the blotting machine itself (incomplete RNA transfer) or the hybridization - complementary PCR 18 - 21 mer primers were used as probes and the stringency

solution used for washing may have been too harsh, despite several attempts to lower the stringency and shorten the washes. Troubleshooting showed that the probes themselves emitted signal and thus were correctly labelled. Since a prestained protein marker was not available to act as a blotting control, an alternative dot-blot control (total RNA) was added to the membrane after blotting and before UV crosslinking. This control did not yield any signal, pointing out that the problem should be hybridization alone. Nevertheless, without proper positive controls, and a non-existing standardised method at the laboratory, I was not able to identify the exact error in our protocol. Since there was not enough time for me to implement a standardised Northern blot protocol, I made use of the functional probes when visualizing the 5' – end size of the transcripts by primer extension. Next to the positive control (5S RNA), only the 6Sc7 putative 6S-like RNA showed a detectable primer extension product of 300 bp. This predicted sequence is located in a gene overlapping region, which could have effect on the transcript amount and therefore on the obtained signal. For the other predictions, the native amount of RNA could have been too low for detection without an amplification step. Altogether, the RT-PCR experiment that verified the presence of 6 of the 7 predicted 6S RNAs was proven a reliable and sensitive detection method as described in literature (Dean et al., 2002).

Semi-quantitative qPCR using SYBR green has been conducted to determine expression profiles of the 6S-like RNAs. Although 6Sc8 transcription was not regarded as positive after RT-PCR, it has been included in the qPCR experiment. The qPCR was an additional experiment, and thus I was not able to repeat it and acquire conclusive data. The preliminary results show consistent expression levels of the endogenous control and its negative control, pointing towards a functional protocol. The absence of significantly differential expression of the 6S-like RNA samples and their negative controls could have been caused by RNA degradation, since the RNA had to be repeatedly treated with DNAse to eliminate gDNA in the samples, detected by the pre-runs of qPCR.

6.3 Bottom-up search for 6S-like RNAs (In new CoIP samples)

After having validated expression of the predicted 6S-like RNAs, I decided to search directly for these transcripts in the CoIP samples. For this, a new CoIP experiment has been set up. This time (unlike the old CoIP sample preparation) I was conducting the experiment myself,

with guidance from Alice Ziková from the Bioinformatics laboratory at IMB, CAS. The western blot control of RNA CoIP of HrdB verified the successful CoIP of the 56kDa large σ^{HrdB}, and the negative control samples were clear. The western blot control of RNA CoIP of RNAP β did not show any band of the size that would indicate the CoIP target – the β subunit of RNAP (128/144kDa). The IgG control banding was caused by the fragmented secondary antibody, that bound the mouse IgG in the IgG control sample and even in the CoIP sample. This was caused by the identical origin of the antibodies used (murine) and did not occur in the HrdB CoIP western blot, where a peroxidase-conjugated primary antibody was used. The sharp band in the lysate sample could be a seemingly slower migrating β subunit of RNAP, although the specific double band created by β and β' cannot be distinguished. As expected, no IgG binding due to the secondary antibody can be seen. Due to an unknown reason, the IP of RNAP β was not successful. The RNA was still included in the following RT-PCR experiment. None of the validated 6S-like RNAs were present in the RNA samples acquired by CoIP of HrdB. As expected, none were found in the RNA samples acquired by CoIP of RNAP β. On the other hand, the 5S RNA endogenous control was detected in both RNA samples, which together with the previous identification of 16S RNA in the old RNA CoIP samples showed the frequent contamination of RNA CoIP samples with ribosomal RNAs. This problem can be addressed by various rRNA cleaning methods in the future (He et al., 2010). Here, the contamination had the role of a positive control of our experiments.

6.4 Reflection

My search for 6S-like RNAs in *Streptomyces coelicolor* did not result in the discovery of any regulatory RNA that would fit the definition of a 6S RNA. By one-step RT-PCR using total RNA from three distinct growth phases of *S. coelicolor*, I managed to detect 6 of 7 RNAs which have been predicted *in silico* based on the suboptimal structure of known 6S RNAs. This finding confirmed the solid prediction technique used (Pánek et al., 2010). Nevertheless, none of the RNAs has been found to interact with the *S. coelicolor* housekeeping σ factor. More research has to be done to find the binding partners of these ncRNAs and to confirm or rule out their association with alternative σ factors. On the other hand, it is possible that despite the structural homology to 6S

RNA the function of these RNAs can be quite different. 6S RNA has not been found in *Mycobacterium smegmatis* nor in *Corynebacterium glutamicum*, both belonging to Actinobacteria (Mentz et al., 2013; Hnilicová et al., 2014). Moreover, a non-DNA binding transcription factor RbpA is specifically prevalent in Actinobacteria and was found to stabilize the RNAP polymerase complex with the housekeeping σ factors by binding directly to the σ subunit (Tabib-Salazar et al., 2013). This points to a unique mechanism of σ factor regulation in Actinobacteria, where, in contrast to the 6S RNA inhibitory mechanism, a stabilizing molecule is needed to secure the vegetative growth RNAP holoenzyme (Hnilicová et al., 2014). The 6Sc4 6S-like RNA *in silico* predicted by Pánek et al., 2010, and described by Mikulík et al., 2014, has structural homology to 6S RNA as well as the ability to serve as a template for RNAP and still is not a true 6S RNA due to the interaction with RNAP core without the involvement of a sigma factor. Therefore, the discovery of structurally similar but functionally distinct regulatory RNAs cannot be ruled out. Taken together, it is possible that no 6S-like RNAs will be found in streptomycetes, but other regulatory RNAs certainly will be identified, and further research is needed to define the functions of the RNAs validated in this thesis.

Following research will be focused on mapping the 5' and 3' ends of the putative 6S-like RNAs by means of RNA Ligase Mediated Rapid Amplification of cDNA Ends (RLM-RACE; Liu & Gorovsky, 1993). When the full transcripts are mapped, the binding partners of the RNAs have to be determined. For this, RNA CoIP with antibodies targeting alternative *S. coelicolor* sigma factors can be used. To maximize the sample value, lysates harvested during different growth phases (as conducted in this thesis) and growth conditions should be combined. This will raise the amount of target RNA-protein complexes present and can raise the chances of identifying RNAs present under specific conditions (Hüttenhofer & Vogel, 2006). Another possibility is the incubation of our putative 6S-like RNAs with binding partner candidates and the detection of complex formation by an Electrophoretic mobility shift assay (EMSA; Hellman & Fried, 2007; Beckmann et al., 2012). Using these techniques, we rely on our predicted model of the putative 6S-like RNAs functions. For a more open-minded approach, high throughput methods such as RNA-protein pull-down could readily identify all binding partners of the putative 6S-like RNAs (Butter et al., 2009; Hnilicová et al., 2014). Follow up mass spectrometry based techniques could not only identify the binding partners of the target RNAs but also reveal the manner of interaction between the two molecules (Kühn-Hölsken et al., 2005; Schmidt et al., 2012).

The resulting findings will show if our primary hypothesis, that a large amount of sigma factors will be accompanied by a proportionate number of regulatory 6S-like RNAs, can be confirmed, or a distinct mechanism of gene expression switching (proposed in Hnilicová et al., 2014) exists in Actinobacteria. When the sigma factor regulation mechanisms are elucidated, the information can be applied in bioengineering approaches to express *Streptomyces* cryptic gene clusters and access the hidden part of their secondary metabolism capacity.

7 Conclusions

The main aim of this thesis was the verification of 6S-like RNAs in *Streptomyces coelicolor*.

- By means of RNA CoIP, RNA co-precipitated with HrdB has been searched. Using a bottom-down search, only ribosomal RNA contamination was detected. Using a bottom-up search, none of the *in silico* predicted target 6S-like RNAs were detected. The 5S RNA endogenous control was positive.
- Six of the seven *in silico* predicted 6S-like RNAs were detected in total RNA samples harvested during the exponential growth phase, transition phase or stationary phase. Five of the RNAs were present in every growth phase.
- The above findings imply the presence of several *S. coelicolor* 6S-like RNAs, that have however not been found to interact with the RNAP – σ^{HrdB} holoenzyme.

The secondary aims of the thesis (characterizing the transcript size and expression profiles) have not been fully met. Follow-up experiments should be conducted to determine the functions of the found putative 6S-like RNAs.

- The 5' end primer extension of the putative 6S-like RNAs pointed towards their low abundance in the samples, since 6Sc7, that is currently mapped on a gene overlapping region, was the only target to produce a primer extension signal.

Overall, the thesis added evidence of an abundance of ncRNAs in *S. coelicolor*, and the function and possible involvement of these putative 6S-like RNAs in developmental transitions will be further studied.

8 References

Al-Bassam, M. M., Bibb, M. J., Bush, M. J., Chandra, G., & Buttner, M. J. (2014). Response regulator heterodimer formation controls a key stage in Streptomyces development. *PLoS genetics*, *10*(8), e1004554.

Allenby, N. E., Laing, E., Bucca, G., Kierzek, A. M., & Smith, C. P. (2012). Diverse control of metabolism and other cellular processes in Streptomyces coelicolor by the PhoP transcription factor: genome-wide identification of in vivo targets. *Nucleic acids research*, *40*(19), 9543-9556.

Altschul, S. F., Madden, T. L., Schäffer, A. A., Zhang, J., Zhang, Z., Miller, W., & Lipman, D. J. (1997). Gapped BLAST and PSI-BLAST: a new generation of protein database search programs. *Nucleic acids research*, *25*(17), 3389-3402.

Aoki, Y., Matsumoto, D., Kawaide, H., & Natsume, M. (2011). Physiological role of germicidins in spore germination and hyphal elongation in Streptomyces coelicolor A3 (2). *The Journal of antibiotics*, *64*(9), 607-611.

Axmann, I. M., Holtzendorff, J., Voß, B., Kensche, P., & Hess, W. R. (2007). Two distinct types of 6S RNA in Prochlorococcus. *Gene*, *406*(1), 69-78.

Babcock, M. J., Buttner, M. J., Keler, C. H., Clarke, B. R., Morris, R. A., Lewis, C. G., & Brawner, M. E. (1997). Characterization of the rpoC gene of Streptomyces coelicolor A3 (2) and its use to develop a simple and rapid method for the purification of RNA polymerase. *Gene*, *196*(1), 31-42.

Baltz, R. H. (2017). Gifted microbes for genome mining and natural product discovery. *Journal of industrial microbiology & biotechnology*, *44*(4-5), 573-588.

Barakat, M., Ortet, P., & Whitworth, D. E. (2010). P2CS: a database of prokaryotic two-component systems. *Nucleic acids research*, *39*(suppl_1), D771-D776.

Barrick, J. E., Sudarsan, N., Weinberg, Z., Ruzzo, W. L., & Breaker, R. R. (2005). 6S RNA is a widespread regulator of eubacterial RNA polymerase that resembles an open promoter. *Rna*, *11*(5), 774-784.

Becker, G., & Hengge-Aronis, R. (2001). What makes an Escherichia coli promoter σS dependent? Role of the− 13/− 14 nucleotide promoter positions and region 2.5 of σS. *Molecular microbiology*, *39*(5), 1153-1165.

Beckmann, B. M., Hoch, P. G., Marz, M., Willkomm, D. K., Salas, M., & Hartmann, R. K. (2012). A pRNA-induced structural rearrangement triggers 6S-1 RNA release from RNA polymerase in Bacillus subtilis. *The EMBO journal*, *31*(7), 1727-1738.

Bentley, S. D., Chater, K. F., Cerdeno-Tarraga, A. M., Challis, G. L., Thomson, N. R., James, K. D., ... & Bateman, A. (2002). Complete genome sequence of the model actinomycete Streptomyces coelicolor A3 (2). *Nature*, *417*(6885), 141-147.

Bibb, M. J., Domonkos, Á., Chandra, G., & Buttner, M. J. (2012). Expression of the chaplin and rodlin hydrophobic sheath proteins in Streptomyces venezuelae is controlled by σBldN and a cognate anti-sigma factor, RsbN. *Molecular microbiology*, *84*(6), 1033-1049.

Bobek, J., Šmídová, K., & Čihák, M. (2017). A waking review: Old and novel insights into the spore germination in Streptomyces. *Frontiers in Microbiology*, *8*, 2205.

Bobek, J., Strakova, E., Zikova, A., & Vohradsky, J. (2014). Changes in activity of metabolic and regulatory pathways during germination of S. coelicolor. *BMC genomics*, *15*(1), 1173.

Brownlee, G. G. (1971). Sequence of 6S RNA of E. coli. *Nature*, *229*(5), 147-149.

Buck, M., Gallegos, M. T., Studholme, D. J., Guo, Y., & Gralla, J. D. (2000). The bacterial enhancer-dependent ς54 (ςN) transcription factor. *Journal of bacteriology*, *182*(15), 4129-4136.

Bush, M. J., Bibb, M. J., Chandra, G., Findlay, K. C., & Buttner, M. J. (2013). Genes required for aerial growth, cell division, and chromosome segregation are targets of WhiA before sporulation in Streptomyces venezuelae. *MBio*, *4*(5), e00684-13.

Bush, M. J., Tschowri, N., Schlimpert, S., Flärdh, K., & Buttner, M. J. (2015). c-di-GMP signalling and the regulation of developmental transitions in streptomycetes. *Nature Reviews Microbiology*, *13*(12), 749-760.

Butter, F., Scheibe, M., Mörl, M., & Mann, M. (2009). Unbiased RNA–protein interaction screen by quantitative proteomics. *Proceedings of the National Academy of Sciences*, *106*(26), 10626-10631.

Buttner, M. J., & Lewis, C. G. (1992). Construction and characterization of Streptomyces coelicolor A3 (2) mutants that are multiply deficient in the nonessential hrd-encoded RNA polymerase sigma factors. *Journal of bacteriology*, *174*(15), 5165-5167.

Campagne, S., Marsh, M. E., Capitani, G., Vorholt, J. A., & Allain, F. H. (2014). Structural basis for− 10 promoter element melting by environmentally induced sigma factors. *Nature structural & molecular biology*, *21*(3), 269-276.

Campbell, E. A., Westblade, L. F., & Darst, S. A. (2008). Regulation of bacterial RNA polymerase σ factor activity: a structural perspective. *Current opinion in microbiology*, *11*(2), 121-127.

Carballido-López, R. (2006). The bacterial actin-like cytoskeleton. *Microbiology and Molecular Biology Reviews*, *70*(4), 888-909.

Cavanagh, A. T., & Wassarman, K. M. (2013). 6S-1 RNA function leads to a delay in sporulation in Bacillus subtilis. *Journal of bacteriology*, *195*(9), 2079-2086.

Chaconas, G., & Chen, C. W. (2005). Replication of linear bacterial chromosomes: no longer going around in circles. In *The bacterial chromosome* (pp. 525-540). American Society of Microbiology.

Chae, H., Han, K., Kim, K. S., Park, H., Lee, J., & Lee, Y. (2011). Rho-dependent Termination of ssrS (6S RNA) Transcription in Escherichia coli implication for 3′ processing of 6s rna and expression of downstream ygfa (putative 5-formyl-tetrahydrofolate cyclo-ligase). *Journal of Biological Chemistry*, *286*(1), 114-122.

Champness, W. C. (1988). New loci required for Streptomyces coelicolor morphological and physiological differentiation. *Journal of bacteriology*, *170*(3), 1168-1174.

Chater, K. F., & Chandra, G. (2008). The use of the rare UUA codon to define "expression space" for genes involved in secondary metabolism, development and environmental adaptation in Streptomyces. *The Journal of Microbiology*, *46*(1), 1-11.

Chater, K. F., Biró, S., Lee, K. J., Palmer, T., & Schrempf, H. (2010). The complex extracellular biology of Streptomyces. *FEMS microbiology reviews*, *34*(2), 171-198.

Chater, K. F., Bruton, C. J., Plaskitt, K. A., Buttner, M. J., Méndez, C., & Helmann, J. D. (1989). The developmental fate of S. coelicolor hyphae depends upon a gene product homologous with the motility σ factor of B. subtilis. *Cell*, *59*(1), 133-143.

Chen, J., Wassarman, K. M., Feng, S., Leon, K., Feklistov, A., Winkelman, J. T., ... & Darst, S. A. (2017). 6S RNA Mimics B-Form DNA to Regulate Escherichia coli RNA Polymerase. *Molecular cell*, *68*(2), 388-397.

Chiller, K., Selkin, B. A., & Murakawa, G. J. (2001). Skin microflora and bacterial infections of the skin. In *Journal of Investigative Dermatology Symposium Proceedings* (Vol. 6, No. 3, pp. 170-174). Elsevier.

Claessen, D., Rink, R., de Jong, W., Siebring, J., de Vreugd, P., Boersma, F. H., ... & Wösten, H. A. (2003). A novel class of secreted hydrophobic proteins is involved in aerial hyphae formation in Streptomyces coelicolor by forming amyloid-like fibrils. *Genes & development*, *17*(14), 1714-1726.

Cosma, C. L., Sherman, D. R., & Ramakrishnan, L. (2003). The secret lives of the pathogenic mycobacteria. *Annual Reviews in Microbiology*, *57*(1), 641-676.

Čihák, M. (2017). Verification of secondary metabolites production during germination of Streptomyces coelicolor. Master thesis, University of Chemistry and Technology Prague, Prague.

Dalton, K. A., Thibessard, A., Hunter, J. I., & Kelemen, G. H. (2007). A novel compartment, the 'subapical stem'of the aerial hyphae, is the location of a sigN-dependent, developmentally distinct transcription in Streptomyces coelicolor. *Molecular microbiology*, *64*(3), 719-737.

Dean, J. D., Goodwin, P. H., & Hsiang, T. (2002). Comparison of relative RT-PCR and northern blot analyses to measure expression of β-1, 3-glucanase inNicotiana benthamiana infected withColltotrichum destructivum. *Plant Molecular Biology Reporter*, *20*(4), 347-356.

Den Hengst, C. D., Tran, N. T., Bibb, M. J., Chandra, G., Leskiw, B. K., & Buttner, M. J. (2010). Genes essential for morphological development and antibiotic production in Streptomyces coelicolor are targets of BldD during vegetative growth. *Molecular microbiology*, *78*(2), 361-379.

Dharmaraj, S. (2010). Marine Streptomyces as a novel source of bioactive substances. *World Journal of Microbiology and Biotechnology*, *26*(12), 2123-2139.

Eaton, D. A. V. I. D., & Ensign, J. C. (1980). Streptomyces viridochromogenes spore germination initiated by calcium ions. *Journal of bacteriology*, *143*(1), 377-382.

Eckburg, P. B., Bik, E. M., Bernstein, C. N., Purdom, E., Dethlefsen, L., Sargent, M., ... & Relman, D. A. (2005). Diversity of the human intestinal microbial flora. *science*, *308*(5728), 1635-1638.

Elliot, M. A., Buttner, M. J., & Nodwell, J. R. (2008). 24 Multicellular Development in Streptomyces. In *Myxobacteria* (pp. 419-438). American Society of Microbiology.

Fadouloglou, V. E., Glykos, N. M., & Kokkinidis, M. (2000). A fast and inexpensive procedure for drying polyacrylamide gels. *Analytical biochemistry*, *287*(1), 185-186.

Fillinger, S., Chaveroche, M. K., Van Dijck, P., de Vries, R., Ruijter, G., Thevelein, J., & d'Enfert, C. (2001). Trehalose is required for the acquisition of tolerance to a variety of stresses in the filamentous fungus Aspergillus nidulans. *Microbiology*, *147*(7), 1851-1862.

Flärdh, K. (2003). Essential role of DivIVA in polar growth and morphogenesis in Streptomyces coelicolor A3 (2). *Molecular microbiology*, *49*(6), 1523-1536.

Flärdh, K., & Buttner, M. J. (2009). Streptomyces morphogenetics: dissecting differentiation in a filamentous bacterium. *Nature Reviews Microbiology*, *7*(1), 36-49.

Flärdh, K., Findlay, K. C., & Chater, K. F. (1999). Association of early sporulation genes with suggested developmental decision points in Streptomyces coelicolor A3 (2). *Microbiology*, *145*(9), 2229-2243.

Flärdh, K., Leibovitz, E., Buttner, M. J., & Chater, K. F. (2000). Generation of a non-sporulating strain of Streptomyces coelicolor A3 (2) by the manipulation of a developmentally controlled ftsZ promoter. *Molecular microbiology*, *38*(4), 737-749.

Fuchino, K., Bagchi, S., Cantlay, S., Sandblad, L., Wu, D., Bergman, J., ... & Ausmees, N. (2013). Dynamic gradients of an intermediate filament-like cytoskeleton are recruited by a polarity landmark during apical growth. *Proceedings of the National Academy of Sciences*, *110*(21), E1889-E1897.

Gerber, N. N., & Lechevalier, H. A. (1965). Geosmin, an earthy-smelling substance isolated from actinomycetes. *Applied microbiology*, *13*(6), 935-938.

Gildehaus, N., Neußer, T., Wurm, R., & Wagner, R. (2007). Studies on the function of the riboregulator 6S RNA from E. coli: RNA polymerase binding, inhibition of in vitro transcription and synthesis of RNA-directed de novo transcripts. *Nucleic acids research*, *35*(6), 1885-1896.

Görke, B., & Stülke, J. (2008). Carbon catabolite repression in bacteria: many ways to make the most out of nutrients. *Nature Reviews Microbiology*, *6*(8), 613-624.

Graham, J. E. (2004). Sequence-specific Rho–RNA interactions in transcription termination. *Nucleic acids research*, *32*(10), 3093-3100.

Gruber, T. M., & Gross, C. A. (2003). Multiple sigma subunits and the partitioning of bacterial transcription space. *Annual Reviews in Microbiology*, *57*(1), 441-466.

Haimes, J., & Kelley, M. (2010). Demonstration of a ΔΔCq Calculation Method to Compute Relative Gene Expression from qPCR Data. *Thermo Scientific Tech Note*, 1-4.

Haselwandter, K., & Ebner, M. R. (1994). Microorganisms surviving for 5300 years. *FEMS Microbiology Letters*, *116*(2), 189-193.

Hassan, S. S., Anjum, K., Abbas, S. Q., Akhter, N., Shagufta, B. I., Shah, S. A. A., & Tasneem, U. (2017). Emerging biopharmaceuticals from marine actinobacteria. *Environmental toxicology and pharmacology*, *49*, 34-47.

He, S., Wurtzel, O., Singh, K., Froula, J. L., Yilmaz, S., Tringe, S. G., ... & Hugenholtz, P. (2010). Validation of two ribosomal RNA removal methods for microbial metatranscriptomics. *Nature methods*, *7*(10), 807-812.

Heckman, D. S., Geiser, D. M., Eidell, B. R., Stauffer, R. L., Kardos, N. L., & Hedges, S. B. (2001). Molecular evidence for the early colonization of land by fungi and plants. *Science*, *293*(5532), 1129-1133.

Hellman, L. M., & Fried, M. G. (2007). Electrophoretic mobility shift assay (EMSA) for detecting protein–nucleic acid interactions. *Nature protocols*, *2*(8), 1849-1861.

Helmann, J. D., & Chamberlin, M. J. (1988). Structure and function of bacterial sigma factors. *Annual review of biochemistry*, *57*(1), 839-872.

Hempel, A. M., Wang, S. B., Letek, M., Gil, J. A., & Flärdh, K. (2008). Assemblies of DivIVA mark sites for hyphal branching and can establish new zones of cell wall growth in Streptomyces coelicolor. *Journal of bacteriology*, *190*(22), 7579-7583.

Heueis, N., Vockenhuber, M. P., & Suess, B. (2014). Small non-coding RNAs in streptomycetes. *RNA biology*, *11*(5), 464-469.

Higo, A., Horinouchi, S., & Ohnishi, Y. (2011). Strict regulation of morphological differentiation and secondary metabolism by a positive feedback loop between two global regulators AdpA and BldA in Streptomyces griseus. *Molecular microbiology*, *81*(6), 1607-1622.

Hnilicová, J., Jirát Matějčková, J., Šiková, M., Pospíšil, J., Halada, P., Pánek, J., & Krásný, L. (2014). Ms1, a novel sRNA interacting with the RNA polymerase core in mycobacteria. *Nucleic acids research*, *42*(18), 11763-11776.

Hopwood, D. A. (1999). Forty years of genetics with Streptomyces: from in vivo through in vitro to in silico. *Microbiology*, *145*(9), 2183-2202.

Hopwood, D. A. (2007). *Streptomyces in nature and medicine: the antibiotic makers*. Oxford University Press.

Hošťálek, Z. (1980). Catabolite regulation of antibiotic biosynthesis. *Folia microbiologica*, *25*(5), 445-450.

Hsu, L. M., Zagorski, J., Wang, Z., & Fournier, M. J. (1985). Escherichia coli 6S RNA gene is part of a dual-function transcription unit. *Journal of bacteriology*, *161*(3), 1162-1170.

Hüttenhofer, A., & Vogel, J. (2006). Experimental approaches to identify non-coding RNAs. *Nucleic acids research*, *34*(2), 635-646.

Jeong, Y., Kim, J. N., Kim, M. W., Bucca, G., Cho, S., Yoon, Y. J., ... & Cho, B. K. (2016). The dynamic transcriptional and translational landscape of the model antibiotic producer Streptomyces coelicolor A3 (2). *Nature communications*, *7*.

Jishage, M., & Ishihama, A. (1998). A stationary phase protein in Escherichia coli with binding activity to the major σ subunit of RNA polymerase. *Proceedings of the National Academy of Sciences*, *95*(9), 4953-4958.

Jogler, C., Waldmann, J., Huang, X., Jogler, M., Glöckner, F. O., Mascher, T., & Kolter, R. (2012). Identification of proteins likely to be involved in morphogenesis, cell division, and signal transduction in Planctomycetes by comparative genomics. *Journal of bacteriology*, *194*(23), 6419-6430.

Jones, S. E., & Elliot, M. A. (2018). 'Exploring'the regulation of Streptomyces growth and development. *Current Opinion in Microbiology*, *42*, 25-30.

Kallifidas, D., Thomas, D., Doughty, P., & Paget, M. S. (2010). The σR regulon of Streptomyces coelicolor A3 (2) reveals a key role in protein quality control during disulphide stress. *Microbiology*, *156*(6), 1661-1672.

Kelemen, G. H., Brian, P., Flärdh, K., Chamberlin, L., Chater, K. F., & Buttner, M. J. (1998). Developmental regulation of transcription ofwhiE, a locus specifying the polyketide spore pigment in Streptomyces coelicolor A3 (2). *Journal of bacteriology*, *180*(9), 2515-2521.

Kieser, T., Bibb, M. J., Buttner, M. J., Chater, K. F., & Hopwood, D. A ., (2000) Practical Streptomyces Genetics. The John Innes Foundation, Norwich, UK.

Kim, K. S., & Lee, Y. (2004). Regulation of 6S RNA biogenesis by switching utilization of both sigma factors and endoribonucleases. *Nucleic acids research*, *32*(20), 6057-6068.

Klocko, A. D., & Wassarman, K. M. (2009). 6S RNA binding to Eσ70 requires a positively charged surface of σ70 region 4.2. *Molecular microbiology*, *73*(2), 152-164.

Kodani, S., Hudson, M. E., Durrant, M. C., Buttner, M. J., Nodwell, J. R., & Willey, J. M. (2004). The SapB morphogen is a lantibiotic-like peptide derived from the product of the developmental gene ramS in Streptomyces coelicolor. *Proceedings of the National Academy of Sciences of the United States of America*, *101*(31), 11448-11453.

Kondo, J., Dock-Bregeon, A. C., Willkomm, D. K., Hartmann, R. K., & Westhof, E. (2013). Structure of an A-form RNA duplex obtained by degradation of 6S RNA in a crystallization droplet. *Acta Crystallographica Section F: Structural Biology and Crystallization Communications*, *69*(6), 634-639.

Kormanec, J., Sevcikova, B., Novakova, R., Homerova, D., Rezuchova, B., & Mingyar, E. (2016). The complex roles and regulation of stress response σ factors in streptomyces coelicolor. *Stress and environmental regulation of gene expression and adaptation in bacteria*, 328-343.

Kreader, C. A. (1996). Relief of amplification inhibition in PCR with bovine serum albumin or T4 gene 32 protein. *Applied and environmental microbiology*, *62*(3), 1102-1106.

Kühn-Hölsken, E. V. A., Lenz, C., Sander, B., Lührmann, R., & Urlaub, H. (2005). Complete MALDI-ToF MS analysis of cross-linked peptide–RNA oligonucleotides derived from nonlabeled UV-irradiated ribonucleoprotein particles. *RnA*, *11*(12), 1915-1930.

Lahdenpera, M. L. (2000). How Mycostop acts in the control of fungal plant diseases. *Infoletter Verdera*, *5*, 1-2.

Lee, D. J., Minchin, S. D., & Busby, S. J. (2012). Activating transcription in bacteria. *Annual review of microbiology*, *66*, 125-152.

Lerat, S., Simao-Beaunoir, A. N., & Beaulieu, C. (2009). Genetic and physiological determinants of Streptomyces scabies pathogenicity. *Molecular plant pathology*, *10*(5), 579-585.

Liu, X., & Gorovsky, M. A. (1993). Mapping the 5′ and 3′ ends of Tetrahymena thermophila mRNAs using RNA ligase mediated amplification of cDNA ends (RLM-RACE). *Nucleic acids research*, *21*(21), 4954-4960.

Losick, R., & Pero, J. (1981). Cascades of sigma factors. *Cell*, *25*(3), 582-584.

Lozada, M., & Dionisi, H. M. (2015). Microbial bioprospecting in marine environments. In *Springer Handbook of Marine Biotechnology* (pp. 307-326). Springer Berlin Heidelberg.

Lybecker, M., Bilusic, I., & Raghavan, R. (2014). Pervasive transcription: detecting functional RNAs in bacteria. *Transcription*, *5*(4), e944039.

Maeda, H., Fujita, N., & Ishihama, A. (2000). Competition among seven Escherichia coli σ subunits: relative binding affinities to the core RNA polymerase. *Nucleic acids research*, *28*(18), 3497-3503.

Manulis, S., Shafrir, H., Epstein, E., Lichter, A., & Barash, I. (1994). Biosynthesis of indole-3-acetic acid via the indole-3-acetamide pathway in Streptomyces spp. *Microbiology*, *140*(5), 1045-1050.

Marchuk, D., Drumm, M., Saulino, A., & Collins, F. S. (1991). Construction of T-vectors, a rapid and general system for direct cloning of unmodified PCR products. *Nucleic acids research*, *19*(5), 1154.

Mauri, M., & Klumpp, S. (2014). A model for sigma factor competition in bacterial cells. *PLoS computational biology*, *10*(10), e1003845.

Mazza, P., Noens, E. E., Schirner, K., Grantcharova, N., Mommaas, A. M., Koerten, H. K., ... & Wohlleben, W. (2006). MreB of Streptomyces coelicolor is not essential for vegetative growth but is required for the integrity of aerial hyphae and spores. *Molecular microbiology*, *60*(4), 838-852.

McCormick, J. R., & Flärdh, K. (2011). Signals and regulators that govern Streptomyces development. *FEMS microbiology reviews*, *36*(1), 206-231.

McDonald, B. R., & Currie, C. R. (2017). Lateral Gene Transfer Dynamics in the Ancient Bacterial Genus Streptomyces. *mBio*, *8*(3), e00644-17.

Mentz, A., Neshat, A., Pfeifer-Sancar, K., Pühler, A., Rückert, C., & Kalinowski, J. (2013). Comprehensive discovery and characterization of small RNAs in Corynebacterium glutamicumATCC 13032. *BMC genomics*, *14*(1), 714.

Menzel, P., Gorodkin, J., & Stadler, P. F. (2009). The tedious task of finding homologous noncoding RNA genes. *RNA*, *15*(12), 2075-2082.

Miguélez, E. M., Hardisson, C., & Manzanal, M. B. (1999). Hyphal death during colony development in Streptomyces antibioticus: morphological evidence for the existence of a process of cell deletion in a multicellular prokaryote. *The Journal of cell biology*, *145*(3), 515-525.

Mikulík, K., Bobek, J., Zídková, J., & Felsberg, J. (2014). 6S RNA modulates growth and antibiotic production in Streptomyces coelicolor. *Applied microbiology and biotechnology*, *98*(16), 7185-7197.

Moran, M. A., Rutherford, L. T., & Hodson, R. E. (1995). Evidence for indigenous Streptomyces populations in a marine environment determined with a 16S rRNA probe. *Applied and environmental microbiology*, *61*(10), 3695-3700.

Myers, T. W., & Gelfand, D. H. (1991). Reverse transcription and DNA amplification by a Thermus thermophilus DNA polymerase. *Biochemistry*, *30*(31), 7661-7666.

Otani, H., Higo, A., Nanamiya, H., Horinouchi, S., & Ohnishi, Y. (2013). An alternative sigma factor governs the principal sigma factor in Streptomyces griseus. *Molecular microbiology*, *87*(6), 1223-1236.

Paget, M. S. (2015). Bacterial sigma factors and anti-sigma factors: structure, function and distribution. *Biomolecules*, *5*(3), 1245-1265.

Paget, M. S., & Helmann, J. D. (2003). The σ 70 family of sigma factors. *Genome biology*, *4*(1), 203.

Paget, M. S., Kang, J. G., Roe, J. H., & Buttner, M. J. (1998). σ R, an RNA polymerase sigma factor that modulates expression of the thioredoxin system in response to oxidative stress in Streptomyces coelicolor A3 (2). *The EMBO journal*, *17*(19), 5776-5782.

Pánek, J., Bobek, J., Mikulík, K., Basler, M., & Vohradský, J. (2008). Biocomputational prediction of small non-coding RNAs in Streptomyces. *Bmc Genomics*, *9*(1), 217.

Panek, J., Krásný, L., Bobek, J., Ježková, E., Korelusova, J., & Vohradský, J. (2010). The suboptimal structures find the optimal RNAs: homology search for bacterial non-coding RNAs using suboptimal RNA structures. *Nucleic acids research*, *39*(8), 3418-3426.

Pathom-Aree, W., Stach, J. E., Ward, A. C., Horikoshi, K., Bull, A. T., & Goodfellow, M. (2006). Diversity of actinomycetes isolated from Challenger Deep sediment (10,898 m) from the Mariana Trench. *Extremophiles*, *10*(3), 181-189.

Patikoglou, G. A., Westblade, L. F., Campbell, E. A., Lamour, V., Lane, W. J., & Darst, S. A. (2007). Crystal structure of the Escherichia coli regulator of σ 70, Rsd, in complex with σ 70 domain 4. *Journal of molecular biology*, *372*(3), 649-659.

Podgornaia, A. I., & Laub, M. T. (2013). Determinants of specificity in two-component signal transduction. *Current opinion in microbiology*, *16*(2), 156-162.

Rediger, A., Geißen, R., Steuten, B., Heilmann, B., Wagner, R., & Axmann, I. M. (2012). 6S RNA–an old issue became blue-green. *Microbiology*, *158*(10), 2480-2491.

Rigali, S., Titgemeyer, F., Barends, S., Mulder, S., Thomae, A. W., Hopwood, D. A., & Van Wezel, G. P. (2008). Feast or famine: the global regulator DasR links nutrient stress to antibiotic production by Streptomyces. *EMBO reports*, *9*(7), 670-675.

Romero-Rodríguez, A., Robledo-Casados, I., & Sánchez, S. (2015). An overview on transcriptional regulators in Streptomyces. *Biochimica et Biophysica Acta (BBA)-Gene Regulatory Mechanisms*, *1849*(8), 1017-1039.

Romero-Rodríguez, A., Rocha, D., Ruiz-Villafan, B., Tierrafría, V., Rodríguez-Sanoja, R., Segura-González, D., & Sánchez, S. (2016). Transcriptomic analysis of a classical model of carbon catabolite regulation in Streptomyces coelicolor. *BMC microbiology*, *16*(1), 77.

Ruban-Ośmiałowska, B., Jakimowicz, D., Smulczyk-Krawczyszyn, A., Chater, K. F., & Zakrzewska-Czerwińska, J. (2006). Replisome localization in vegetative and aerial hyphae of Streptomyces coelicolor. *Journal of bacteriology*, *188*(20), 7311-7316.

Sanchez, S., Chávez, A., Forero, A., García-Huante, Y., Romero, A., Sánchez, M., ... & Rodríguez-Sanoja, R. (2010). Carbon source regulation of antibiotic production. *The Journal of antibiotics*, *63*(8), 442-459.

Sanger, F., Nicklen, S., & Coulson, A. R. (1977). DNA sequencing with chain-terminating inhibitors. *Proceedings of the national academy of sciences*, *74*(12), 5463-5467.

Sardi, P., Saracchi, M., Quaroni, S., Petrolini, B., Borgonovi, G. E., & Merli, S. (1992). Isolation of endophytic Streptomyces strains from surface-sterilized roots. *Applied and Environmental Microbiology*, *58*(8), 2691-2693.

Schmidt, C., Kramer, K., & Urlaub, H. (2012). Investigation of protein–RNA interactions by mass spectrometry—Techniques and applications. *Journal of proteomics*, *75*(12), 3478-3494.

Seipke, R. F., Kaltenpoth, M., & Hutchings, M. I. (2012). Streptomyces as symbionts: an emerging and widespread theme? *FEMS microbiology reviews*, *36*(4), 862-876.

Sharma, C. M., & Vogel, J. (2009). Experimental approaches for the discovery and characterization of regulatory small RNA. *Current opinion in microbiology*, *12*(5), 536-546.

Sharma, C. M., Hoffmann, S., Darfeuille, F., Reignier, J., Findeiß, S., Sittka, A., ... & Stadler, P. F. (2010). The primary transcriptome of the major human pathogen Helicobacter pylori. *Nature*, *464*(7286), 250-255.

Shinkawa, H., Hatada, Y., Okada, M., Kinashi, H., & Nimi, O. (1995). Nucleotide sequence of a principal sigma factor gene (hrdB) of Streptomyces griseus. *The Journal of Biochemistry*, *118*(3), 494-499.

Sola-Penna, M., & Meyer-Fernandes, J. R. (1998). Stabilization against thermal inactivation promoted by sugars on enzyme structure and function: why is trehalose more effective than other sugars? *Archives of biochemistry and biophysics*, *360*(1), 10-14.

Staroń, A., Sofia, H. J., Dietrich, S., Ulrich, L. E., Liesegang, H., & Mascher, T. (2009). The third pillar of bacterial signal transduction: classification of the extracytoplasmic function (ECF) σ factor protein family. *Molecular microbiology*, *74*(3), 557-581.

Steuten, B., & Wagner, R. (2012). A conformational switch is responsible for the reversal of the 6S RNA-dependent RNA polymerase inhibition in Escherichia coli. *Biological chemistry*, *393*(12), 1513-1522.

Steuten, B., Schneider, S., & Wagner, R. (2014). 6S RNA: recent answers–future questions. *Molecular microbiology*, *91*(4), 641-648.

Steuten, B., Setny, P., Zacharias, M., & Wagner, R. (2013). Mapping the spatial neighborhood of the regulatory 6S RNA bound to Escherichia coli RNA polymerase holoenzyme. *Journal of molecular biology*, *425*(19), 3649-3661.

Swiercz, J. P., Bobek, J., Haiser, H. J., Di Berardo, C., Tjaden, B., & Elliot, M. A. (2008). Small non-coding RNAs in Streptomyces coelicolor. *Nucleic acids research*, *36*(22), 7240-7251.

Tabib-Salazar, A., Liu, B., Doughty, P., Lewis, R. A., Ghosh, S., Parsy, M. L., ... & Paget, M. S. (2013). The actinobacterial transcription factor RbpA binds to the principal sigma subunit of RNA polymerase. *Nucleic acids research*, *41*(11), 5679-5691.

Tahvonen, R. T. (1988). Microbial control of plant diseases with Streptomyces spp. *Eppo Bulletin*, *18*(1), 55-59.

Tillotson, R. D., Wösten, H. A. B., Richter, M., & Willey, J. M. (1998). A surface active protein involved in aerial hyphae formation in the filamentous fungus Schizophillum commune restores the capacity of a bald mutant of the filamentous bacterium Streptomyces coelicolor to erect aerial structures. *Molecular microbiology*, *30*(3), 595-602.

Trotochaud, A. E., & Wassarman, K. M. (2005). A highly conserved 6S RNA structure is required for regulation of transcription. *Nature structural & molecular biology*, *12*(4), 313-319.

Tschowri, N., Schumacher, M. A., Schlimpert, S., babu Chinnam, N., Findlay, K. C., Brennan, R. G., & Buttner, M. J. (2014). Tetrameric c-di-GMP mediates effective transcription factor dimerization to control Streptomyces development. *Cell*, *158*(5), 1136-1147.

Ulrich, L. E., Koonin, E. V., & Zhulin, I. B. (2005). One-component systems dominate signal transduction in prokaryotes. *Trends in microbiology*, *13*(2), 52-56.

Urem, M., Świątek-Połatyńska, M. A., Rigali, S., & van Wezel, G. P. (2016). Intertwining nutrient-sensory networks and the control of antibiotic production in Streptomyces. *Molecular microbiology*, *102*(2), 183-195.

Ventura, M., Canchaya, C., Tauch, A., Chandra, G., Fitzgerald, G. F., Chater, K. F., & van Sinderen, D. (2007). Genomics of Actinobacteria: tracing the evolutionary history of an ancient phylum. *Microbiology and molecular biology reviews*, *71*(3), 495-548.

Viollier, P. H., Kelemen, G. H., Dale, G. E., Nguyen, K. T., Buttner, M. J., & Thompson, C. J. (2003). Specialized osmotic stress response systems involve multiple SigB-like sigma factors in Streptomyces coelicolor. *Molecular microbiology*, *47*(3), 699-714.

Vockenhuber, M. P., Sharma, C. M., Statt, M. G., Schmidt, D., Xu, Z., Dietrich, S., ... & Suess, B. (2011). Deep sequencing-based identification of small non-coding RNAs in Streptomyces coelicolor. *RNA biology*, *8*(3), 468-477.

Vohradsky, J., Li, X. M., Dale, G., Folcher, M., Nguyen, L., Viollier, P. H., & Thompson, C. J. (2000). Developmental Control of Stress Stimulons inStreptomyces coelicolor Revealed by Statistical Analyses of Global Gene Expression Patterns. *Journal of bacteriology*, *182*(17), 4979-4986.

Wassarman, K. M., & Saecker, R. M. (2006). Synthesis-mediated release of a small RNA inhibitor of RNA polymerase. *Science*, *314*(5805), 1601-1603.

Wassarman, K. M., & Storz, G. (2000). 6S RNA regulates E. coli RNA polymerase activity. *Cell*, *101*(6), 613-623.

Watanabe, T., Sugiura, M., & Sugita, M. (1997). A novel small stable RNA, 6Sa RNA, from the cyanobacterium Synechococcus sp. strain PCC6301. *FEBS letters*, *416*(3), 302-306.

Weaver, D., Karoonuthaisiri, N., Tsai, H. H., Huang, C. H., Ho, M. L., Gai, S., ... & Chen, C. W. (2004). Genome plasticity in Streptomyces: identification of 1 Mb TIRs in the S. coelicolor A3 (2) chromosome. *Molecular microbiology*, *51*(6), 1535-1550.Wildermuth, H. (1970). Development and organization of the aerial mycelium in Streptomyces coelicolor. *Microbiology*, *60*(1), 43-50.

Willey, J., Santamaria, R., Guijarro, J., Geistlich, M., & Losick, R. (1991). Extracellular complementation of a developmental mutation implicates a small sporulation protein in aerial mycelium formation by S. coelicolor. *Cell*, *65*(4), 641-650.

Wohl, D. L., & McArthur, J. V. (2001). Aquatic actinomycete-fungal interactions and their effects on organic matter decomposition: a microcosm study. *Microbial ecology*, *42*(3), 446-457.

Supplementary data

Sequences and genetic neighborhood of *in silico* predicted *S. coelicolor* 6S RNAs

6Sc1

```
  1 uggacggcug uugguacgca cggaccgggc gggguguuca gccgggcccu cgcgccgccc
 61 ccgaucggca cccuccgcau ccggagcgcg acgcaccguu gcgaucacgg agcggaauga
121 cugcuucagc gaaucugcac aucgaaugcc caacccgguc acucccguug gcgcaucugc
181 acaagcccgc g
```

GenBank accession: AL939106 Region: 206114..206304

Position: intergenic, upstream - SCO0752 protease precursor;
downstream - SCO0754 putative secreted protein

6Sc2

```
  1 acguucccgc ucguggcuuu uccucgaaaa aacuuuccga ggggccggcu guugccgauu
 61 ggcggcgaau gugccguauu gcgugucuuu gugucguacg gguucgcgca gucggucagu
121 gucggucccg ccggcugggu ugccgguuug uucaugagga cgugcccgga gccuaaaugg
181 uucaugcguc g
```

GenBank accession: AL939125 Region: 81627..81817

Position: intergenic, upstream - SCO5821 putative serine protease,
SCO5820 HrdB; downstream - SCO5822 putative DNA gyrase
subunit B

6Sc3

```
  1 guagaacauc ugaggcaccc uagcguucgc cgucgcauuc cguaaaacac ucgacgucau
 61 ucccgcauuu cggguucuug gguacggugu gaguaccgug cgaguacccc guaauccggg
121 aacucggccu ccccggacgc gcgacggacc ucacguggag cgcccuguuu gucaugacac
181 aucauuacug a
```

GenBank accession: AL939113 Region: 124603..124793

Position: intergenic, downstream – tRNA-Gly, tRNA-Pro;
upstream - SCO2622 putative integral membrane protein

6Sc5

```
  1 ggaccccgaa cgccgcaugu cggugacaug gcucauagcc aggcuuccgg acaaccucuc
 61 ccgaccccuu gacaggcccg cgcacgacac cuucaacacc ccugcucgcc cgcgauccau
121 ggucggauaa cgagaaauuc cgcagaucuu ccggccggaa gggcagauuc ccgcaaaggu
181 ucggucguga u
```

GenBank accession: AL939123 Region: 38742..38932

Position: intergenic, downstream – SCO5260 secreted protein;
upstream - SCO5261 putative malate oxidoreductase

6Sc6

```
  1 cccaaagugg cugccuaaag ccguggagcc gaccgcgcca gccacagagg gugucucccc
 61 acuucaugcc cgcagccgcc gggcgcggcc agccggggcg aggacaggag gcgggccgcg
121 ccguagaggc ggcgcgcgcc cgcgccgugc gcgggccuug augaaguagg gaaagucuua
181 ucccacugug a
```

GenBank accession: AL939124 Region: 156538..156728

Position: intergenic, downstream – SCO5637 mutT-like protein, SCO5636 transcriptional regulator;
upstream - SCO5638 integral membrane protein

6Sc7

```
  1 cucggcagca ccacgaaccc cuucggaucg ucgguccguu ugacgaccuc cacggccagg
 61 gcgaguuucu cgcgggccca gucgaugagg gaugguguaa ccgccgucgg cccagaccag
121 gcagaugucc cggugcagcu cacgcagccg ggucaacagg ccgguggccg ccucgcgguc
181 cccgauguuc g
```

GenBank accession: AL939104 Region: 65790..65980

Position: complete gene overlap, SCO0076 putative transposase

6Sc8

```
  1 ugccuccuug ggcgucggcg gcgcguggcu cgcgccggga cgaucugguu cagucucccc
 61 ucaugccugg ucguagcgcc accauguccc gguaacgggc ugggaguguu uucgaccaca
121 cggggcgccg gggcgcgagc gugaccaguu caagcgcggg ugagcgacgu cucccgcgcc
181 cguuucgggc c
```

GenBank accession: AL939113 Region: 162695..162885

Position: intergenic, downstream - SCO2657 putative ROK-family transcriptional regulatory protein; upstream - SCO2655 conserved hypothetical protein SC8E4A.25c